

# CHARLES UNIVERSITY IN PRAGUE

**Faculty of Pharmacy in Hradec Králové**

**Department of Pharmaceutical Chemistry and Drug Control**



## **Inhibitors of mitochondrial enzymes as potential therapeutics for Alzheimer's disease**

**Dissertation work**

**Mgr. Lukáš Hroch**

**Course: Pharmaceutical Chemistry**

**Supervisor:**

**assoc. prof. PharmDr. Kamil Musílek, Ph.D.**

**Supervisor – consultant:**

**prof. PharmDr. Martin Doležal, Ph.D.**

**Hradec Králové, June 2017**

## **Acknowledgement**

Firstly, I would like to extend a thank you to my supervisor assoc. prof. PharmDr. Kamil Musílek, Ph.D. and my consultant prof. PharmDr. Martin Doležal, Ph.D. for their guidance and project coordination throughout the doctoral studies. Sincere appreciation goes to Department of Pharmaceutical Chemistry and Drug Control (Faculty of Pharmacy in Hradec Králové, Charles University in Prague and Biomedical Research Centre (University Hospital of Hradec Králové), where I was allowed to performed substantial part of experimental work. Gratitude goes to my project collaborator, colleague and friend Mgr. Ondřej Benek, Ph.D. and to graduate students Mgr. Matěj Chříbek and Mgr. Vendula Králová for their contribution to the project.

Acknowledgement goes to our close project collaborators from University of St. Andrews, namely prof. Frank Gun-Moore, Dr. Rona R. Ramsay, Dr. Laura Aitken and Dr. Patrick Guest.

Last, but not least, I would like to express my appreciation to the following parties providing generous financial support.

Project financial support: Ministry of Health of the Czech Republic (no. NV15-28967A), Ministry of Education, Youth and Sports of the Czech Republic (SVV 260 401), Grant Agency of Charles University in Prague (GAUK B-CH/992214) and European Social Fund and the state budget of the Czech Republic (TEAB, no. CZ.1.07/2.3.00/20.0235).

Traineeships/Internships financial support: Australian Government Endeavour Fellowship programme (6-months, Hobart, Australia), Erasmus+ programme of the European Union (5-months, Cardiff, United Kingdom), FAFIS + COST CM1103 (2-months, St. Andrews, United Kingdom), COST CM1103 (1-month, Istanbul, Turkey).

## **Declaration**

I hereby declare, that I am the sole author of presented dissertation. Neither any part of the dissertation nor the whole dissertation has been submitted to claim any other degree. I certify that, presented dissertation is a result of my independent work. Any other material (published or otherwise) and work of other people are fully acknowledged and/or listed in reference chapter according to standard referencing practice.

Hradec Králové, 12.6.2017

.....

Mgr. Lukáš Hroch

# Content

<b>List of Abbreviations .....</b>	<b>9</b>
<b>1. Concept and aims of the project .....</b>	<b>11</b>
<b>2. Introduction .....</b>	<b>13</b>
2.1. Alzheimer's disease as an illness .....	14
2.2. Hypotheses involved in AD pathogenesis.....	14
2.2.1. Cholinergic hypothesis .....	14
2.2.2. Tau protein hypothesis .....	15
2.2.3. Amyloid cascade hypothesis .....	16
2.3. Biomarkers and symptoms onset.....	16
2.4. Current treatment strategies.....	17
2.5. AD and A $\beta$ supported by genetics.....	20
2.6. Formation of A $\beta$ species .....	21
2.7. A $\beta$ deposition .....	23
2.8. Intracellular A $\beta$ .....	24
2.9. Mitochondrial A $\beta$ .....	25
2.9.1. Implications of A $\beta$ presence in mitochondria .....	26
2.9.2. A $\beta$ entry points to mitochondria.....	26
2.9.3. Mitochondrial proteins interacting with A $\beta$ .....	27
2.10. Amyloid $\beta$ -binding alcohol dehydrogenase .....	27
2.10.1. Structure and catalysis of ABAD .....	28
2.10.2. Enzymatic function of ABAD .....	29
2.10.3. Physiological function of ABAD .....	30
2.10.4. Interaction of A $\beta$ and ABAD .....	30
2.10.5. Consequences of A $\beta$ and ABAD interaction.....	32
2.10.6. ABAD – a potential drug target .....	34
2.10.7. Small molecules targeting ABAD or A $\beta$ -ABAD interaction .....	35
2.11. Benzothiazoles – scaffold of interest for CNS targeted drugs .....	36
2.12. Multi-target-directed strategies .....	36
<b>3. Results and Discussion .....</b>	<b>38</b>

3.1.	Synthesis and evaluation of frentizole-based indolyl thiourea analogues as MAO/ABAD inhibitors for Alzheimer's disease treatment .....	38
3.1.1.	Design and chemistry .....	38
3.1.2.	Results and discussion.....	39
3.1.3.	Conclusion.....	40
3.2.	Design, synthesis and <i>in vitro</i> evaluation of riluzole-based ureas as potential ABAD/17β-HSD10 modulators for Alzheimer's disease treatment .....	41
3.2.1.	Design and chemistry .....	41
3.2.2.	Results and discussion.....	42
3.2.3.	Conclusion.....	43
3.3.	Design, synthesis and evaluation of further analogues.....	43
3.3.1.	Exploration of distal phenyl ring substitutions.....	43
3.3.2.	Fluorinated distal phenyl ring substitutions.....	47
3.3.3.	Scaffold linker modifications .....	49
3.3.4.	Physical-chemical properties of designed series .....	52
3.3.5.	Fragments based on 2-aminoindole-3-carboxylic acid derivatives .....	53
3.3.6.	Derivatives of National Cancer Institute Diversity IV library hits.....	55
<b>4.</b>	<b>Conclusion.....</b>	<b>57</b>
<b>5.</b>	<b>Experimental section.....</b>	<b>58</b>
5.1.	Chemicals and instrumentation .....	58
5.2.	Synthesis and characterisation data of intermediates and final compounds .....	59
5.3.	Biological evaluation of final compounds.....	82
<b>6.</b>	<b>Abstract (English).....</b>	<b>83</b>
<b>7.</b>	<b>Abstrakt (Czech).....</b>	<b>84</b>
<b>8.</b>	<b>Outputs.....</b>	<b>85</b>
8.1.	Publications .....	85
8.2.	Conference communications .....	86
<b>9.</b>	<b>References .....</b>	<b>89</b>
<b>10.</b>	<b>Attachments .....</b>	<b>102</b>

## List of Abbreviations

A $\beta$	Amyloid $\beta$ -peptide
ABAD	A $\beta$ -binding alcohol dehydrogenase
AD	Alzheimer's disease
ACh	Acetylcholine
AChE	Acetylcholinesterase
AChEI	Acetylcholinesterase inhibitor
ApoE	Apolipoprotein E
APP	Amyloid precursor protein
BACE	$\beta$ -site APP cleaving enzymes
BBB	Blood brain barrier
Boc <sub>2</sub> O	Di- <i>tert</i> -butyl dicarbonate
CDI	<i>N,N'</i> -Carbonyldiimidazole
CNS	Central nervous system
CoA	Coenzyme A
CSF	Cerebrospinal fluid
EOAD	Early-onset Alzheimer's disease
ER	Endoplasmic reticulum
ERAB	ER-associated amyloid-binding protein
Ep-1	Endophilin-1
DCE	1,2-Dichloroethane
DCM	Dichloromethane
DMAP	4-(Dimethylamino)pyridine
DMF	<i>N,N</i> -Dimethylformamide
DMSO	Dimethyl sulfoxide
DP	Decoy peptide
EA	Elemental analysis
ELISA	Enzyme-linked immunosorbent assay
EtOAc	Ethyl acetate
FAD	Familial Alzheimer's disease
FDG	Fluorodeoxyglucose
HNE	4-Hydroxynonenal
HRMS	High-resolution mass spectra
HRP	Horseradish peroxidase
IC <sub>50</sub>	Concentration required for 50% inhibition of target
LDH	Lactate dehydrogenase

LOAD	Late-onset Alzheimer's disease
MAO-A/B	Monoamine oxidase A/B
MAP	Microtubule-associated proteins
MAM	Mitochondria associated membrane
MDA	Malondialdehyde
MHBD	2-Methyl-3-hydroxybutyryl-CoA dehydrogenase
MRI	Magnetic resonance imaging
MTDL	Multi-target-directed ligands
MTT	3-(4,5-Dimethylthiazol-2-yl)-2,5-diphenyltetrazolium bromide
NAD <sup>+</sup>	Nicotinamide adenine dinucleotide, oxidised
NADH	Nicotinamide adenine dinucleotide, reduced
ND	Not determined
NFT	Neurofibrillary tangles
NMDA	<i>N</i> -Methyl- <i>D</i> -aspartate
NMR	Nuclear magnetic resonance
PAMPA	Parallel artificial membrane permeability assay
Pd/C	Palladium on activated carbon
PE	Petroleum ether
PET	Positron emission tomography
Prdx-2	Peroxiredoxin-2
PHF	Paired helical filaments
ROS	Reactive oxygen species
SAD	Sporadic Alzheimer's disease
SCHAD	Short chain L-3-hydroxyacyl-CoA dehydrogenase
SDR	Short-chain dehydrogenase/reductase
SF	Straight filaments
SP	Senile plaques
SPECT	Single photon emission computed tomography
RT	Room temperature
THF	Tetrahydrofuran
TIM	Translocase of the inner membrane
TLC	Thin-layer chromatography
TMS	Tetramethylsilane
TOM	Translocase of the outer membrane

## **1. Concept and aims of the project**

The dissertation project is intended to form integral part of a newly established long-term project of assoc. prof. PharmDr. Kamil Musílek, Ph.D. at Biomedical Research Centre, University Hospital Hradec Králové. The long-term project is dedicated to the preparation and investigation of small molecules interacting with selected mitochondrial enzymes, which might hold therapeutic potential for neurodegenerative disorders, such as Alzheimer's disease (AD).

The workgroup of assoc. prof. PharmDr. Kamil Musílek, Ph.D. pursues pharmaceutical chemistry aspects of the project such as drug design, synthesis, and elucidation of structure and activity relationships etc. Furthermore, the project also builds on already established international cooperation with University of St. Andrews, United Kingdom. The workgroups of prof. Frank Gunn-Moore and Dr. Rona R. Ramsay possess desired expertise in molecular biology and biochemistry aspects of neurodegenerative disorders.

Presented work is focused on selected aspects:

### **Review of AD towards the involvement of mitochondrial enzymes in disease pathology**

Although there is a vast pool of literature sources covering aspects of AD, the involvement of selected mitochondrial enzymes comes only in limited numbers. Therefore, the introduction part attempts to cover the very most important aspects of AD with progressive focus on mitochondrial enzymes involved in AD, especially enzyme called amyloid  $\beta$ -binding alcohol dehydrogenase (ABAD). Introduction starts as a broader topic and gradually narrows the subject to key aspects of the presented work. As AD represents a multifactorial disease, multi-target-directed ligand (MTDL) strategies will be discussed with emphasis on secondary targets, monoamine oxidases (MAO). Since further investigation will be focused around frentizole, a review of benzothiazole scaffold acting in central nervous system (CNS) was prepared and it is enclosed as a sole attachment A1.

### **Design and synthesis of novel potential modulators of mitochondrial enzymes**

There is a limited number of small molecules known to interact and modulate the activity of ABAD. Among those few, the project is focused on the earlier identified scaffold, frentizole, which demonstrated valuable properties for further investigation. The aim of the project is to build rationally diverse pool of compounds, which would help to identify structural features necessary for interaction with ABAD. The overall design will be coordinated and based on the long-term project interests.



### **Biological evaluation of prepared compounds**

While the most important goals of the dissertation project are design and synthesis of small molecules, it is imperative to evaluate compounds' potential activity towards the desired biological targets, such as ABAD. The project will utilize already established inter-workgroup collaborations (both domestic and international) to assess biological properties of prepared compounds. Author's international internships were planned to contribute to biological evaluation of prepared compounds.

### **Molecular basis and structural features underlying modulation of ABAD**

Series of prepared compounds will be gradually subjected to investigation and establishment of structure and activity relationships for ABAD. Initial series of compounds will be designed with emphasis on fast and straightforward process to readily build a limited pool of compounds. The foremost purpose of initial series will be identification of very basic structural aspects underlying modulation of ABAD enzymatic activity. Based on the initially acquired data, further design will follow to extend available pool of compounds. Moreover, follow-up design will consider possible improvements and limitations (such as potency/selectivity towards biological targets or physical-chemical properties) of investigated scaffold in order to provide comprehensive pharmacophore information.

### **Supporting documents**

Presented work is accompanied by five attachments – A1-A5.

**Attachment A1:** A review of benzothiazole scaffold with focus on CNS, which serves as a complementary chapter to the project introduction.

**Attachments A2-A4:** Original papers, which include discussed experimental work directly related to the project.

**Attachment A5:** Additional experimental work conducted during doctoral research stay at Cardiff University, though not directly related to the discussed project.

## 2. Introduction

One hundred and ten years ago, Dr. Alois Alzheimer gave a lecture, where he presented remarkable pathological and clinical findings of a new disease, which were afterwards published one year later [1]. The presented data already included histological findings such as senile plaques (SP) and neurofibrillary tangles (NFT), nowadays well-known hallmarks in Alzheimer's disease research community [1, 2]. Three years later, this disease was named after Dr. Alois Alzheimer by his colleague Dr. Emil Kraepelin [3]. After next 70 years, AD has been acknowledged as a “major killer” along other diseases [4]. Along with population aging, AD became a major health issue problem of the world population. In the United States of America, it is estimated that 5.4 million people have AD, where 5.1 million are  $\geq 65$  years old. In 2015, about 50 million people around the world will be living with a form of dementia and it is estimated that the number will raise close 130 million by the year of 2050. Today, AD (as a form of dementia) is the most common cause of dementia with its estimation from 60 to 80 percent of overall cases [5, 6]. Over the century, both academic research institutions and research corporations have put enormous efforts into the research of AD. Numerous papers have been published describing various pathophysiological changes, constructing new hypotheses and challenging new avenues, leading to valuable knowledge about disease progression. However, up to date, both the aetiology of the disease and ability, how to tackle the treatment remain unclear.

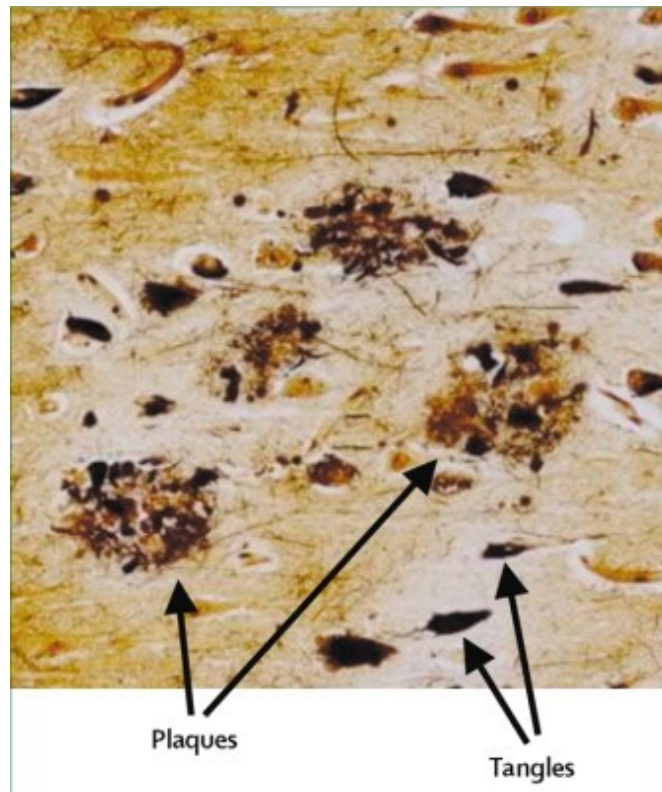


**Figure 1.** Deposition of senile plaques and neurofibrillary tangles in the cerebral cortex in AD (Blennow *et al.*, 2006) [6].

## **2.1. Alzheimer's disease as an illness**

AD is neurodegenerative disorder, currently considered as an irreversible disease. In addition, AD is a multifactorial disorder with its recognised complexity. Such complexity includes alterations in proteins function, neuroinflammation, oxidative stress, impairment in neuronal signalling pathways and many others, consequently resulting in neuronal degeneration [6, 7]. Occurrence, frequency and severity of the symptoms correlate with progression of the disease and loss of neurons in particular brain areas. The first symptoms manifest as difficulties in remembering of new information (short-term memory impairment). As the disease progresses, memory loss is accompanied with other cognitive symptoms such as general difficulties in learning, perception, judgement, emotional behaviour disturbances or disruption of daily life routines [8, 9]. Later then, patients either fail to partially or completely take care of themselves and they are becoming fully dependent on family and health care system. Such medically handicapped patients with severe progression of AD are generally susceptible to other illnesses (for example bacterial or viral infections) with marginal probability for successful recovery, thus eventually leading to early deaths [5, 6].

## **2.2. Hypotheses involved in AD pathogenesis**

Due to the complex nature of AD pathogenesis, enormous efforts and intensive research were conducted in order understand the pathogenesis of AD. Therefore over the last decades, numerous hypotheses were proposed, which resulted in profiling into the three most commonly recognised hypotheses – cholinergic, tau and amyloid  $\beta$ -peptide (A $\beta$ ) hypotheses. However, there are many other hypotheses, whose importance may promptly arise as new aspects and insights into AD pathogenesis are continually documented. These hypotheses includes ongoing pathophysiological events such as oxidative stress, cellular ion homeostasis, mitochondrial and energy metabolism, neuroinflammation, neurotransmitters dysregulation and others [10].

### **2.2.1. Cholinergic hypothesis**

Cholinergic hypothesis represents the oldest hypothesis with remarkable insights into AD pathogenesis. The origin of hypothesis dates back to the beginning of the twentieth century, when Henry Dale and Otto Loewi published their novel research focused on acetylcholine (ACh) and its function as a chemical neurotransmitter with further identification of ACh presence in mammalian tissue [11–13]. In 1936, both authors received and shared Nobel Prize for their novel research in chemical neurotransmission and characterization of firstly identified neurotransmitter, ACh. Since then, the field of chemical neurotransmission became of great interest and cholinergic neurotransmission has been repeatedly associated with many brain functions and numerous neurological disorders such as depression, schizophrenia, affective disorders, sleep regulation and

so on [14]. Second half of the twentieth century brought in many intensive studies focused on cholinergic association with AD pathogenesis. Among the first ones, histological post-mortem investigation of human brain tissue showed reduced activity of choline acetyltransferase and acetylcholinesterase (AChE) in cerebral cortex [15, 16]. Later on, studies of both post-mortem and cerebral biopsy tissues showed different abnormalities in cholinergic neurotransmission system. These abnormalities involved shortages in synthesis of ACh via choline acetyltransferase, decreased choline uptake, reduced ACh uptake, different stage deterioration or a complete loss of cholinergic neurons [17–20]. Consequently, overall degradation of cholinergic neurons in basal forebrain and decline of cholinergic neurotransmission are fundamental events of cholinergic hypothesis. Thus, abovementioned pathophysiological changes have been associated with AD patients' symptoms (such as cognitive decline, memory loss or behavioural changes), where cholinomimetic treatment shows amelioration of AD symptoms [21–23].

### **2.2.2. Tau protein hypothesis**

The basis of the tau protein hypothesis is established on hyperphosphorylation of tau protein with consequent formation of NFT. The presence of NFT has already been discovered by Dr. Alois Alzheimer, but fundamental involvement of tau protein in NFT formation was described in late eighties of the twentieth century [1, 24, 25]. Tau protein gene is located on chromosome 17 and transcription process with its alternative splicing can produce up to six isoforms, which are commonly present in adult brain. It is largely expressed in neurons and marginally in other neuronal cells such as astrocytes or oligodendrocytes [24, 26, 27]. Tau protein belongs to microtubule-associated proteins (MAP), which are important parts in development of cell cytoskeleton. Neuronal cell cytoskeleton is fundamental part for organised transport of organelles and molecules within neuronal cell body, dendrites or axons. Cytoskeleton is formed by three fibre structures – microtubules, microfilaments and neurofilaments. Tau protein binds with tubulins (structural part of microtubules) through its specific microtubule-binding domain and it facilitates nucleation, co-polymerisation and stabilisation of microtubules forming functional part of neuronal cell cytoskeleton. The affinity towards microtubules is regulated via phosphorylation of tau protein, where higher level of tau protein phosphorylation causes a decrease in its binding affinity [26, 28]. In the regard of such case, the tau protein hyperphosphorylation may occur under various pathophysiological conditions. Hyperphosphorylation along with reduced tau protein binding affinity towards microtubules can cause tau protein to misfold, aggregate and polymerize forming oligomers, aggregates, straight filaments (SF), paired helical filaments (PHF) and eventually NFT. Therefore, it is presumed that these abnormally formed tau protein structures are the cause of neuronal damage in AD brain [25, 29, 30]. Tau protein hyperphosphorylation is not merely exclusive to AD, but it was reported as pathophysiological condition in various other neurological disorders. Thus, such conditions are generally recognised as tauopathies (for example Guam

parkinsonism dementia complex, Niemann-Pick type C, pugilistic dementia, and Pick's diseases) [28]. General phosphorylation process is maintained by enzymes called kinases. pathophysiological hyperphosphorylation of tau protein has already been associated with several known kinases (e.g. glycogen synthase kinase 3 $\beta$ , cAMP dependent protein kinase or extracellular signal-regulated kinase 2). Therefore targeting such kinases is considered as a perspective strategy in drug discovery of novel AD therapeutics [31].

### **2.2.3. Amyloid cascade hypothesis**

Similar to tau protein hypothesis, foundation of amyloid cascade hypothesis dates back to Dr. Alois Alzheimer's discovery, where he described two histological findings characteristic for AD pathology. Besides firstly abovementioned presence of NFT, secondly the presence A $\beta$  depositions as SP has been described [1, 2]. Amyloid cascade hypothesis proposed that A $\beta$  as the central structural element of SP is a causative component to AD pathology. Amyloid cascade hypothesis presumes, that A $\beta$  deposition and consequent formation of extracellular SP triggers a cascade of toxic events (e.g. neuronal damage, hyperphosphorylation of tau protein, formation of NFT) ultimately leading to the neuronal cell death [32, 33]. Great attention has been focused on amyloid cascade hypothesis with its numerous iterations [33]. It has become widely discussed and elaborated on as many A $\beta$  pathophysiological events has been proposed. Still, full picture of A $\beta$  involvement and its toxicity remains unclear.

## **2.3. Biomarkers and symptoms onset**

Tau protein and amyloid cascade hypotheses formed two most commonly monitored biomarkers - A $\beta$  peptide species and tau protein. Both A $\beta$  species and tau protein are fluid biomarkers in cerebrospinal fluid (CSF) as their levels were found changed throughout the development of AD [34]. There are several A $\beta$  species, while A $\beta_{42}$  is the most amyloidogenic one. A $\beta_{42}$  is more hydrophobic than other A $\beta$  peptides, fibrillogenic and it more readily aggregates forming SP. Therefore, A $\beta_{42}$  is more closely monitored [35, 36]. Formation of various A $\beta$  species will be discussed later on (chapter 2.6.). Non-invasive imaging methods are used to monitor A $\beta$  depositions such as positron emission tomography (PET), single photon emission computed tomography (SPECT) or magnetic resonance imaging (MRI). Both PET and SPECT imaging methods utilize various radiolabelled tracers (e.g. Thioflavin-T based Pittsburgh compound B for PET) to monitor A $\beta$  depositions or more recently tangles formation [37]. Additionally, there are other biomarkers which are more or less followed through the disease progression [34].

Figure 2 depicts the changes in monitored biomarkers with correlation to expected first symptoms onset. Elevated CSF levels of A $\beta_{42}$  (twenty-five years before expected symptoms) are followed by appearance of A $\beta$  deposits (PET imaging) along with elevated CSF levels of tau

protein (fifteen years before expected symptoms). Deteriorating changes of neuronal metabolism monitored with fluorodeoxyglucose (FDG) are usually observed ten years before expected symptoms onset [38–40].

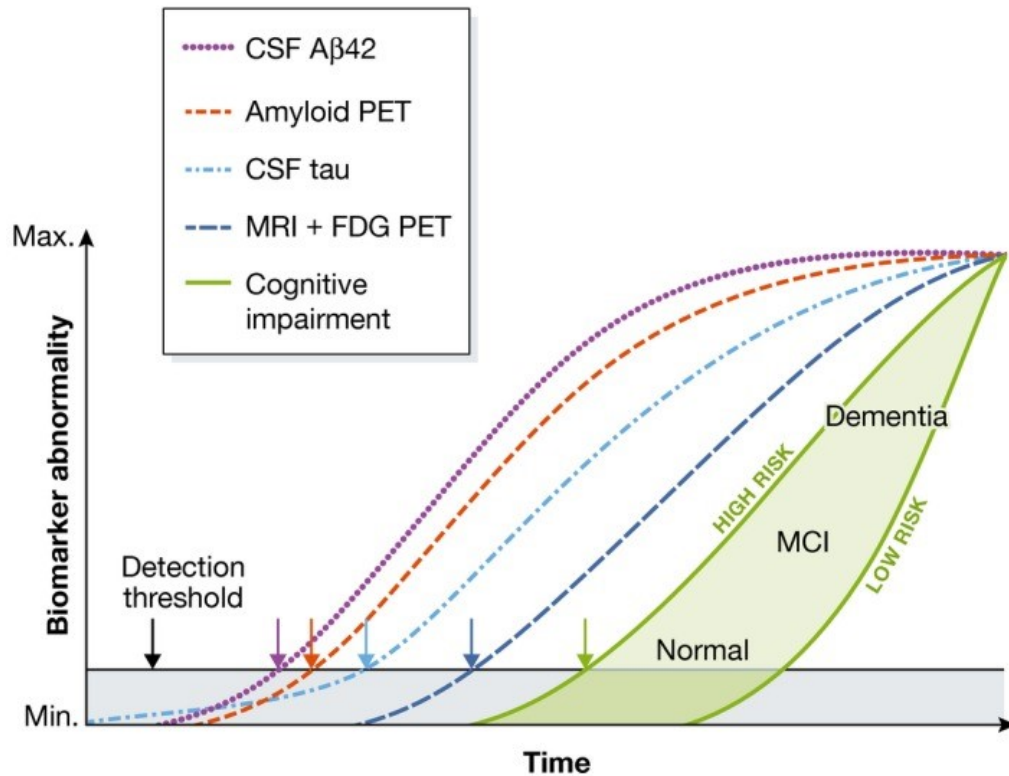


**Figure 2.** A hypothetical temporal model integrating Alzheimer’s disease biomarkers. The threshold for the first detection of biomarkers associated with pathophysiological changes is denoted by the black horizontal line. The gray area denotes the zone in which abnormal pathophysiological changes lie below this biomarker detection threshold. In this model, the occurrence of tau pathology can precede A $\beta$  deposition in time, but only early on at a sub-threshold biomarker detection level. A $\beta$  deposition occurs independently and rises above the biomarker detection threshold (purple and red arrows). This induces acceleration of tauopathy, and CSF tau then rises above the detection threshold (light blue arrow). Later still, changes in FDG PET and MRI (dark blue arrow) rise above the detection threshold. Finally, cognitive impairment becomes evident (green arrow), with a wide range of cognitive responses that depend on the individual’s risk profile (light green-filled area). Note that while CSF A $\beta_{42}$  alteration is plotted as a biomarker (purple), this represents a decrease in CSF A $\beta_{42}$  levels and is a surrogate for an increase in parenchymal A $\beta_{42}$  and changes in other A $\beta$  peptides in the brain tissue. MCI, mild cognitive impairment. (Selkoe *et al.*, 2016) [40].

## 2.4. Current treatment strategies

Even though AD has been studied over a century, there are currently only four commercially available drugs (Figure 3 and Figure 4), namely donepezil, rivastigmine, galantamine and memantine. Additionally, three of them share the same base mechanism of action [41].

Three of the abovementioned drugs (Figure 3: donepezil, rivastigmine and galantamine) target cholinergic neurotransmission as they inhibit AChE, enzyme responsible for degradation of neurotransmitter ACh, thus commonly known as acetylcholinesterase inhibitors (AChEIs). However, they differ in their pharmacological profile, which is taken into account in dose-determination and treatment strategies. All three AChEIs are relatively well tolerated with known dose-dependent and manageable adverse effects. AChEIs are used for treatment of mild to moderate cognitive impairment [41, 42]. Originally, there was a fourth commercially available AChEI – tacrine (Figure 3). However, later studies showed elevation of serum alanine aminotransferase (ALT) levels indicating hepatic toxicity of tacrine [43]. Therefore, the use of tacrine became limited and carefully monitored. Later on, production of commercially available tacrine ceased [10].

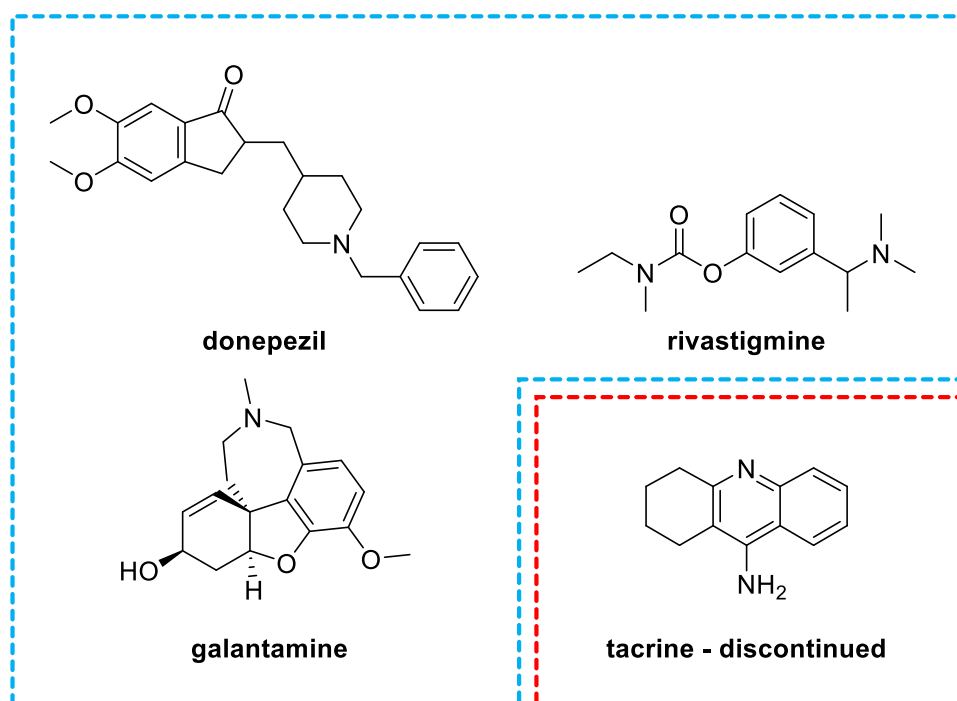
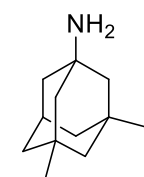


**Figure 3.** Clinically used cholinergic treatment for AD. Four AChEIs were originally available, while tacrine was discontinued due to its hepatotoxicity.

The last abovementioned clinically used drug is memantine (Figure 4). Memantine acts as *N*-methyl *D*-aspartate (NMDA) antagonist, hence targeting glutamatergic system. Glutamine is another neurotransmitter supposedly closely tied up to the AD pathology [41], however not yet discussed in context of mentioned hypotheses. Glutamine is a major excitatory neurotransmitter and it is involved in neuronal plasticity, therefore responsible for memory formation or learning processes. However in AD pathology, the A $\beta$ -induced over-stimulation of glutamatergic system leads to excitotoxicity, high intracellular calcium levels, and neuronal cell homeostasis misbalance eventually resulting in neuronal cell dysfunction [44, 45]. Memantine is used for treatment of

moderate to severe cognitive impairment. Memantine is well tolerated drug, with minimal adverse effects [41].



**memantine**

**Figure 4.** Clinically used NMDA antagonism treatment for AD - memantine.

Nevertheless, both AChEIs and memantine belong to symptomatic (or palliative) treatment strategies, hence not targeting the disease aetiology. Thus, there is still no effective disease modifying treatment available on the market.

There are numerous reported experimental strategies (both symptomatic and disease modifying approaches) for possible treatment of AD. Please see below adopted table from Anand *et al.* review for general picture to illustrate the complexity of AD pathology and high number of considered targets and strategies [10].

**Table 1.** Therapeutic strategies in Alzheimer’s disease treatment (Anand *et al.*, 2014) [10].

1. Modulating neurotransmission	4. Modulating intracellular signalling cascades
a. Cholinesterase inhibitors	5. Oxidative stress reduction
b. NMDA receptor antagonism	a. Exogenous antioxidant supplementation
c. GABAergic modulation	b. Augmenting endogenous defence
d. Serotonin receptor modulation	6. Mitochondrial targeted therapy
e. Histaminergic modulation	7. Modulation of cellular calcium homeostasis
f. Adenosine receptor modulation	8. Anti-inflammatory therapy
2. Tau based therapies	9. Others
a. Tau phosphorylation inhibition	a. Gonadotropin supplementation
b. Microtubule stabilization	b. Lipid modifiers - Statins
c. Blocking Tau oligomerization	c. Growth factor supplementation
d. Enhancing Tau degradation	d. Metal chelation
e. Tau based immunotherapy	e. Epigenetic modifiers
3. Amyloid based strategies	f. Caspase inhibitors
a. Secretase enzymes modulation	g. Nitric oxide synthase modulation
b. Amyloid transport	h. Nucleic acid drugs
c. Preventing amyloid aggregation	i. Multi-target directed ligands
d. Promoting amyloid clearance	
e. Amyloid based immunotherapy	



The provided list of approaches (Table 1) hardly covers all investigated strategies, however it highlights the most discussed ones. A $\beta$ -based strategies and especially investigation of  $\gamma$ -secretases modulation (protein complexes responsible for generation of A $\beta$  species, see chapter 2.6. for more details) received a great deal of attention over the last few years [46–48]. It was presumed that by the year 2014 one of the  $\gamma$ -secretases inhibitors might be approved for AD treatment. So it was an unexpected disappointment, when such potential drug candidates (in this case, semagacestat) failed to pass the clinical trials [49, 50].

## 2.5. AD and A $\beta$ supported by genetics

Base on the AD genetics research of past years, AD has been categorised into two distinctive forms - familiar AD (FAD) and sporadic AD (SAD). Furthermore, AD forms and also differs based on various age disease onset [6].

In most cases, FAD form is characterised by disease onset before 65 years, therefore also often referred to as early-onset AD (EOAD). It is estimated that about 50% people with FAD genetic predispositions develop FAD between the age of ~30-50 years [51]. Up to date, FAD has been associated with numerous mutations in three different genes [52]. All of them are associated with formation of A $\beta$ , which will be discussed later on. The manifestation of majority FAD cases are caused by mutations in presenilin 1 (30-70% of FAD) and presenilin 2 (less than 5% of FAD) genes located on chromosome 14 and 1, respectively [53–55]. The third contributing gene mutations responsible for FAD are located on chromosome 21, encoding amyloid precursor protein (APP) (16% of FAD) [55, 56]. However, FAD caused by autosomal dominant mutations in abovementioned three genes is quite rare, and it only accounts for about 1-6% of overall AD cases [57]. Even though FAD contributes to the overall AD cases marginally, FAD patients share a very similar pathological profile. Therefore, the study of early-onset mutations provides valuable genetic based profile as a convenient and useful tool for deeper understanding of AD pathogenesis [48].

The rest of AD cases (more than 90%) are accounted for SAD. Due to the usual late-onset of the disease, SAD is also referred to as late-onset AD (LOAD). Currently the only established genetic risk contributing to SAD is gene polymorphism encoding apolipoprotein E (ApoE) located on chromosome 19 [58]. ApoE is responsible for lipid transports and it has been associated with cardiovascular, neurodegenerative and infectious diseases [59]. ApoE gene occurs in three type of alleles ( $\epsilon$ 2,  $\epsilon$ 3,  $\epsilon$ 4) encoding three different ApoE isoforms (ApoE2, ApoE3, ApoE4), where most common isoform in general population is ApoE3 with prevalence 77-78% [60, 61]. ApoE2 is found in 7-8% of population and it is associated with type III hyperlipoproteinaemia, where ApoE4 is found in 14-15% of population with association to AD, Lewy body disease and frontal lobe dementia [60, 62]. Allele  $\epsilon$ 4 of ApoE gene has been recognised to have major causative risk factor

for development of SAD, where contributing risk of homozygotes is five times higher compared to heterozygotes [63, 64]. Whereas ApoE2 and ApoE3 showed to promote proteolytic degradation and clearance of A $\beta$ , ApoE4 isoform displayed lowered A $\beta$  proteolytic activity and also enhanced A $\beta$  fibril formation [65, 66].

The overall described genetic factors showed their association with A $\beta$  pathways thus supporting the idea of amyloid cascade hypothesis. However, more genetic predisposing factors may yet to be discovered. Heterogeneous nature of the disease funds intensive research focused on susceptibility gene polymorphism for LOAD and characterization of novel AD genes, which points to several loci on various chromosomes, however the precise genes haven't been identified yet [67, 68].

## 2.6. Formation of A $\beta$ species

All A $\beta$  species are products of proteolytic cleavage of APP, which is a ubiquitous protein with its gene located on chromosome 21 [69]. Even though the physiological function of APP is not yet completely understood, much more focus is drawn to its pathophysiological turnover in development of AD demonstrated by enormous amount of scientific debate to its regard. APP is a single-passing transmembrane glycoprotein with large extracellular domain, whose alternate APP gene splicing can produce up to 8 APP's isoforms [70]. The most commonly occurring isoforms are the 695 amino acid form (mainly expressed in CNS) along with the 751 and 770 amino acid forms (with more ubiquitous expression) [71]. This protein undergoes two different pathways of proteolytic processing (Figure 5), which are often mentioned as (non)amyloidogenic or  $\alpha$ - and  $\beta$ -pathway (based on their cleavage proteins). The first proteolytic step includes cleavage of APP extracellular domain with either  $\alpha$ - or  $\beta$ -secretases releasing soluble sAPP $\alpha$  or sAPP $\beta$  fragments, respectively. Proteolytic  $\beta$ -secretases are also well known as  $\beta$ -site APP cleaving enzymes and abbreviated as BACE. Second proteolytic cleavage of remaining transmembrane fragment is controlled with  $\gamma$ -secretases, where cleavage of C83 or C99 transmembrane APP fragment produces either non-pathogenic p3 peptide or cytotoxic A $\beta$  for either  $\alpha$ -pathway or  $\beta$ -pathway, respectively [72]. Therefore, the distinguishing step of (non)amyloidogenic pathway lies in different APP cleavage site of  $\alpha$ -secretases and  $\beta$ -secretases. The  $\alpha$ -secretases are responsible for physiologic cleavage, which occurs in A $\beta$  domain region of APP, thus consequently producing non-amyloidogenic APP fragments. On the other hand, the  $\beta$ -secretases cleavage with subsequent  $\gamma$ -secretases cleavage releases amyloidogenic fragments [52]. BACE-1, a  $\beta$ -secretase associated with cleavage of APP, is a well-characterised protease [71]. However, the identification of  $\gamma$ -secretases, proteases responsible for cleavage of APP, struggled [73]. Presenilins (presenilin 1, presenilin 2) are proteins primarily expressed in neurones. Both presenilins were formerly associated with  $\gamma$ -secretases as they may have been either  $\gamma$ -secretases or more likely presenilins

form a complex as subunits of  $\gamma$ -secretase regulating its proteolytic activity [73]. For example, presenilins knockout animal experiments displayed complete disappearance of  $\gamma$ -secretase activity. Still, enzymatic protease activity hasn't been directly associated with presenilins themselves [73]. Later on as other parts of presumed protein complex became recognised and associated with  $\gamma$ -secretase activity, presenilins were confirmed to form a multi-protein complex along with additional three proteins – nicastrin, presenilin enhancer 2 and anterior pharynx defective 1 [48]. Such  $\gamma$ -secretase multi-protein complex with enzymatic protease activity is responsible for intramembranous cleavage of remaining APP segment. In fact, two  $\gamma$ -secretase cleavages occur. The  $\epsilon$ -cleavage releases intracellular APP domain (AICD), whereas the  $\gamma$ -cleavage releases extracellular APP domain, i.e. p3 protein or A $\beta$  protein for non-amyloidogenic or amyloidogenic pathway, respectively [48, 72]. Such A $\beta$  protein can form extracellular depositions or cause cytotoxic effects.

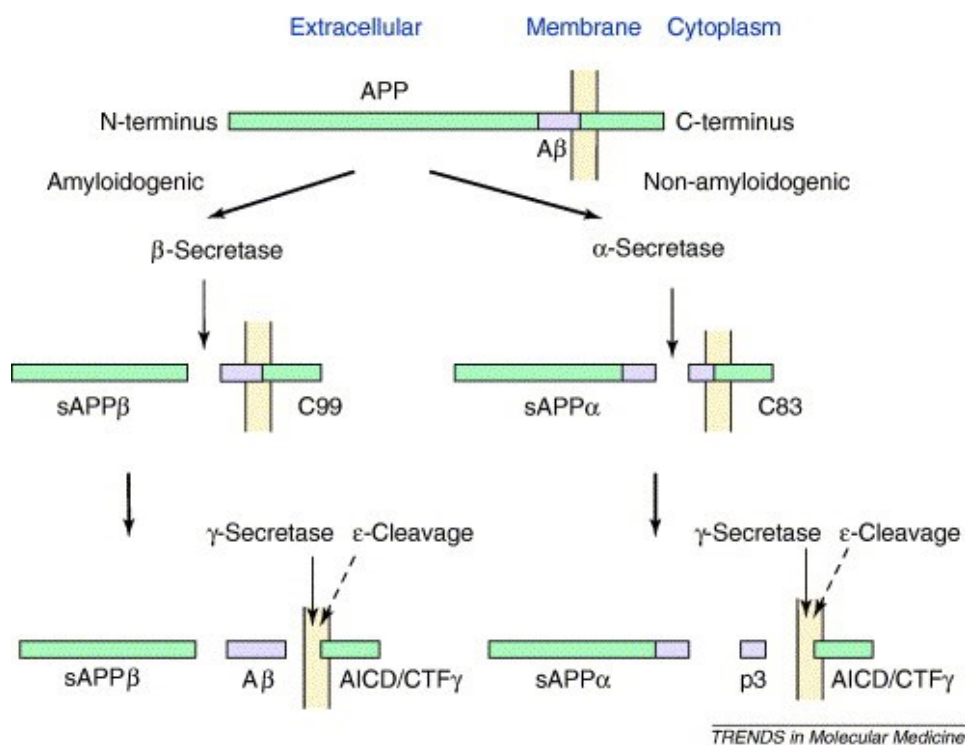


**Figure 5.** Amyloidogenic (left) and non-amyloidogenic (right) proteolytic processing pathways of APP (Vardy *et al.*, 2005) [72].

Products of amyloidogenic cleavage of APP are generally hydrophobic A $\beta$  peptides constituting of 37-43 amino acids. They tend to aggregate in various lengths, sizes or manners after their cleavage and release from APP [74, 75]. The overall pool of A $\beta$  species comprises from A $\beta$  of various lengths, where most common species are peptides having 38 (A $\beta_{38}$ , A $\beta_{1-38}$ ), 40 (A $\beta_{40}$ , A $\beta_{1-40}$ ) and 42 (A $\beta_{42}$ , A $\beta_{1-42}$ ) amino acid residues, with their pool representation of 16%, 50% and 10%, respectively (values refer to CSF levels of A $\beta$  species) [76].

## 2.7. A $\beta$ deposition

After the final transmembrane cleavage of APP, A $\beta$  species are released as the soluble peptides. Since some of the A $\beta$  species (e.g. A $\beta$  with 16 or 17 residues) are present under physiological conditions, there are several physiological pathways regulating the clearance of formed A $\beta$  peptides [36, 77]. However, these mechanisms gradually fail to clear other A $\beta$  species formed in amyloidogenic pathways resulting in steady built-up of amyloidogenic A $\beta$  levels. Changes in A $\beta$  metabolism involves increased A $\beta$  production, deviations in A $\beta$  species ratios or impaired clearance and degradation of A $\beta$  species [74]. While A $\beta_{40}$  is the most abundant peptide, A $\beta_{42}$  is more hydrophobic and it tends to aggregate, thus more readily forms amyloid plaques and concomitantly becoming more neurotoxic than other A $\beta$  species. Therefore, insoluble amyloid plaques are predominantly formed of A $\beta_{42}$  species [35, 36, 74]. Monomers of A $\beta$  aggregates in  $\beta$ -sheet structure forming complex structures. Extracellular insoluble A $\beta$  deposits are gradually building up through various assembly stages: low molecular weight oligomers, assemblies, protofibrils, fibrils, diffusible and deposited plaques (Figure 6) [74, 78, 79]. As SP were the firstly identified, they became one of the most discussed and followed hallmarks of AD progression. Though, low molecular weight oligomeric A $\beta$  forms have started to draw much more attention as they were found to be possibly one of the most pathological ones responsible for impairment of synaptic functions, consequently undesirably affecting learning and memory processes [80, 81].

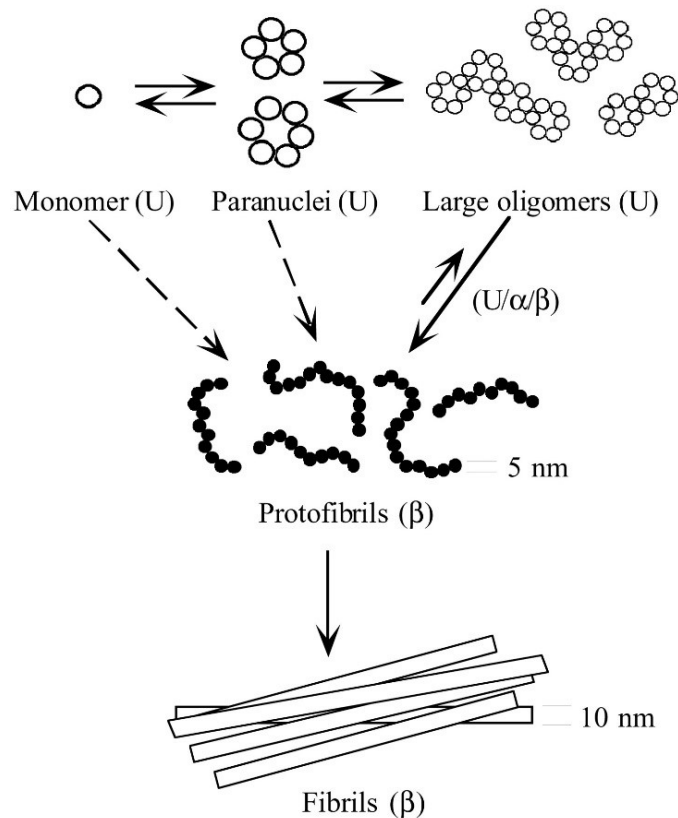


**Figure 6.** Assembly scheme of various A $\beta$  protein species (Bitan *et al.*, 2003) [36].

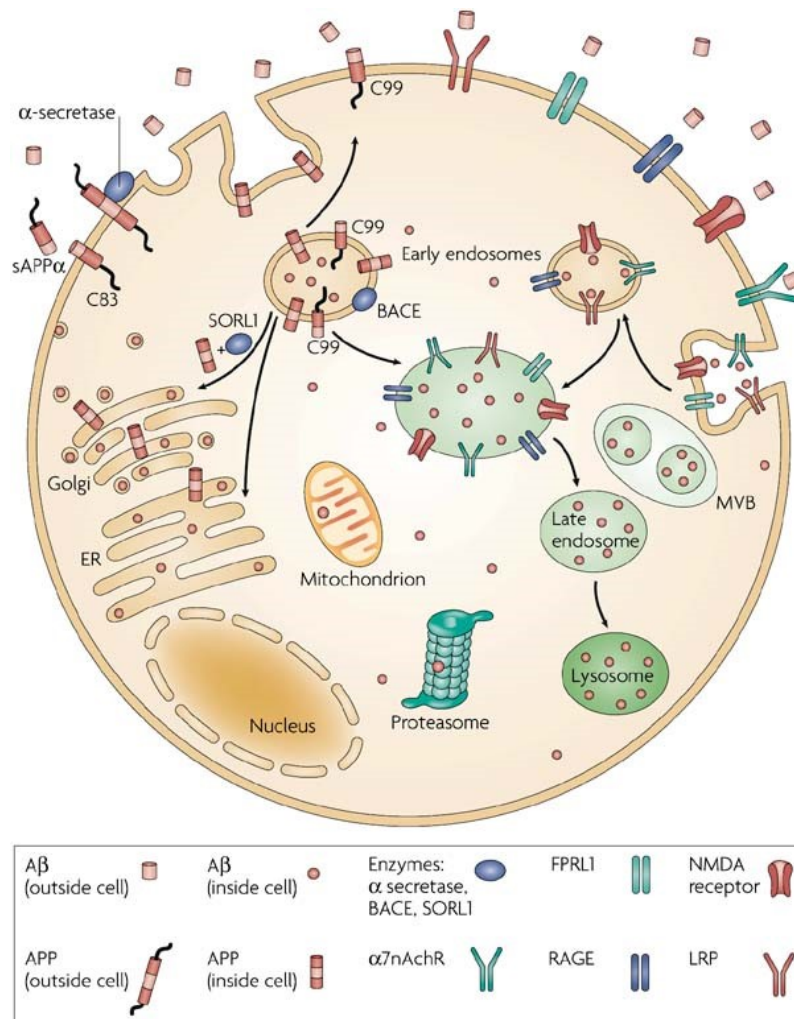
Furthermore, the level ratios of the most amyloidogenic species ( $A\beta_{42}/A\beta_{40}$ ) are frequently used as biomarkers for interpretation of  $A\beta$ -induced pathophysiological events. For example, increased  $A\beta_{42}/A\beta_{40}$  ratio was correlated with FAD forms [82] or changes in CSF levels of  $A\beta_{42}/A\beta_{40}$  were associated with depositions of  $A\beta$  in brain tissue [83].

## 2.8. Intracellular $A\beta$

It has passed a long time since the discovery of extracellular SP in the beginning of twentieth century. Later on, the general concept of classical amyloid cascade hypothesis was established on extracellular  $A\beta$  deposition being responsible for triggering pathophysiological cascade leading to overall neuronal dysfunction [32, 33]. However since the  $A\beta$  identification being a key component of SP, classical amyloid cascade hypothesis started to be repeatedly questioned as new reports of possible presence of intracellular  $A\beta$  started to emerge [84]. It was shown that most of the intracellular produced  $A\beta$  is  $A\beta_{42}$  in contrast to  $A\beta_{40}$  [85]. Furthermore, both presynaptic and postsynaptic multivesicular bodies (endosomal cellular compartments) were identified as intracellular sites of  $A\beta_{42}$  build-up. Thus, such intracellular  $A\beta_{42}$  has been associated with neuronal impairment [86]. Over the time, numerous reports confirmed the existence of intracellular  $A\beta$  and two possible ways were suggested to explain the presence of intracellular  $A\beta$  – intracellular  $A\beta$  production and extracellular  $A\beta$  cell reuptake (Figure 7) [87].

Firstly,  $A\beta$  could be produced in cells and not secreted. Production of  $A\beta$  by cleavage of APP is known to be localised in cell plasma membrane. However, localisation of APP is not exclusive to cell plasma membrane. It is also localised in membrane of intracellular compartments (such as endoplasmic reticulum, trans-Golgi network, mitochondria, lysosomes, endosomes or nucleus) [88]. So in order to reach extracellular space,  $A\beta$  could be produced by cleavage of APP localised either on cell plasma membrane or on membrane cell secretory pathway compartments. However, when APP cleavage occurs in other cell compartments (e.g. mitochondrial membrane), intracellular  $A\beta$  is produced and deposited within the cell [84, 87, 89].

Besides the plasma membrane and intracellular  $A\beta$  production, it is assumed that extracellular  $A\beta$  could be taken up back to cell's intracellular cytosol. It is known that  $A\beta$  is able to bind with a vast number of biomolecules (such lipids, proteins, etc.). Thus, focus was centred on the identification of possible transports and options facilitating  $A\beta$  reuptake to the cells. For example, *N*-methyl-D-aspartate (NMDA), formyl peptide receptor-like 1 (FPRL1),  $\alpha 7$  nicotinic acetylcholine receptor ( $\alpha 7nAChR$ ), scavenger receptor for advanced glycation end products (RAGE) or ApoE belong among the few identified  $A\beta$  re-uptake transporters/facilitators (Figure 7) [84, 87]. Thus, such targets have shown great deal of interest for their possible pharmacological modulation. For example,  $A\beta$  cell reuptake was shown to be enhanced by integrin antagonists and blocked by NMDA receptor antagonists [90].



Nature Reviews | Neuroscience

**Figure 7.** Possible sites of cellular Aβ production. (a) Intracellular APP cleavage located on cellular compartments such as Golgi network, endoplasmic reticulum or endosomes. (b) Extracellular Aβ reuptake by transporters/facilitators (LaFerla *et al.*, 2007) [87].

As the evidence of intracellular Aβ have been numerously reported, more studies described the pathophysiological consequences of intracellular Aβ occurrence, such as proteasome dysfunction, hyperphosphorylation of tau protein, mitochondria function impairment, disturbance in intracellular calcium levels and overall cell homeostasis disbalance [86, 87].

## 2.9. Mitochondrial Aβ

Mitochondria are key cell organelles, responsible for generation and level maintenance of high-energy compounds, calcium homeostasis or regulation of cell death. Therefore, mitochondria play vital role in overall cell survivability. Mitochondria also maintain their pools of reactive oxygen species (ROS), for example due to the presence of electron transport chain and transfer of electrons within the organelle. Consequently, impairment of normal mitochondrial processes can

cause not only severe mitochondrial dysfunction, but also overall cell damage. Furthermore, it has been reported that mitochondrial functions have been negatively affected throughout aging and by numerous neurodegeneration diseases [91, 92].

### **2.9.1. Implications of A $\beta$ presence in mitochondria**

The existence, role and pathophysiological effects of A $\beta$  in mitochondria have been reported many times, yet not fully understood. To demonstrate possible sites of A $\beta$ -induced mitochondrial dysfunction, A $\beta$  was described to (list based on the review Tillement *et al.*, 2011) [93]:

- disturb membrane properties
- disturb calcium homeostasis
- affect oxidative phosphorylation
- influence ROS production
- induce apoptosis
- enhance mitochondrial vulnerability to other toxics (tau protein toxicity, nitric oxide production, cytokine production and neuroinflammation)
- affect other mitochondrial functions (disturb organelle dynamics, effect mitochondrial DNA and RNA)

### **2.9.2. A $\beta$ entry points to mitochondria**

Similar to existence of intracellular A $\beta$  (see chapter 2.8), there may be two possible ways to explain the presence of mitochondrial A $\beta$  – either direct A $\beta$  transport into the mitochondria or localised A $\beta$  production. There are several reports confirming and explaining A $\beta$  presence in mitochondrial space, still the complete understanding of processes remains unclear [89].

To facilitate import of proteins, mitochondria possess translocase system, which includes translocase of the outer membrane (TOM) and translocase of inner the membrane (TIM). A $\beta$  has been shown to take advantage of this mitochondrial transport system and it can be imported via the TOM complexes (TOM20, TOM40 and TOM70) into the mitochondria [94]. In addition, A $\beta$  precursor (APP) is able to interact and bind with both TIM and TOM complexes. Then, APP restrained in translocase complex is cleaved by Omi protease localised in mitochondrial inter membrane space (IMS). The rest of APP processing is controlled by secretases localised in mitochondrial membranes resulting in release of A $\beta$  to mitochondrial space [95, 96]. On the other hand, APP can also be held in the TOM/TIM complexes, thus causing an impairment of physiological protein trafficking within mitochondria [89]. Further possible entry point of A $\beta$  into the mitochondria is via mitochondria-associated membranes (MAMs). These MAMs are close contact points, which are used for direct transport between mitochondria and another cellular compartment. Hence, MAMs of endoplasmic reticulum (ER) are close contact points between ER

and mitochondria responsible for transport of e.g. fatty acids, cholesterol, glucose metabolites [97]. Moreover, several studies showed altered MAM functions or enriched regions with both presenilins having increased  $\gamma$ -secretase activity [89, 96].

### 2.9.3. Mitochondrial proteins interacting with A $\beta$

Formed A $\beta$  species were described to interact with a vast number of biological targets. As the localisation of A $\beta$  in mitochondria was reported, studies showing the cytotoxic implications of mitochondrial A $\beta$  has started to emerge [93]. More than twenty proteins have been identified to interact with A $\beta$ , while five of them present evidence with potential to be a viable drug target [89, 96, 98]. Selected enzymes below belong among the most therapeutically promising drug targets:

- Amyloid  $\beta$ -binding alcohol dehydrogenase (ABAD)
- Cyclophilin D (CypD)
- $\gamma$ -secretase
- Glyceraldehyde-3-phosphate dehydrogenase (GAPDH)
- Insulin-degrading enzyme (IDE)

For more comprehensive list and additional information about mitochondrial proteins interacting with A $\beta$ , please see Benek *et al.*, Table 16) [98].

## 2.10. Amyloid $\beta$ -binding alcohol dehydrogenase

In 1997, ABAD has been identified by Yan *et al.*, however that day referred to as ER-associated amyloid-binding protein (ERAB) [99]. Same year, Furuta *et al.* reported cloning and expression of cDNA for a newly identified isozyme of bovine liver 3-hydroxyacyl-CoA dehydrogenase and its import into mitochondria [100]. In the beginning of next year, He *et al.* identified a human brain L-3-hydroxyacyl-CoA dehydrogenase [101], which was identical to an A $\beta$  binding protein involved in AD [99].

Over the years of studying ABAD, ABAD has become a protein of many names due to its identification, localisation and substrate specificity. Other possible names for ABAD protein were summarised in Table 2. As functions and properties of ABAD are described in following chapters, all alternative names will become more clear and rational. Nevertheless, presented work holds its relation to AD and A $\beta$ , thus protein will be mostly addressed as ABAD outside the introduction section (if not stated otherwise).

As pointed out before, ABAD was initially thought to be localised in ER (therefore named as ERAB) [99], however later several studies confirmed localisation of ABAD within the mitochondria [102–104]. Moreover, ABAD (as 17 $\beta$ -hydroxysteroid dehydrogenase type 10) mitochondrial localisation is distinct in comparison with other 17 $\beta$ -hydroxysteroid dehydrogenases



(more than ten different types were already reported). ABAD is constitutively expressed in liver, brain, gonads and other tissues [104].

**Table 2.** Chronological list of ABAD alternative names (Yang *et al.*, 2005) [105].

Year	Name	Acronym	Ref.
1995	Short-chain 3-hydroxy-2-methylacyl-CoA dehydrogenase	SC-HMAD	[106]
1996	3-Hydroxyacyl-CoA dehydrogenase type II	HADH II	[107]
1997	ER-associated amyloid-binding protein	ERAB	[99]
1998	Short chain L-3-hydroxyacyl-CoA dehydrogenase	SCHAD	[101]
1999	Amyloid $\beta$ -binding alcohol dehydrogenase	ABAD	[108]
2001	17 $\beta$ -hydroxysteroid dehydrogenase type 10	17 $\beta$ -HSD10	[104]
2003	2-Methyl-3-hydroxybutyryl-CoA dehydrogenase	MHBD	[109]

### 2.10.1. Structure and catalysis of ABAD

Enzyme ABAD is encoded by SCHAD gene, which consists of six exons and five introns. It is localised on chromosome X [101]. In general, second copy of chromosome X is subjected to inactivation process. However, SCHAD gene belongs to cluster, which is not affected by inactivation process. Therefore, females have two active SCHAD gene forms in comparison with males [105, 110].

The crystal structure of ABAD was reported several times. It includes crystal structures bound with co-factor and substrates [111], A $\beta$  [112] or ABAD inhibitor [113]. ABAD is a homotetrameric protein with molecular mass about 108 kDa (27 kDa per unit). Protein structure includes Rossmann fold dinucleotide-binding motif, an evolutionary common motif among dehydrogenases [114]. The residues of the catalytic triad (Ser155, Tyr168 and Lys172) form a core of enzyme active site. They are highly conserved and characteristic for short-chain dehydrogenase/reductase (SDR) family [111]. Powell *et al.* proposed the mechanism of reduction via hydride transfer based on the shared SDR catalysis principles (Figure 8) [115]. Stabilised formation of proposed proton donor Tyr168 in catalysis is achieved by following H-bond formations. Firstly, suggested proton donor Tyr168 is stabilised in position with 3'-hydroxyl group of ribose. Secondly, protonated Lys172 residue is thought to decrease pKa of hydroxyl group of Tyr168. Thirdly, another H-bond contact is formed with Ser155, which is suggested to share proton with Tyr168 after catalysis completion. Such stabilised Tyr168 allows the activation of substrate carbonyl group (3-oxobutyrate) via its hydroxyl

proton. Then, hydride of NADH co-factor is transferred to carbon of activated carbonyl group followed by proton transfer from Tyr168 [111].

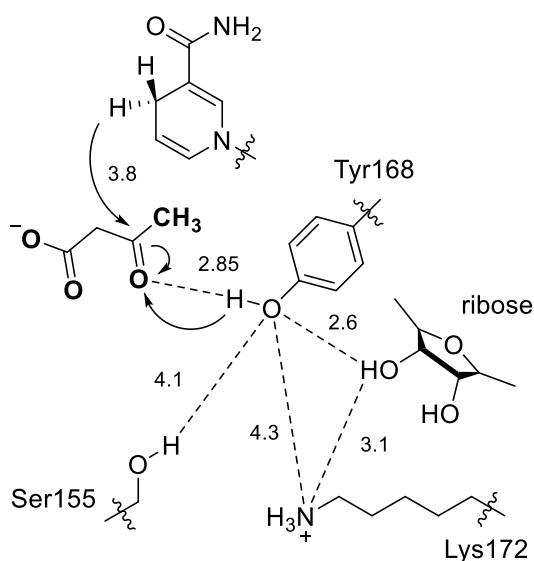


**Figure 8.** Schematic diagram showing the proposed reaction mechanism of reduction of 3-oxobutyrates by ABAD (adopted from Powell *et al.*, 2000) [111].

Structural comparison with other members of SDR includes two distinct insertions in ABAD protein sequence. First insertion is at residues 100–110 and second insertion is at 140–150 residues. While the first insertion forms a short  $\beta$ -hairpin structure and extends the enzyme surface on one side of the substrate-binding cleft, the second insertion does not lie near the active site. Both insertions were suggested to support the binding of coenzyme A (CoA) substrates as CoA substrates were found to be more readily processed by ABAD enzyme. Such hypothesis is supported by knowledge that phosphate groups negative charges of CoA substrates interact with positive charges of 100-110 residues (Lys99, His102, Lys104 and Lys105) [111, 113]. More importantly, first insertion was found to be responsible for interaction with A $\beta$  [112].

### 2.10.2. Enzymatic function of ABAD

As mentioned above, ABAD belongs to SDR family and this enzyme utilizes NAD<sup>+</sup>/NADH co-factors for its enzymatic function. Its function is to catalyse oxidation of alcohols and reduction of aldehydes or ketones to their corresponding products (Figure 9).

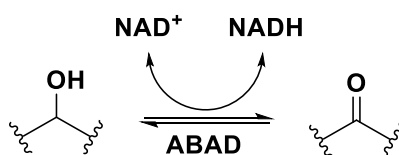


**Figure 9.** Oxidation and reduction of alcohols and aldehydes/ketones by ABAD (Muirhead *et al.*, 2010) [89].

Enzyme ABAD is a quite promiscuous with low specificity towards its substrates. Therefore, ABAD is able to catalyse oxido-reductive reactions for wide range of substrates. For example, ABAD is able to catalyse oxidation or reduction reactions for following substrates:

- acyl-CoA derivatives (e.g. acetoacetyl-CoA,  $\beta$ -hydroxybutyryl-CoA, 2-methyl-3-hydroxybutyryl-CoA, 3-oxooctanoyl-CoA) [101, 108, 116]
- simple alcohols (e.g. ethanol, 2-propanol, *n*-propanol, *n*-butanol, octanol, *n*-decanol) [108, 116]
- steroids (e.g. 17 $\beta$ -estradiol, androsterone, 5 $\alpha$ -dihydrotestosterone, progesterone, cortisone) [102, 108, 116]

Suffice to say, reported substrates turnover rates quite differ, even for same substrates (possible due to different assay conditions). Moreover, reported ABAD ability to catalase particular reaction *in vitro* does not have to correlate with its *in vivo* function. So under physiological conditions, ABAD itself does not have to necessary catalyse wide range of reactions, however its promiscuity might be related to some of the protein's pathophysiological turn-overs [89].

### 2.10.3. Physiological function of ABAD

Several physiological function of ABAD were reported. It is responsible for isoleucine degradation and short branched-chain fatty acid  $\beta$ -oxidation process. It also catalyses oxidation step of 2-methyl-3-hydroxybutyryl-CoA [106]. Point mutations in SCHAD gene responsible for ABAD/MHBD deficiency can result in mild to progressive neurodegenerative symptoms [117, 118]. Metabolism of steroids is also secured by ABAD. It takes part in sex steroid hormone metabolism, such as oxidation of 17 $\beta$ -estradiol, generation of 5 $\alpha$ -dihydrotestosterone or participation in androgens synthesis. Furthermore, ABAD is suggested to play a role in neuroactive steroid metabolism including oxidative 3 $\alpha$ -HSD activity or neurosteroidogenesis [105]. It is also one the components of mitochondrial RNase P, which is a tRNA processing enzyme. Thus, ABAD assists in protein synthesis [119]. More recently, another function of ABAD has been described, where cardiolipin is oxidised by ABAD [120].

### 2.10.4. Interaction of A $\beta$ and ABAD

In 1997, Yan *et al.* presented data for a yeast two-hybrid screen, which allowed identifying molecules binding to A $\beta$ . Four clones were identified and all of them shared the same cDNA sequence leading to identification of ABAD as protein binding with A $\beta$  [99]. Later on, more studies confirmed the A $\beta$ -ABAD interaction with various techniques such as nuclear magnetic resonance (NMR), surface plasmon resonance, immunoprecipitation or crystallography [112, 121, 122].

It was demonstrated, that A $\beta$  is able to bind to ABAD within low nanomolar range of  $K_D$ . Both A $\beta_{40}$  and A $\beta_{42}$  showed affinity towards the ABAD [99]. Also, both A $\beta_{40}$  and A $\beta_{42}$  were able to inhibit ABAD enzymatic function within low micromolar  $K_i$  (e.g.  $K_i$  1.6  $\mu$ M for S-acetoacetyl-CoA, 3.2  $\mu$ M for 17 $\beta$ -estradiol and 2.6  $\mu$ M for (2)-2-octanol) [108]. Interestingly, the binding of A $\beta$  to ABAD is observed within nanomolar range, however the inhibition of ABAD function within micromolar range. Therefore, it can be assumed, that A $\beta$  monomers can bind to ABAD, however not sufficiently to inhibit enzymatic function. Higher concentration levels might promote further A $\beta$  aggregation, which can then hinder the enzyme activity [89].

Studies of related A $\beta$  species showed that ABAD binds to A $\beta_{1-40}$  and A $\beta_{1-20}$ , however not A $\beta_{25-35}$  suggesting approximate residues necessary for A $\beta$ -ABAD interaction. Two years later, Oppermann *et al.* narrowed down the optimal sequence for A $\beta$  binding to ABAD to residues 12-24. Remarkably, area necessary for A $\beta$  aggregation and fibril formation is 16-20, where overlapping area 13-22 is crucial for both A $\beta$  aggregation and A $\beta$ -ABAD interaction [103].

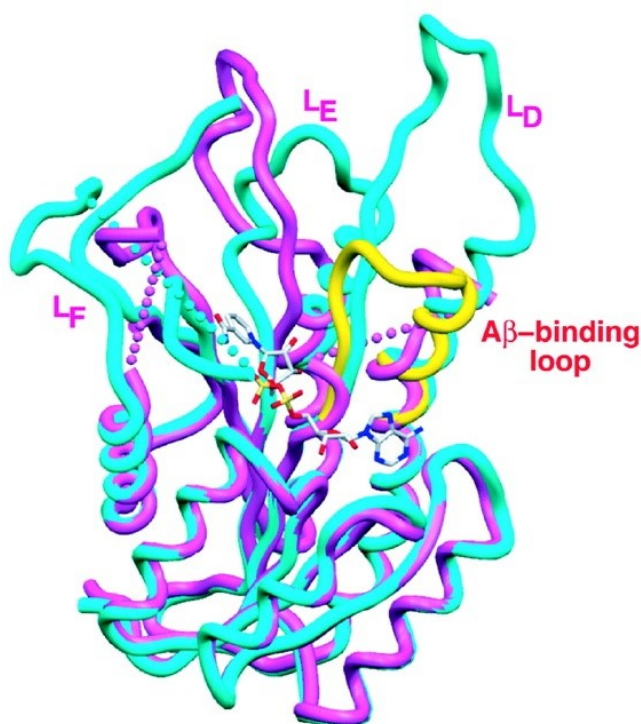


**Figure 10.** Superposition of A $\beta$ -bound human ABAD (pink) and rat ABAD in complex with NAD (blue). The L<sub>D</sub> loop of 3 $\alpha$ -hydroxysteroid dehydrogenase (3 $\alpha$ -HSD) (PDB code 1FJH) is shown in yellow. NAD is shown as a stick model with gray for carbon atoms, red for oxygen atoms, blue for nitrogen atoms, and yellow for phosphate atoms. The proposed A $\beta$ -binding loop is indicated (adopted from Lustbader *et al.*, 2004) [112].

Initial crystallography study of ABAD's A $\beta$ -binding site showed that NAD<sup>+</sup> was not bound to ABAD. Therefore, it was proposed that A $\beta$  prevents co-factor binding to ABAD, suggesting

possible mechanism of ABAD inhibition. The crystal structure of ABAD with A $\beta$  had certain degree of distortion of co-factor binding pocket, catalytic triad pocket and also so-called Loop D (residue 100-110) [112]. Binding studies with A $\beta$  and glutathione *S*-transferase–ABAD truncation mutants and site-directed mutagenesis within and beyond the disordered Loop D (residues 95-113) identified two regions (residue 98-101 and 108-110), which were important for A $\beta$  binding to ABAD [112]. It is worth reminding (chapter 2.10.1, last paragraph), that Loop D is unique to ABAD among other members of SDR family, therefore A $\beta$  binding properties seems to be unique to ABAD [111].

#### **2.10.5. Consequences of A $\beta$ and ABAD interaction**

The molecular basis of A $\beta$  interaction with ABAD was described earlier. However, consequences and precise A $\beta$ -ABAD mediated toxicity has not been fully understood. Still, there are several reported insights shedding light onto A $\beta$ -ABAD mediated pathophysiological outcomes. Currently reported A $\beta$ -mediated mitochondrial cytotoxic effects are displayed in Figure 11, which also includes other consequences of mitochondrial A $\beta$  (such as mitochondrial transport disturbance, interaction with other proteins, effects on other cellular targets) [123].

It was demonstrated that A $\beta$  binds to ABAD in much lower concentration range (nanomolar) than the actual inhibition of ABAD function occurs (micromolar). In addition, A $\beta$  exerted cytotoxicity in cell cultures already within A $\beta$  binding concentration levels. On the other hand, cell cultures expressing catalytically inactive ABAD mutant with A $\beta$  presence did not show enhanced cytotoxicity [108]. Cytotoxic effects such as DNA fragmentation and cell apoptosis were reported for cell cultures expressing both A $\beta$  and ABAD. Similar to previous findings, such cytotoxic effects were not observed with inactive ABAD mutant [99, 108]. Surprisingly, both wild type and mutant form of ABAD shared similar binding affinity ( $K_D$  of 64.5 nM and 38.9 nM, respectively). It can be assumed, that inhibition of ABAD does not contribute to A $\beta$ -mediated cytotoxicity, but A $\beta$  rather triggers cytotoxic effects via binding to catalytically active ABAD, which promotes other pathophysiological cascade. This hypothesis also suggests that A $\beta$ -mediated cytotoxicity is caused in combination with catalytically active ABAD [89].

Elevated levels of ROS, lipid peroxidation end products and increased oxidative stress were associated with neurodegenerative diseases. In particular, increased levels of 4-hydroxynonenal (HNE) and malondialdehyde (MDA) were found in AD models [124]. Assuming that ABAD could be responsible for detoxification of oxidative stress products, Murakami *et al.* demonstrated, that ABAD can have cytoprotective role against reactive aldehydes such as HNE and MDA. Therefore, A $\beta$ -impaired ABAD function can result in increased levels of ROS [125].

Other hypothesis assumes that A $\beta$ -ABAD interaction negatively effects metabolism of steroid molecules. Increased levels of ABAD expression along with abundance of ABAD were found in

hippocampus of mouse AD models. Hence, it can be presumed that decreased levels of 17 $\beta$ -estradiol may contribute to neuronal and synaptic loss with impairment of hippocampal-dependent learning and memory [126].

Furthermore, changes in expression levels of two proteins were described due to A $\beta$ -ABAD interaction, peroxiredoxin-2 (Prdx-2) and endophilin-1 (Ep-1). First protein (Prdx-2) is protein possessing antioxidative properties. Thus, its upregulation can indicate increased oxidative stress [127], supporting previous findings [124]. Second protein (Ep-1) was associated with several neurodegenerative diseases (e.g. AD, Parkinson disease or Huntington disease). Increased levels of Ep-1 were correlated with elevated activity of stress kinase c-Jun *N*-terminal kinase (JNK), which starts signalling cascade leading up to the neuronal cell death [128, 129].

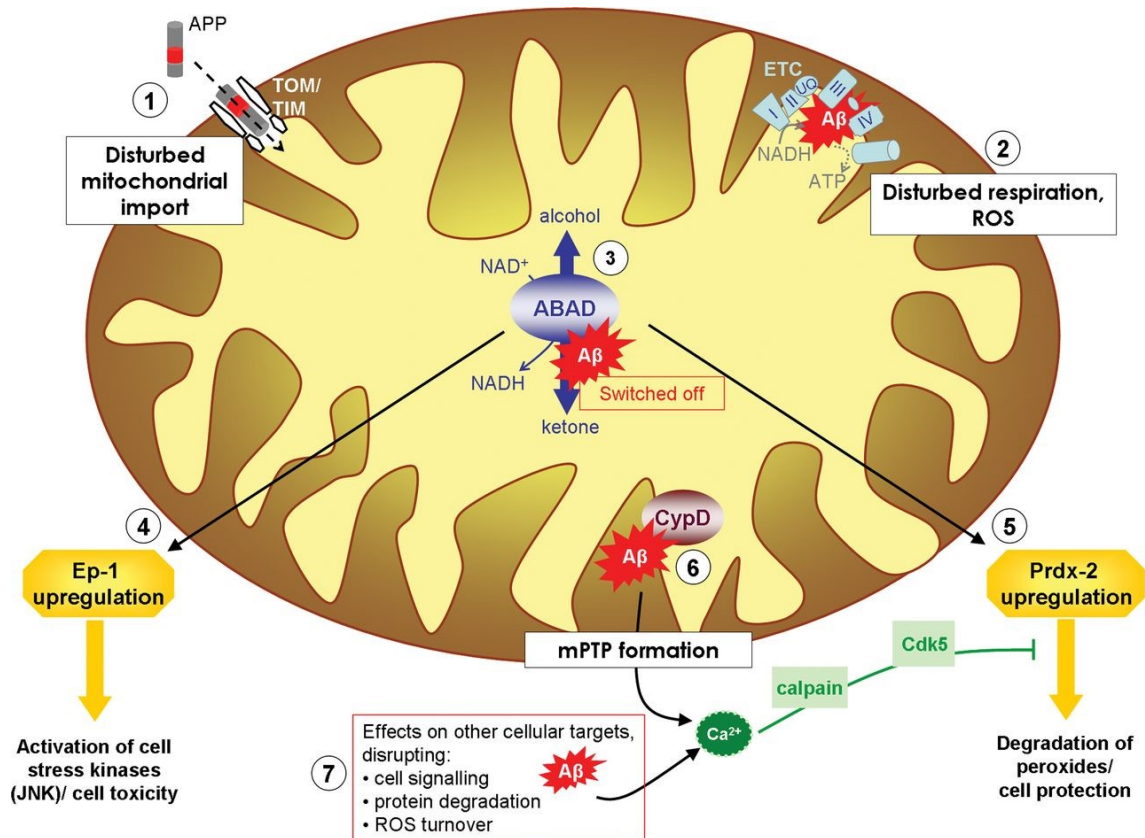


**Figure 11.** Consequences of mitochondrial A $\beta$ : APP can be transported to mitochondria, where it interacts with TOM and TIM, disturbing mitochondrial protein import (1). A $\beta$  can be imported into mitochondria via TIM and TOM and is found associated with the inner mitochondrial membrane, disrupting mitochondrial respiration and leading to an excess production of ROS (2). A $\beta$  has been found to interact with ABAD in the mitochondrial matrix, inhibiting enzyme activity (3). The A $\beta$ -ABAD interaction also leads to an up-regulation of AD biomarkers Ep-1 (4) and Prdx-2 (5). At the inner mitochondrial membrane, A $\beta$  can interact with CypD, which is involved in the formation of mPTP and Ca<sup>2+</sup>-release from mitochondria (6). A $\beta$  can be found in the cytosol, disturbing cell signalling, protein degradation and causing ROS production, which leads to an increase in cytosolic Ca<sup>2+</sup> (7). Ca<sup>2+</sup>-mediated Cdk5 activation has been found to inhibit Prdx-2's antioxidant function (Borger *et al.*, 2011) [123].

### 2.10.6. ABAD – a potential drug target

In chapter 2.10.4, interaction between A $\beta$  and ABAD was described. Loop D region was identified as A $\beta$ -ABAD binding site with X-ray crystallography [112]. Milton *et al.* used a different approach utilizing antisense DNA strand technique. Analysis of the ABAD antisense amino acid sequence identified ABAD residues 99-108 to be responsible for binding to A $\beta$  [130] via previously reported A $\beta$  sequence residues 16-20 [103]. Synthetic peptide of antisense DNA strand was able to inhibit A $\beta$ -induced cytotoxicity for A $\beta$ <sub>1-42</sub>, A $\beta$ <sub>1-40</sub> and A $\beta$ <sub>17-42</sub> using mouse myeloma cells. Positive results were shown on post mitotic NT2 neurons lowering A $\beta$ -induced cytotoxicity [130]. Later, Lustbader *et al.* prepared synthetic peptide, comprised of residues 92-120 of Loop D region, acting as a decoy peptide (DP). Constructed DP mimics ABAD's Loop D residues and competitively inhibited binding between A $\beta$  and ABAD, which was confirmed by surface plasma resonance experiments. Cell-based studies demonstrated protective effect of DP against A $\beta$ -induced cytotoxicity [112]. Transgenic mouse AD model *in vivo* studies showed that DP can reverse elevated Prdx-2 and Ep-1 expression to their physiological levels [127, 129]. Transgenic mice treated with DP showed substantial improvement in selected cognitive functions [131]. Taken together, these results suggest that ABAD may be a viable target for investigation of novel AD treatment approaches.

There may be two different approaches how to target ABAD. Firstly, the inhibition of A $\beta$ -ABAD interaction presents the most viable and reasonable way. However as described above, interaction of A $\beta$ -ABAD did not switch off ABAD catalytic function (at least not in binding concentration levels), but rather altered ABAD enzyme function resulting in pathophysiological turnover. Therefore, inhibition of ABAD itself (thus interrupting A $\beta$ -induced cytotoxicity) represents a second approach how to target ABAD. Understandable drawback of inhibition ABAD function might be reduced ABAD catalytic activity necessary for physiological functions. Inhibition of ABAD function might help in understanding of A $\beta$ -induced cytotoxic effects in neuronal cells. While doing so, the investigation of A $\beta$ -induced ABAD cytotoxic turnover may help in understanding of not yet described AD pathology.

Inhibition of ABAD function might also be beneficial in investigation and/or treatment of certain type of cancers. As described above, ABAD can take place in catalysis of various steroid sex hormones synthesis [105]. Selected types of prostate cancer showed elevated levels of ABAD, which can enable prostate cancer cells to generate dihydrotestosterone via alternative enzymatic route in absence of testosterone [132]. Hence, it also renders ABAD as possible cancer drug target in steroid biosynthesis [133].

### 2.10.7. Small molecules targeting ABAD or A $\beta$ -ABAD interaction

As only antisense/decoy peptide was developed, there was an apparent need for search of small molecules targeting ABAD or A $\beta$ -ABAD interaction. However, there is only a limited number of reported small molecules targeting ABAD or A $\beta$ -ABAD interaction.

In order to identify small molecule moieties, which would inhibit A $\beta$ -ABAD interaction, Xie *et al.* utilised ELISA-based (enzyme-linked immunosorbent assay) screening assay. They identified several hit scaffolds, in particular Congo Red, Thioflavine-T and resveratrol. While Congo Red retained high toxicity profile, resveratrol did not display further activity in assay. Interestingly, secondary screen based on Thioflavine-T scaffold identified frentizole as a promising hit (Figure 12). Frentizole is FDA-approved immunosuppressive drug, which showed inhibition of A $\beta$ -ABAD interaction with IC<sub>50</sub> of 200  $\mu$ M. Synthesis of frentizole analogue library identified two benzothiazole urea analogues with IC<sub>50</sub> of  $\sim$ 6.5  $\mu$ M (Figure 12). However, any further data regarding A $\beta$  and ABAD were not reported [121].

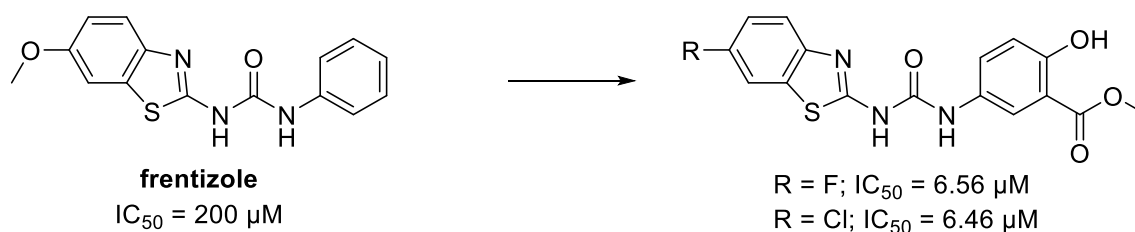


**Figure 12.** Chemical structures of currently known A $\beta$ -ABAD interaction inhibitors.

There are currently three known scaffolds, which were identified to inhibit ABAD function (Figure 13). Compound AG18021 is potent ABAD inhibitor (IC<sub>50</sub> = 92 nM), however it binds covalently with NAD<sup>+</sup> cofactor [113]. Still, AG18021 displayed amelioration of A $\beta$ -induced toxicity [134]. Compound RM-532-46 (IC<sub>50</sub> = 0.55  $\mu$ M) and its analogues (displayed only the most potent one) were reported as reversible ABAD inhibitors with association to AD and prostate cancer [133]. More recently while project progressed, a benzothiazole phosphonate analogues with moderate inhibitory activity (IC<sub>50</sub> = 53  $\mu$ M) was reported with cytoprotective effects against A $\beta$ -induced toxicity [135].



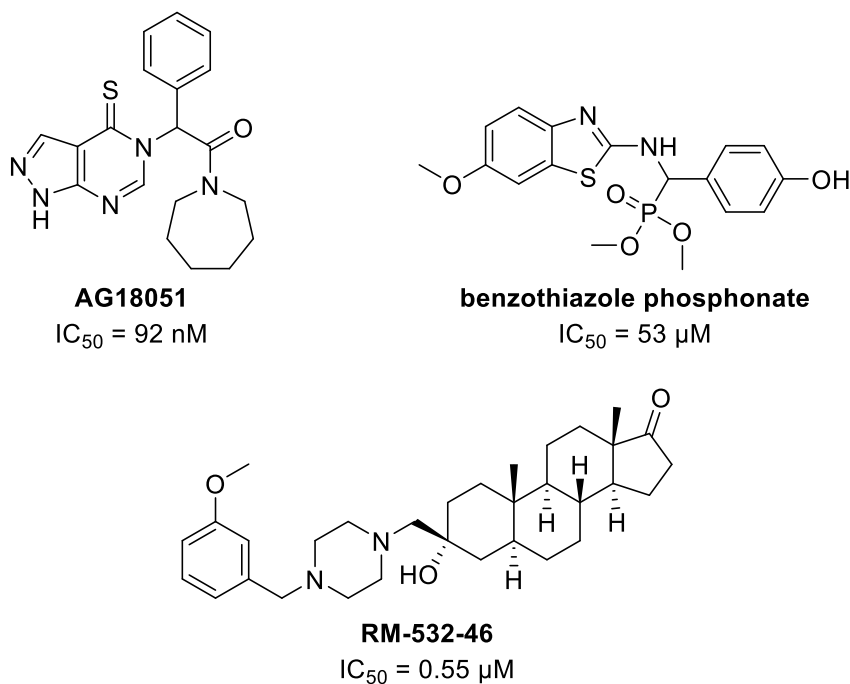


**Figure 13.** Chemicals structures of currently known ABAD inhibitors.

## 2.11. Benzothiazoles – scaffold of interest for CNS targeted drugs

Abovementioned frenzizole derivatives showed promising features with only limited amount of data reported [121]. Therefore, benzothiazole-based scaffolds were of main interest and results were reported in following chapter 3. As such, a review of benzothiazoles as scaffold of interest for CNS targeted drugs was conducted and reported (attachment A1, [37]). Attachment A1 is proposed to serve as a complementary chapter to the introduction part.

Various natural compounds or drugs possess heterocyclic benzothiazole moiety. Benzothiazole skeleton is an essential part of compounds having numerous biological activities (such as antitumor, antimicrobial, anthelmintic, antiparasitic, antituberculous, antidiabetic, antiinflammatory, antidiuretic and so on). More importantly, benzothiazole scaffold is part of compounds, which are biologically active in CNS. Benzothiazole-based compounds were reported to have e.g. anticonvulsant, neuroprotective or  $A\beta$ -binding properties. While some compounds are already used for treatment or diagnostic of CNS-related disorders, many novel CNS-targeted compounds having benzothiazole in their structure are reported [37].

## 2.12. Multi-target-directed strategies

Chapter adopted and extended based on attachment A2 [136].

As discussed before, AD involves multiple pathogenic factors rendering AD as one of the many multifactorial diseases (e.g. several other neurodegenerative syndromes, cancer, diabetes or cardiovascular disorders). Therefore, single target directed approach has been questioned, whether

it could produce desirable therapeutic effects in AD treatment [137]. Over the past recent years, there is an apparent trend to refocus the efforts from single-target-directed ligand to multi-target-directed ligand (MTDL) approach in development of novel AD drugs. It is presumed that simultaneous modulation of several pathophysiological factors may have a greater contribution to the therapeutic effect than the former approach [137, 138]. Reviewing the literature, there is a number of evidences that MTDL approach has been adopted and accepted by many research groups [139–142]. Furthermore, it is worth mentioning that MTDL approach may show up as viable strategy, for example in the case of the compound ladostigil (Figure 14), which has reached clinical trials [143, 144].

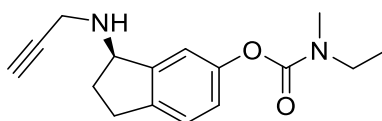


**Figure 14.** Chemicals structure of ladostigil.

While several deficiencies in cholinergic system were already well established in previous chapters, dysregulations of other neurotransmitter systems were also reported in the brain of AD patients. It includes for example dopaminergic or serotonergic neurotransmitter systems. Observed behavioural syndromes in AD patients are then attributed to the impairment of monoamine neurotransmitter systems [145]. Therefore, monoamine neurotransmitter metabolizing enzymes, such as MAO, were proposed as feasible target strategy for AD treatment [144]. There are two distinct isoforms of MAO (MAO-A and MAO-B). They have different localisation, substrates and inhibitors specificities [144, 146, 147]. Pathophysiological changes of both MAO isoforms (activity changes, elevated enzyme levels or localisation expression changes) were reported in brains of AD patients [148–150]. Elevated levels of MAO-B are well described. However, pathophysiological deviations in MAO-A activity seems to be rather more complex and not yet fully understood [151]. Inhibition of MAO-A is well known for its potential side effects, in particular for tyramine-induced hypertension (commonly known as “cheese reaction” or “cheese effect”). Such side effects are triggered by dietary amines after the inhibition of intestinal MAO-A. However, it is only caused by irreversible inhibition of peripheral MAO-A, where the MAO-A inhibitor is covalently bound to the enzyme (generally via hydrazine or propargyl-amino moiety) [144]. Both MAO isoforms can generate toxic metabolites (e.g. aldehydes or hydrogen peroxide) [152]. As such, elevated oxidative stress levels in AD are thought to be worsening due to raised levels of MAO isoforms [153]. For these reasons, the inhibition of both MAO isoforms is considered as a possible approach with beneficial therapeutic effects in AD treatment.

### 3. Results and Discussion

Following chapters were divided based on the synthesised series of compounds. First two series of compounds were published, while further series are currently in progress of publishing.

To prevent any data duplication, first two chapters (3.1. and 3.2.) serves as commentary sections to already published data (attachment A2 and A3). Rest of the chapters (3.x.) provides full data sets.

Same principle applies for experimental section, where characterisation data for published compounds were omitted, as these data are available in accompanied attachments (A2 and A3).

Compounds numbering reflects attachment A2 and A3, and continues with unpublished compounds as follows:

- Numbers **1-23** refer to compounds in attachment A2 [136].
- Numbers **24-32** were not used throughout the whole dissertation. They do not relate to any compounds in dissertation attachments/publications. They were skipped to keep compounds numbers synchronised between dissertation and two commented publications (attachments A2 and A3).
- Numbers **33-50** refer to compounds in attachment A3 [154].
- Numbers **51-131** refer to unpublished compounds and intermediates.

#### 3.1. Synthesis and evaluation of frentizole-based indolyl thiourea analogues as MAO/ABAD inhibitors for Alzheimer's disease treatment

The following chapter is a commentary section for attachment A2 [136], which serves as reference for any information provided in current chapter.

##### 3.1.1. Design and chemistry

Design of initial series of compounds exploits the MTDL approach with an intent to target both ABAD and MAO enzymes (Figure 15). Selected structural key aspects were altered to investigate the limitations of frentizole scaffold to retain both ABAD and MAO inhibitory activity. Base scaffold builds up on frentizole moiety, which was modified to ascertain MAO inhibition activity. While bicyclic system in frentizole is attached to the linker via five-membered ring, indole moiety has been flipped to mimic ladostigil scaffold and to explore the effect on ABAD activity. Propargyl-amino moiety was omitted as it is suspected to be responsible for irreversible MAO inhibition. Thiourea linker has been introduced as both thiourea and urea linkers showed beneficial effects.

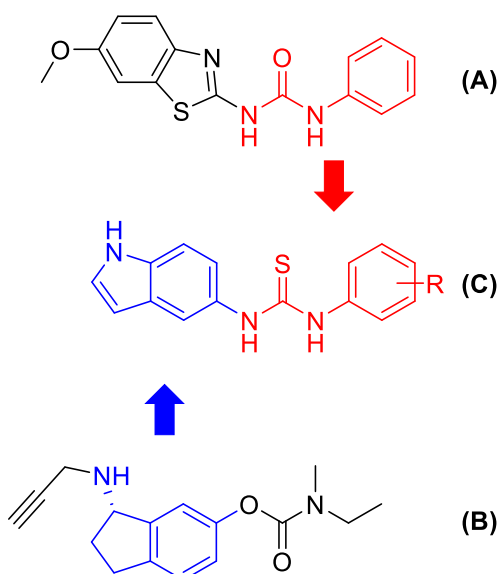
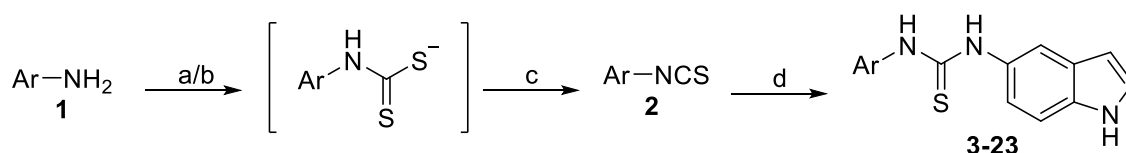


**Figure 15.** Conjunctive design approach combining frentizole (A) and ladostigil (B) to novel MAO/ABAD inhibitors (C) [136].

Disubstituted indolyl thioureas (**3-23**) were prepared with two-step synthesis. Firstly, an amine was converted to dithiocarbamic salt (Scheme 1a/b for electron rich/poor amines, respectively) with subsequent formation of isothiocyanate (Scheme 1c). Then, obtained isothiocyanate was coupled with second amine (Scheme 1d) to yield final disubstituted thiourea (**3-23**) in moderate to excellent yields (38-99%).



**Scheme 1:** Synthesis of indolyl thioureas **3-23**. Reagents and conditions: (a) CS<sub>2</sub>, Et<sub>3</sub>N, THF, RT. (b) CS<sub>2</sub>, NaH, THF, reflux. (c) Boc<sub>2</sub>O, DMAP, 0°C to RT. (d) 1*H*-indole-5-amine, DCM, RT.

### 3.1.2. Results and discussion

ABAD screening assay at fixed 100 μM concentration showed that most of the compounds did not substantially inhibit ABAD function. However two compounds (**17** and **21**) showed noteworthy decrease in ABAD activity (~50% and ~60%). Both active compounds possess hydroxyl substitution at *para* position of distal phenyl ring. Additionally, chlorine substitution is present in single *meta* position (**17**) or in both *meta* positions (**21**). This supports our concurrently obtained data [154], which will be discussed further in next chapter (3.2.).

The investigation of MAO inhibition with coupled fluorescence assay revealed potent (low micromolar range) inhibitors of MAO enzymes. However, same results were not obtained with spectrophotometric assay. Thus, it was suspected that compounds could either quench the fluorescence or inhibit horseradish peroxidase (HRP) enzyme used in coupled assay. Further assessment ruled out fluorescence quenching and confirmed inhibition of HRP. Several compounds (mostly with phenolic group) displayed low micromolar IC<sub>50</sub> values for HRP inhibition.

Therefore, kynuramine based spectrophotometric assay was used for further compounds evaluation. Initial MAO studies with purified MAO-A enzyme revealed several compounds with moderate inhibitory activity (**4**, **8**, **15**, **17**, **19**), where compound **10** showed low micromolar IC<sub>50</sub> (5.9 μM). Selectivity studies were performed with membrane-bound MAO-A and MAO-B enzymes. Most of the evaluated compounds were moderately selective towards MAO-B. Interestingly, *para* bromine substitution showed stronger inhibition towards MAO-A than MAO-B (**10**). Compounds having *ortho* substituted hydroxyl inhibited both MAO-A and MAO-B (**4**), especially with additional presence of chlorine substitution (**19**). In comparison with parent compound with no substitution (**3**), *ortho*-hydroxyl substitution (**4**) displayed by 15-fold stronger inhibition of MAO-B (4.0 μM) compared to MAO-A (only 4-fold). The IC<sub>50</sub> value was further pushed down to high nanomolar range (0.30 μM) with additional presence of chlorine in *para* position (**19**).

Notably, cytotoxicity screen showed low cytotoxicity profile for majority of compounds in whole series (one order magnitude higher compared to frentizole). Compounds **9** and **12**, both having additionally phenyl ring attached, showed higher cytotoxicity profile. Nevertheless, they did not express any interesting biological activity.

### 3.1.3. Conclusion

A series of novel disubstituted thioureas was synthesised and evaluated for ABAD, MAO-A and MAO-B inhibitory activity. In case of ABAD inhibition, only two compounds showed noteworthy activity towards ABAD. Still, in terms of structure and activity relationship and building library of compounds targeted towards ABAD, they did provide significant insight for future development. More interestingly, several compounds showed promising MAO inhibition activity (micromolar range) with certain selectivity towards MAO-B isoform. Thus, a novel class of MAO inhibitors was reported. Compounds revealed significant inhibitory activity towards HRP, demonstrating potential limitations of enzyme-coupled assays and emphasizing the need for cautious data interpretation.

### 3.2. Design, synthesis and *in vitro* evaluation of riluzole-based ureas as potential ABAD/17 $\beta$ -HSD10 modulators for Alzheimer's disease treatment

The following chapter is a commentary section for attachment A3 [154], which serves as reference for any information provided in current chapter.

#### 3.2.1. Design and chemistry

Design of this series of compounds (**33-50**) builds on the previously prepared compounds (attachment A3: **5-32**). The initial screen showed that the inhibition of ABAD is restricted to 3-chloro-4-hydroxy substitution pattern of distal phenyl ring (in context of prepared series). However, different halogen substitution (fluorine and chlorine) of 6-position of benzothiazole ring did not show any notable effect on ABAD activity. In light of these findings, riluzole-based ureas were prepared as subsequent series (Figure 16). As substitution of benzothiazole ring did not influenced ABAD activity, trifluoromethoxy substitution was introduced in the moiety with intent to mimic riluzole, neuroprotective compounds with multiple mechanism of actions. Distal phenyl ring includes mostly oxygen-containing substitutions with two aspects in mind. Firstly, ABAD inhibitory activity was observed for compounds with hydroxyl group supported with additional chlorine substitution. Secondly, our pool of compounds contained only limited number diversity. Therefore, several substitutions overlapped with previous series to receive exhaustive pool of data, which could tackle possible diversity-based structure and activity issues.

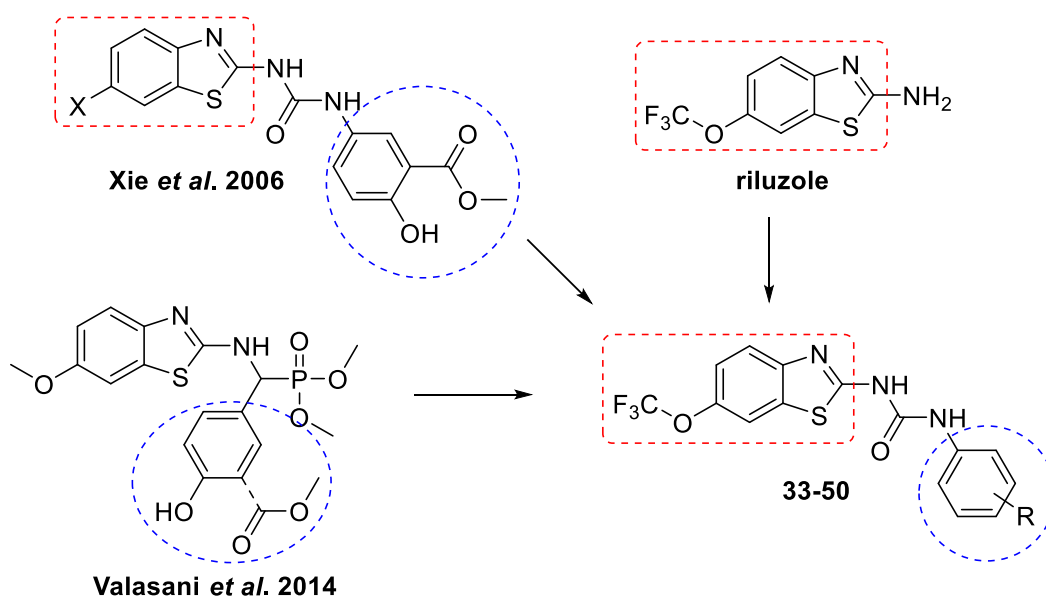
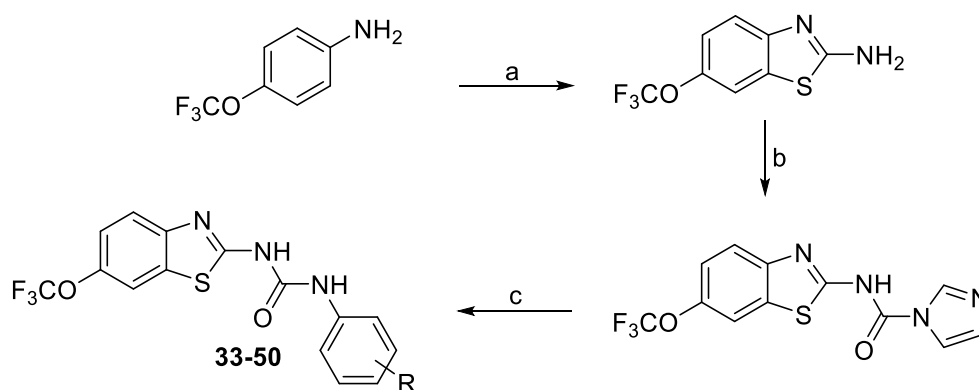


**Figure 16.** Design of riluzole-based ureas as ABAD inhibitors [154].

Riluzole-based disubstituted ureas were synthesised in three steps (Scheme 2). Riluzole (6-(trifluoromethoxy)benzo[*d*]thiazol-2-amine) was prepared from its corresponding *para*-substituted aniline derivative. Subsequently, riluzole was treated with *N,N'*-carbonyldiimidazole (CDI) to obtain *N*-(6-(trifluoromethoxy)benzo[*d*]thiazol-2-yl)-1*H*-imidazole-1-carboxamide, followed by subsequent reaction with a substituted aromatic amine to produce final ureas (**33-50**) in moderate to excellent yields (50-99%).



**Scheme 2:** Synthesis of benzothiazolyl ureas (**33-50**). Reagents and conditions: (a) Br<sub>2</sub>, KSCN, CH<sub>3</sub>COOH. (b) CDI, DCM, reflux. (c) Ar-NH<sub>2</sub>, MeCN, reflux.

### 3.2.2. Results and discussion

Compounds were screened at fixed 25  $\mu$ M concentration for ABAD inhibitory activity. Compound **37** with 3-chloro-4-hydroxy substitution showed the most promising inhibition towards ABAD. Compound **39** with additional chlorine (3,5-dichloro-4-hydroxy substitution) displayed comparable inhibitory activity as compound **37**. Trifluoromethoxy substitution improved the inhibition (~80%) in comparison with 6-halogen substituted analogues (~60%). Furthermore, compounds with a single phenolic group (**34**, **35**), 4-chloro-2-hydroxy substitution pattern (**38**) and isosteric hydroxyl-thiol group exchange (**50**) showed less pronounced inhibition activity (~20-35%).

Physical-chemical properties for compounds **37** and **39** were calculated (HBA, HBD, TPSA, Clog*P*, Clog*D*) and correlated with experimentally obtained ones (Elog*P*, Elog*D*). In terms of Lipinski rule of five, selected values fluctuated near upper cut-off values, still rationally conforms to proposed guidelines. Both experimentally obtained values (Elog*P*, Elog*D*) are in a good agreement with calculated values. Additionally, blood-brain barrier (BBB) penetration was predicted using parallel artificial membrane permeability assay (PAMPA). While experimental data for compound **39** suggested high penetration to CNS, compound **37** gave rather uncertain prediction for BBB penetration.

Lastly, acute cytotoxic profile (MTT and LDH assay) was determined for compounds **37** and **39** with correlation to frentizole and parent riluzole. Compound **39** showed comparable cytotoxicity with frentizole ( $IC_{50} = 30\text{-}46\ \mu\text{M}$ ), while compound **37** displayed slightly higher cytotoxicity ( $IC_{50} = 7\text{-}8\ \mu\text{M}$ ). Cytotoxicity levels of parent compound riluzole were approximately one order of magnitude lower ( $IC_{50}$  of  $310\ \mu\text{M}$  and  $480\ \mu\text{M}$  for MTD and LDH, respectively) than discussed urea derivatives (**39**).

### 3.2.3. Conclusion

A series of riluzole-based ureas was designed and synthesised. ABAD inhibition studies showed that the most promising feature in structure and activity relationship is the presence of 3-chloro-4-hydroxy substitution pattern on distal phenyl ring, which is in agreement with our previous findings. Prediction studies using PAMPA assay showed possible high BBB penetration for compound **39**. Compound **39** also displayed comparable cytotoxicity with frentizole (as a standard and FDA-approved drug).

## 3.3. Design, synthesis and evaluation of further analogues

This chapter includes additional series of compounds prepared for the discussed project, which were not yet published. The sub-chapters (3.3.x) were based on smaller series of compounds with follow-up design, chemistry and *in vitro* evaluation (if available).

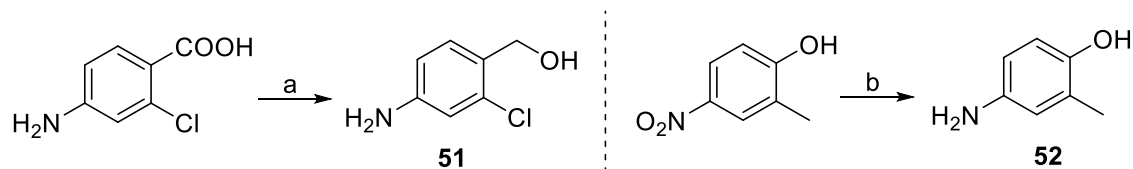
### 3.3.1. Exploration of distal phenyl ring substitutions

#### Design and chemistry

Design of the current series is a direct follow-up of previously reported compounds [154]. While benzothiazole scaffold and urea linker were kept intact, further substitution changes into the distal phenyl ring were introduced. Methoxy substitution in position six of benzothiazole was selected and based on the comparable inhibitory activity with halogenated analogues and due to availability of starting material. Substitution selection of distal phenyl ring were designed to more exhaustively explore possible variations in phenyl ring pattern, which were not yet investigated and evaluated.

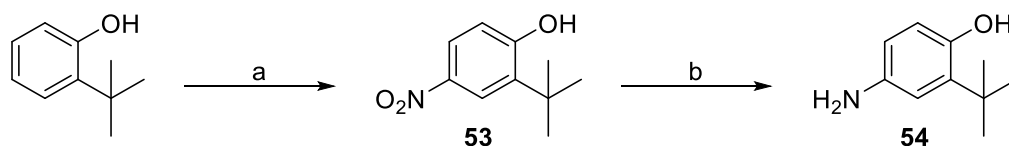
While previously reported compounds had more or less readily available reagents, this series of compounds required to prepare selected intermediates. Primary alcohol group in *para* position (**51**) was generated via reduction of carboxylic acid analogue with lithium aluminium hydride (Scheme 3a). In general, reduction of substituted nitrobenzenes into the corresponding anilines (e.g. **52**) was achieved with palladium on activated carbon (Pd/C) catalysed hydrogenation reaction (Scheme 3b).





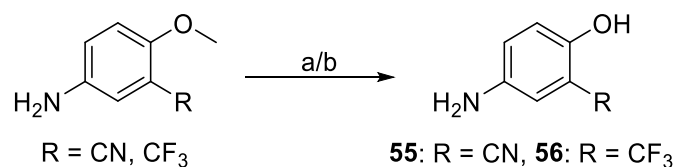
**Scheme 3:** Synthesis of **51-52**. Reagents and conditions: (a)  $\text{LiAlH}_4$ , THF,  $-5^\circ\text{C}$  to RT. (b) Pd/C,  $\text{H}_2$ , EtOH, RT.

2-(*Tert*-butyl)phenol was selected as a starting material for introduction of *tert*-butyl group into the *meta* position of distal phenyl ring. Firstly, nitration was achieved with nitric acid in presence of acetic acid as reaction solvent (Scheme 4a) to obtain intermediate **53**. Secondly, introduced nitro group was reduced to 4-amino-2-(*tert*-butyl)phenol (**54**). Initially, the reduction was attempted with Pd/C catalysed hydrogenation (Scheme 3b). However, a complex mixture of decomposed starting material was received. Thus, reduction was accomplished using iron powder and ammonium chloride (Scheme 4b) to successfully obtain intermediate **54**.



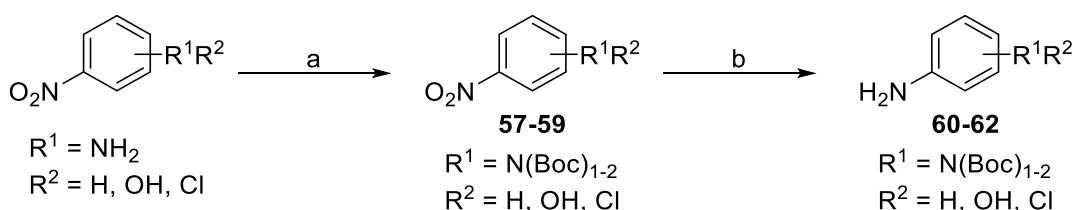
**Scheme 4:** Synthesis of **53-54**. Reagents and conditions: (a)  $\text{HNO}_3/\text{CH}_3\text{COOH}$ , RT. (b) Fe,  $\text{NH}_4\text{Cl}$ , MeOH: $\text{H}_2\text{O}$ , RT.

Methoxy analogues were demethylated using two different reactions. While de-methylation proceeded readily with help of aluminium chloride (Scheme 5a) for 3-cyano substitution (**55**), this approach failed in presence of 3-trifluoromethyl substitution (**56**). Therefore, de-methylation was successfully achieved with hydrobromic acid (Scheme 5b) for intermediate **56**.



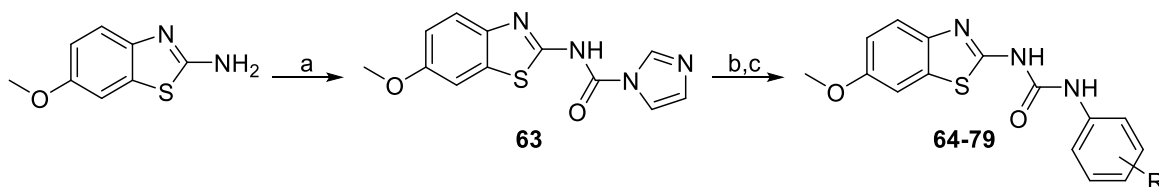
**Scheme 5:** Synthesis of **55-56**. Reagents and conditions: (a)  $\text{AlCl}_3$ , DCM, reflux (**55**). (b) HBr,  $\text{CH}_3\text{COOH}$ , reflux (**56**).

*N*-Boc (de)protection was selected for final compounds with free amine group on distal phenyl ring. Firstly, amine group of nitroaniline was protected with di-*tert*-butyl dicarbonate (Scheme 6a) to yield intermediates **57-59**. Secondly, nitro group was reduced with Pd/C catalysed hydrogenation to obtain intermediates **60-62** (Scheme 6b). Final *N*-Boc acidic deprotection was performed after urea formation (Scheme 7c).



**Scheme 6:** Synthesis of **57-62**. Reagents and conditions: (a) (Boc)<sub>2</sub>O, DMAP, THF, RT. (b) Pd/C, H<sub>2</sub>, EtOH, RT.

Benzothiazole ureas were formed with following two-step reaction process. Initially, 6-methoxybenzo[*d*]thiazol-2-amine was activated with CDI (Scheme 7a). Subsequently, intermediate **63** was reacted with previously prepared aniline intermediates (Scheme 7b) to give final disubstituted ureas (**64-79**). *N*-Boc protection group was cleaved under acidic conditions (Scheme 7c) to receive compounds **77-79**.



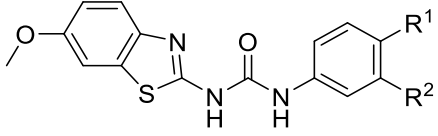
**Scheme 7:** Synthesis of **63-79**. Reagents and conditions: (a) CDI, DCM, RT. (b) Amine, MeCN, reflux. (c) 4 M HCl, dioxane, RT (for *N*-Boc protected ureas).

## Results and discussion

Compounds **64-79** (Table 3) were screened at fixed 25 μM concentration for ABAD inhibitory activity. Results were correlated with standard compound with already established biologically activate substitution pattern (3-chloro-4-hydroxy) of distal phenyl ring. The introduction of small alkyl group (methyl, **64**) instead of chlorine showed ~35% decrease in ABAD activity. However, ABAD inhibitory activity with more bulky alkyl (*tert*-butyl, **65**) substitution completely diminished. Introduction of different halogens (**66**, **67** and **88**) showed comparable results with chlorine substitution. Both fluorine (**88**, Table 4, prepared in following series) and bromine (**66**) demonstrated ~85% decrease in ABAD activity. Substitution with iodine caused ~95% decrease in

ABAD activity. Determination of IC<sub>50</sub> displayed comparable low micromolar values for **66** and **67** (1.33 μM and 1.66 μM, respectively).

**Table 3.** Substitution pattern and *in vitro* data for compounds **64-79**.



Compound	R <sup>1</sup>	R <sup>2</sup>	Relative % activity remaining @ 25 μM	IC <sub>50</sub> (μM)
control	-	-	100.00 ± 0.21	-
standard	OH	Cl	10.00 ± 0.39	0.79
<b>64</b>	OH	CH <sub>3</sub>	66.07 ± 1.38	-
<b>65</b>	OH	C(CH <sub>3</sub> ) <sub>3</sub>	94.35 ± 2.95	-
<b>66</b>	OH	Br	13.45 ± 0.58	1.30
<b>67</b>	OH	I	6.72 ± 0.46	1.66
<b>68</b>	OH	CN	67.63 ± 2.25	-
<b>69</b>	OH	CF <sub>3</sub>	-	-
<b>70</b>	OH	NO <sub>2</sub>	-	-
<b>71</b>	CH <sub>2</sub> OH	Cl	103.10 ± 5.61	-
<b>72</b>	6-hydroxypyridin-3-yl <sup>a</sup>		73.50 ± 3.36	-
<b>73</b>	4-hydroxycyclohexyl <sup>a</sup>		106.30 ± 0.85	-
<b>77</b>	H	NH <sub>2</sub>	92.18 ± 2.88	-
<b>78</b>	OH	NH <sub>2</sub>	96.69 ± 0.83	-
<b>79</b>	NH <sub>2</sub>	Cl	108.6 ± 2.92	-

<sup>a</sup> Substitution pattern replacement of whole distal phenyl ring.

Compounds **68-70** demonstrates additional introduction of electron withdrawing groups (cyano, trifluoro and nitro). Substitution with cyano group showed only moderate decrease (~30%) in ABAD activity. *In vitro* data for compounds with trifluoromethyl (**69**) and nitro (**70**) substitutions were not yet determined.

The exchange of phenol group with hydroxymethyl (**71**) did not show any inhibitory activity, proving the necessity of phenolic group in potency of discussed compounds. Compounds **72-73** introduce initial changes into the distal phenyl ring itself. 6-Hydroxypyridin-3-yl (**72**) substitution retained some inhibitory activity (~25%), while any inhibitory potency diminished for saturated ring (**73**, 4-hydroxycyclohexyl). Suffice to say, compounds **72** and **73** only outline possible changes into distal phenyl ring and there is still a vast number of potential modifications to explore. Either introduction or exchange of phenolic/chlorine groups with amino group (**77-79**) did not display any significant decrease in ABAD activity.

### 3.3.2. Fluorinated distal phenyl ring substitutions

Compounds **83-103** were prepared by Mgr. Matěj Chřibek (already graduated master student) under my experimental supervision. Therefore, experimental data were not included in this dissertation. They are attached in his Master thesis [155]. Following chapter will outline design and chemistry used to obtain these compounds. Furthermore, biological data will be commented in context of discussed project.

#### Design and chemistry

Concurrently to previously discussed compounds **64-79**, a fluorinated series of compounds was designed to explore the combination of halogen/hydroxyl/methoxy substitution effect on ABAD inhibitor activity. Distal phenyl ring substitutions include combination of fluorine(s) and hydroxyl/methoxy groups. These substitutions are either analogous to already prepared chlorine counterparts or novel substitution patterns, which were not readily available in combination with chlorine. Three alternating substitution (fluorine, chlorine, methoxy) in position six of benzothiazole moiety were selected based on inhibitory activity towards ABAD.

Intermediates and final compounds (**83-103**) were prepared according to already mentioned procedures. Intermediates were prepared from starting material having either nitro group or methoxy group. Nitro derivatives were reduced using iron powder and ammonium chloride (Scheme 4b). Methoxy derivatives were demethylated utilizing aluminium chloride (Scheme 5a). Final compounds were obtained using established two-step process (Scheme 7a-b).

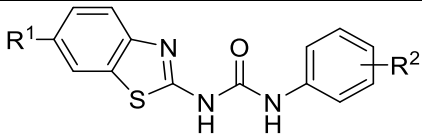
#### Results and discussion

Compounds **83-103** (Table 4) were screened at fixed 25  $\mu\text{M}$  concentration for ABAD inhibitory activity. The most promising inhibitory activity towards ABAD was seen for compounds with 3-fluoro-4-hydroxy substitution pattern of distal phenyl ring (**86-88**). Compound **88** with 6-methoxy group of benzothiazole showed  $\sim 85\%$  decrease in ABAD activity, while halogenated analogues less pronounced inhibition ( $\sim 65-75\%$ ). In comparison with compounds having 3-halogen-4-hydroxy substitution, substitution with fluorine (**88**) showed comparable inhibitory activity with bromine analogue (**66**). Surprisingly, the addition of secondary fluorine (**98-100**) caused partial loss of ABAD inhibition potency ( $\sim 30-45\%$ ). In contrast, compound with two chlorines in both *meta* positions (**39**) showed comparable activity with its single chlorine analogue (**37**).

Trinity of compounds having 2-hydroxy-4-fluoro substitution (**89-91**) showed interesting drop in ABAD activity ( $\sim 41-66\%$ ). Compounds having *ortho* hydroxyl showed moderate decrease ABAD activity [154]. In this case, displacement of hydroxyl to fluorine in *para* position caused increase of inhibition potency. Additionally, compounds **83-85** with 3-fluoro-2-methoxy substitution pattern also showed moderate decrease in ABAD activity ( $\sim 30-55\%$ ). Rest of the

evaluated compounds (**92-97**, **101-103**) did not show any inhibitory activity. Interestingly, some of these compounds showed slightly elevated activity levels (~5-15%), which we were already described earlier ([154] and unpublished data).

**Table 4.** Substitution pattern and *in vitro* data for compounds **83-103**.



Compound	R <sup>1</sup>	R <sup>2</sup>	Relative % activity remaining @ 25 μM
<b>control</b>	-	-	100 ± 0.21
<b>standard</b>	-OCH <sub>3</sub>	3-Cl, 4-OH	10.00 ± 0.95
<b>83</b>	-F	2-OCH <sub>3</sub> , 3-F	71.7 ± 0.95
<b>84</b>	-Cl	2-OCH <sub>3</sub> , 3-F	44.0 ± 0.94
<b>85</b>	-OCH <sub>3</sub>	2-OCH <sub>3</sub> , 3-F	56.7 ± 1.31
<b>86</b>	-F	3-F, 4-OH	23.3 ± 0.33
<b>87</b>	-Cl	3-F, 4-OH	33.9 ± 0.52
<b>88</b>	-OCH <sub>3</sub>	3-F, 4-OH	14.2 ± 0.46
<b>89</b>	-F	2-OH, 4-F	48.2 ± 0.56
<b>90</b>	-Cl	2-OH, 4-F	33.7 ± 0.23
<b>91</b>	-OCH <sub>3</sub>	2-OH, 4-F	58.7 ± 0.55
<b>92</b>	-F	2-F, 4-OH	110.50 ± 0.60
<b>93</b>	-Cl	2-F, 4-OH	110.79 ± 1.08
<b>94</b>	-OCH <sub>3</sub>	2-F, 4-OH	110.25 ± 1.17
<b>95</b>	-F	2-OCH <sub>3</sub> , 4-F	115.57 ± 0.61
<b>96</b>	-Cl	2-OCH <sub>3</sub> , 4-F	113.19 ± 1.29
<b>97</b>	-OCH <sub>3</sub>	2-OCH <sub>3</sub> , 4-F	95.70 ± 0.66
<b>98</b>	-F	3,5-F, 4-OH	68.24 ± 0.57
<b>99</b>	-Cl	3,5-F, 4-OH	66.94 ± 0.42
<b>100</b>	-OCH <sub>3</sub>	3,5-F, 4-OH	55.34 ± 0.60
<b>101</b>	-F	2-OH, 3,4-F	105.07 ± 1.10
<b>102</b>	-Cl	2-OH, 3,4-F	106.58 ± 1.17
<b>103</b>	-OCH <sub>3</sub>	2-OH, 3,4-F	106.94 ± 0.75

In context of the whole series, potency between trinities followed same tendency in terms of structure and activity relationship. On the other hand, effect benzothiazole substitution (differences among each trinity) did not follow the same trend and structure and activity relationship is not completely clear.

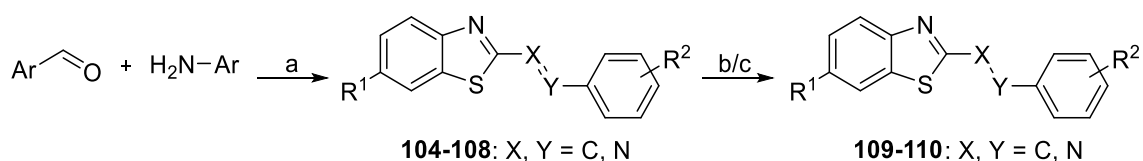
### 3.3.3. Scaffold linker modifications

#### Design and synthesis

While the previous series explored mostly modifications on distal phenyl ring or marginally benzothiazole substitution, the following series was focused on selected modifications in linker part of scaffold. The whole scaffold itself does not possess optimal physical-chemical properties. Therefore, it was designed to break the conjugation of urea linker with benzothiazole ring. Urea linker was replaced with amine/imine moiety having either same or shorter linker length. The most promising distal phenyl ring substitution (3-chlorine-4-hydroxy) was selected with either 6-methoxy or unsubstituted benzothiazole ring. Additionally to concurrently published work [135, 156], dimethyl phosphonates analogues were prepared as standards for comparison between inter-workgroup biological evaluations along with the most promising substitution pattern.

These linker modifications do not exhaustively cover all possibilities. Simultaneously, further linker modifications were also prepared by Dr. Ondřej Benek and discussed in his dissertation [157]. Therefore, compounds were designed to complement other series prepared by ABAD project contributors.

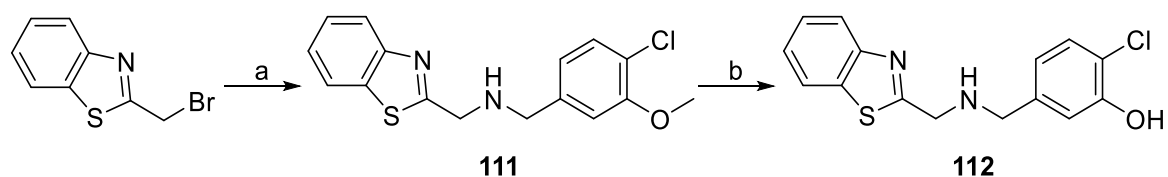
One-atom shorter linkers were prepared via imine/amine approach with two reaction steps. Favourably, this process also allowed using imines as intermediates for both amines (**109-110**) and dimethyl phosphonates (**113-116**). Corresponding aldehyde and amine were coupled at reflux conditions (Scheme 8a) to receive compounds **104-108**. Furthermore, imines were reduced to their amine analogues. Initially, reduction was attempted with sodium borohydride (Scheme 8c). The reaction proceeded readily to yield compound **110**. However, the reaction to receive compound **109** showed difficulties to receive desired product. Then, imine was reduced to corresponding amine (**109**) with Pd/C catalysed hydrogenation (Scheme 8b).



**Scheme 8:** Synthesis of **104-110**. Reagents and conditions: (a) toluene, reflux. (b) Pd/C, H<sub>2</sub>, MeOH, RT (**109**). (c) NaBH<sub>4</sub>, MeOH, RT (**110**).

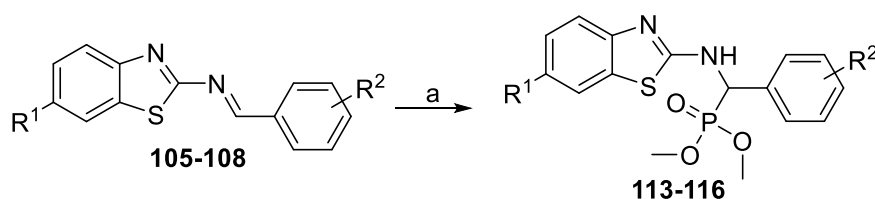
An amine linker having same length as urea was prepared with two-step synthesis. Firstly, (3-chloro-4-methoxyphenyl)methanamine was alkylated using 2-(bromomethyl)benzo[*d*]thiazole (Scheme 9a) to receive compound **111**. Then, compound **111** was demethylated using aluminium chloride (Scheme 9b). Previously, demethylation proceeded quickly in refluxing dichloromethane

(DCM), however not in this case. Therefore, 1,2-dichloroethane (DCE) with higher boiling point was used to set off the reaction at 60°C.



**Scheme 9:** Synthesis of **111-112**. Reagents and conditions: (a) (3-chloro-4-methoxyphenyl)methanamine, DIPEA, DCM, RT. (b) AlCl<sub>3</sub>, DCE, 60°C.

The imines (**105-108**) from previous reaction step were utilised to prepare dimethyl phosphonate linkers. While the originally used reaction conditions proved to be troublesome to receive desired compounds [156], final dimethyl phosphonates (**113-116**) were prepared using dimethyl phosphite and 1,1,3,3-tetramethylguanidine in satisfactory yields (Scheme 10a).



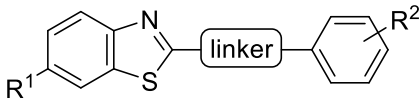
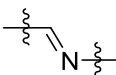
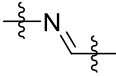
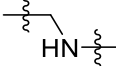
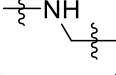
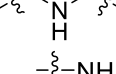
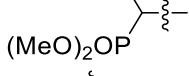
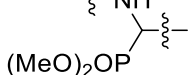
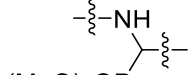
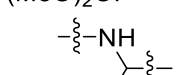
**Scheme 10:** Synthesis of **113-116**. Reagents and conditions: (a) dimethyl phosphite, 1,1,3,3-tetramethylguanidine, THF, 65°C.

## Results and discussion

Compounds **104-116** (Table 5) were screened at fixed 25  $\mu$ M concentration for ABAD inhibitory activity. Imine linkers (**104-105**) did not show any inhibitory activity. Likewise, amine linker with nitrogen adjacent to distal phenyl ring resulted in complete loss of inhibition activity. On the other hand, amine linker with nitrogen adjacent to benzothiazole showed  $\sim$ 70% decrease in ABAD activity. Similarly, amide linkers were prepared and evaluated [157]. Amide with nitrogen adjacent to distal phenyl ring did not show any inhibitory potency, while amide with nitrogen adjacent to benzothiazole showed  $\sim$ 50% decrease in ABAD activity (data not shown). Methylaminomethyl linker (**112**) showed comparable inhibitory activity ( $\sim$ 77%) with aminomethyl linker (**110**). It can be assumed that nitrogen directly attached to distal phenyl ring triggered the loss of inhibitory activity. Moreover, it is not necessary to have nitrogen adjacent directly to benzothiazole (**110** vs. **112**). In contrast, it does not apply for urea linker with clearly retained activity.

Dimethyl phosphonate linkers were prepared as standards for inter-workgroup assay comparisons (**114-116**) [135, 156]. However, they did not show any noteworthy drop in ABAD activity. Dimethyl phosphonate with 3-chloro-4-hydroxy substitution pattern (**113**) was also prepared. Again, no inhibition was observed for compound **113**. Suffice to say, our assay was demonstrated as robust and verified with reference inhibitor [154], while the same cannot be confirmed for concurrently reported phosphonate analogues [135]. Another possibility might be due to compounds chirality and the fact that they were prepared with different procedures. However, this assumption has not been yet investigated.

**Table 5.** Substitution pattern and *in vitro* data for compounds **104-116**.

				
Compound	R <sup>1</sup>	linker	R <sup>2</sup>	Relative % activity remaining @ 25 μM
control	-	-	-	100.00 ± 0.33
<b>104</b>	-H		3-Cl, 4-OH	103.17 ± 2.71
<b>105</b>	-OCH <sub>3</sub>		3-Cl, 4-OH	97.50 ± 0.96
<b>109</b>	-H		3-Cl, 4-OH	98.04 ± 1.09
<b>110</b>	-OCH <sub>3</sub>		3-Cl, 4-OH	29.65 ± 0.56
<b>112</b>	-H		3-Cl, 4-OH	33.21 ± 0.44
<b>113</b>	-OCH <sub>3</sub>		3-Cl, 4-OH	97.83 ± 0.88
<b>114</b>	-OCH <sub>3</sub>		4-F	89.03 ± 0.89
<b>115</b>	-OCH <sub>3</sub>		4-OH	97.28 ± 4.02
<b>116</b>	-OCH <sub>3</sub>		3-COOCH <sub>3</sub> , 4-OH	97.91 ± 3.44



### 3.3.4. Physical-chemical properties of designed series

Optimal physical-chemical properties of compounds represent key aspects for favourable pharmacokinetic profile. Moreover, CNS-acting drugs require penetration through BBB to successfully reach their targets. Thus, selected physical-chemical descriptors were calculated in ACDLabs PhysChem Suite 12.0; logarithm of partition coefficient (*ClogP*), logarithm of distribution coefficient (*ClogD*), topological polar surface area (TPSA), molecular weight (*M<sub>w</sub>*), hydrogen bond acceptors/donors (HBA/D), logarithmic acid dissociation constant (*pK<sub>a</sub>*) and logarithm of solubility (*ClogS*). Calculated descriptors values were correlated with desirable range of CNS drug-like properties [158, 159] and they were summarised in Table 6.

Additionally, selected descriptors were used to calculate multi-parameter optimization (MPO) score. MPO scoring function uses six descriptors (*ClogP*, *ClogD*, TPSA, *M<sub>w</sub>*, HBD and *pK<sub>a</sub>*) to determine overall score with balancing/weighting effect and without hard cut-offs [160].

**Table 6.** Calculated physical-chemical properties for selected compounds.

Comp.	<i>ClogP</i>	<i>ClogD</i> <sup>a</sup>	TPSA	<i>M<sub>w</sub></i>	HBA/D	<i>pK<sub>a</sub></i> <sup>a</sup>	<i>ClogS</i>	MPO
LR5 <sup>b</sup>	≤ 5	0-3	≤ 90	≤ 450	≤ 7 / ≤ 3	≤ 10	-	≥ 3.5
<b>37</b>	4.24	3.92	111.72	403.76	7 / 3	7.39	-4.95	2.6
<b>66</b>	3.85	3.78	111.72	394.24	7 / 3	8.21	-4.71	2.8
<b>67</b>	3.89	3.80	111.72	441.24	7 / 3	8.08	-4.76	2.5
<b>110</b>	3.90	3.89	82.62	320.79	4 / 2	8.28	-4.72	4.0
<b>112</b>	3.61	3.59	73.39	304.80	3 / 2	8.57	-2.87	4.1

<sup>a</sup> pH dependant values refers to pH 7.40

<sup>b</sup> optimal physical-chemical properties [158–160]

Compounds from initial series (**37**, **66**, and **67**) were predicted with mostly physical-chemical properties border lining with optimal values for CNS penetrable drugs. However, later series (**110**, **112**) were designed with partial emphasis on improvement of physical-chemical properties. Compounds **66** and **67** still possess benzothiazol-2-yl-urea moiety. Upon the dismantling of conjugated benzothiazole-2-yl-urea moiety, physical-chemical properties showed clear improvement (**110**, **112**), where MPO score reached ≥ 4 values. Thus, compounds **110** and **112** demonstrated reasonable improvement within the studied scaffold.

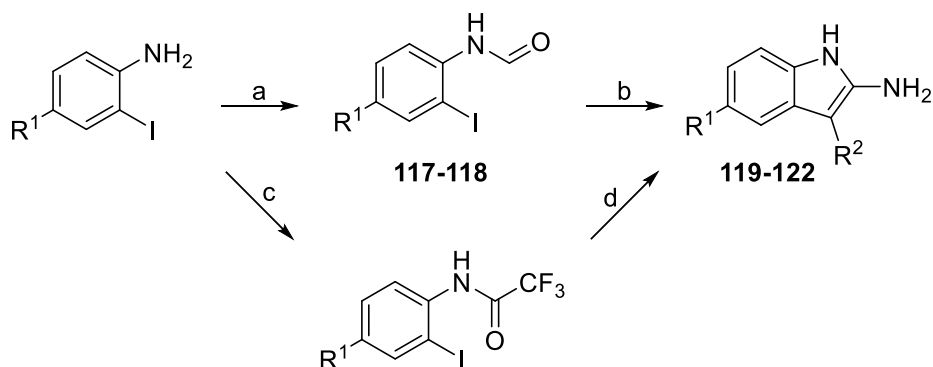
Suffice to say, these data set represents approximation of reality as only calculated values were considered. Later, calculated data will be correlated with experimental ones, which are currently under experimental determination.

### 3.3.5. Fragments based on 2-aminoindole-3-carboxylic acid derivatives

#### Design and chemistry

Design of compounds **119-122** was based on Dr. Laura Aitken screening selection (collaborating workgroup of prof. Frank Gunn-Moore, University of St. Andrews). Briefly, Maybridge fragment database was utilised for initial screening, while several techniques (thermal shift analysis, nuclear magnetic resonance experiments such as saturation transfer difference and water-ligand observation with gradient spectroscopy) were used to narrow down the search of possible fragments interacting with ABAD. Among others, 2-aminoindoles with electron withdrawing group in third position of indole ring (Scheme 11) displayed promising results for interaction with ABAD.

Compounds **119-122** were prepared with two reaction steps. Firstly, selected 2-iodoanilines were formylated using formic acid to yield compounds **117-118**. Then, indole scaffold was formed with 2-cyanoacetic acid derivative catalysed by copper(I) iodide (Scheme 11b) to obtain compounds **119-122**. Later, compounds were also prepared with modified approach. Firstly, 2-iodoanilines were treated with trifluoroacetic acid to yield corresponding trifluoroacetamides (Scheme 11c). Then, indole scaffold was formed in similar manner using L-proline and lower temperature (Scheme 11d). In general, second method (conditions c/d) gave ~10-15% yield improvement over original approach. Additionally, fragments were attempted to incorporate into urea scaffold with distal phenyl ring, however every effort failed to do so.

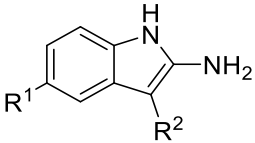


**Scheme 11:** Synthesis of **117-122**. Reagents and conditions: (a)  $\text{HCOOH}$ , toluene, reflux. (b) 2-cyanoacetic derivative,  $\text{K}_2\text{CO}_3$ ,  $\text{CuI}$ ,  $\text{DMSO}:\text{H}_2\text{O}$ ,  $120^\circ\text{C}$ . (c)  $(\text{CF}_3\text{CO})_2\text{O}$ ,  $\text{THF}$ ,  $-15^\circ\text{C}$ . (d) 2-cyanoacetic derivative,  $\text{K}_2\text{CO}_3$ , L-proline,  $\text{CuI}$ ,  $\text{DMSO}:\text{H}_2\text{O}$ ,  $60^\circ\text{C}$ .

## Results and discussion

Initially, compounds **119-122** (Table 7) were screened at fixed 25  $\mu\text{M}$  concentration for ABAD inhibitory activity. However, any of these compounds did not show any substantial decrease in ABAD enzyme activity.

**Table 7.** Substitution pattern and *in vitro* data for compounds **119-122**.



Comp.	R <sup>1</sup>	R <sup>2</sup>	Remaining activity (%) ABAD @ 25 $\mu\text{M}$	MAO-A IC <sub>50</sub> ( $\mu\text{M}$ )	MAO-B IC <sub>50</sub> ( $\mu\text{M}$ )
<b>119</b>	F	CN	90.94 $\pm$ 2.48	-	-
<b>120</b>	Cl	CN	88.13 $\pm$ 5.16	2.80 $\pm$ 0.40	3.89 $\pm$ 0.02
<b>121</b>	F	COOEt	90.31 $\pm$ 1.90	-	-
<b>122</b>	Cl	COOEt	95.00 $\pm$ 1.36	> 30	> 30

Additionally, carbonitrile-containing aminoheterocycles were reported to be potent inhibitors of MAO enzyme isoforms [161]. Therefore, compounds **119-122** were screened against both MAO-A and MAO-B. Initial screen at fixed compounds concentration (50  $\mu\text{M}$  and 5  $\mu\text{M}$ ) showed inhibition of both MAO-A and MAO-B (data not shown). As halogen substitution did not show any substantial deviation between fluorine and chlorine, only one pair of compounds with chlorine substitution (**120** and **122**) was selected for further IC<sub>50</sub> determination. Compound **120** with nitrile substitution inhibited both MAO-A and MAO-B with low micromolar range (2.80  $\mu\text{M}$  and 3.89  $\mu\text{M}$ ). On the other hand, ethyl ester substitution showed higher IC<sub>50</sub> values for both MAO-A and MAO-B.

Compounds **119-122** were not pursued further for inhibition of ABAD. However, obtained initial MAO data were utilised in a follow-up project (attachment A4, [162]). Using MTDL strategy, scaffold of compounds **119-122** was tightly combined with tacrine moiety yielding novel dual MAO and choline esterase inhibitors (Figure 17) [162].

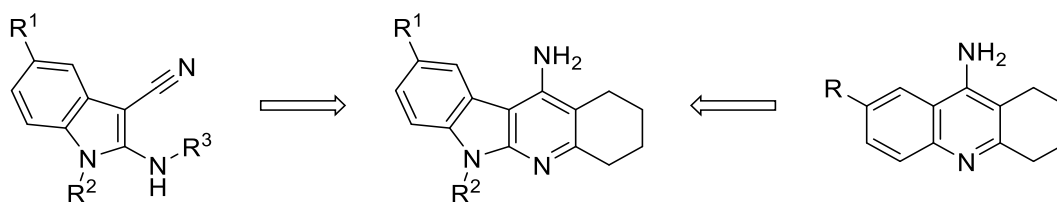


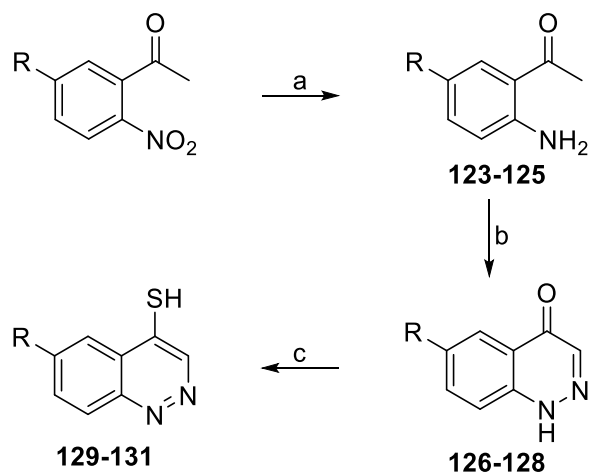
**Figure 17.** Compounds **119-122** based follow-up design of indolotacrine series compounds [162].

### 3.3.6. Derivatives of National Cancer Institute Diversity IV library hits

#### Design and chemistry

Yet another library screen was performed by Dr. Patrick Guest (collaborating workgroup of prof. Frank Gunn-Moore, University of St. Andrews). National Cancer Institute (NCI) Diversity IV compound library was screened with ABAD assay at fixed concentration (100  $\mu$ M) to identify novel scaffolds for future investigations. Based on the library evaluation, compound 17796 (cinnolin-4-thiol) showed a particular interest and additional analogues were screened. Several analogues showed promising inhibition activities towards ABAD. However, upon closer investigation of obtained data, an assumption of possible formation of disulphide bond between cinnolin-4-thiol and enzyme did arise [163].

In order to investigate the hypothesis, a small series of 4,6-disubstituted cinnoline analogues was designed. While cinnolines with 4-amino- and 4-chloro- substitutions were commercially available, cinnoline-4-ones and cinnoline-4-thioles were synthesised. 6-Halogencinnolin-4-thiols were prepared in following three-step process. 1-(2-Amino-5-halogenphenyl)ethan-1-ones (**123-125**) were prepared with reduction of their corresponding nitro analogues (Scheme 12a). Subsequent diazotization (Scheme 12b) followed by ring closure yielded 6-halogencinnolin-4-ones (**126-129**). Final oxygen-sulphur exchange was readily achieved with Lawesson's reagent (Scheme 12c) to obtain desired 6-halogencinnolin-4-thiols (**129-131**).



**Scheme 12:** Synthesis of **123-131**. Reagents and conditions: (a) H<sub>2</sub>, Pd/C, EtOH, RT. (b) NaNO<sub>2</sub>, 6 M HCl, 0°C to RT (overnight), reflux (6 h). (c) Lawesson's reagent, toluene, reflux.

## **Results and discussion**

Study of these compounds was a subject of Dr. Patrick Guest dissertation work, therefore detailed compounds investigation is available in his dissertation [163]. Briefly, compounds **126-131** along with purchased 4-amino and 4-chloro cinnoline derivatives were evaluated for inhibition of ABAD. Only compounds with thiol group demonstrated ability to inhibit ABAD. Additionally, observed ABAD inhibition could be reversed by addition of DTT (dithiothreitol), which further supports originally hypothesis of disulphide bond formation between cinnolin-4-thiol and ABAD. Therefore, investigation of this scaffold was no longer followed [163].

## 4. Conclusion

In summary, about 90 final compounds (78 novel and 12 already reported compounds) were designed, synthesised and evaluated for their potential to inhibit ABAD enzymatic function. Initial series allowed identification of essential structural features underlining the inhibition activity towards ABAD. Scaffold of the most promising compounds builds on benzothiazole moiety attached to additional distal aromatic moiety via urea linker. Diversity of prepared compounds demonstrated, that the most significant features for inhibitory activity lies in proper substitution pattern of distal phenyl ring. The crucial factor is the presence of phenolic group. Although several positional isomers displayed moderate ABAD inhibitory activity, *para* position was the most favoured one. Additionally, presence of chlorine in *meta* position greatly improved activity of the compounds reaching low micromolar IC<sub>50</sub> values (~1-2 μM). Similar inhibition levels were retained for compounds with both occupied *meta* positions (3,5-chloro-4-hydroxyphenyl). Exchange of chlorine with other halogens also demonstrated comparable IC<sub>50</sub> values. Any other substitution of distal phenyl ring did not show any enhancement over 3-halogen-4-hydroxyphenyl substitution pattern. Further modifications to linker or benzothiazole part of the scaffold did not yield any more potent ABAD inhibitors than described earlier. However, several compounds with improved physical-chemical properties managed to retain comparable potency (low micromolar range of IC<sub>50</sub>) with parent ones.

Needless to say, presented work is one of the integral parts of assoc. prof. Kamil Musílek long-term project. Therefore, it is necessary to look at these results from a wider perspective of whole project. About 250 compounds (including those presented in this work) were prepared and already evaluated (though further experiments are still ongoing). Initial biological evaluation and assessment of these results allowed building a substantial pool of compounds for elucidation of structure and activity relationships. However to date, only a limited number of experiments were employed. The most importantly, whole pool of compounds is going to be screened for modulation of Aβ-ABAD interaction, which will allow cross-examining whole data set and distinguishing structural features necessary for inhibition of ABAD and Aβ-ABAD interaction. Most promising compounds were selected for further experiments, which are already in progress. These experiments include cell-based monitoring of ABAD activity in presence of selected inhibitors, selectivity studies towards other types of 17β-hydroxysteroid dehydrogenases, *in vivo* toxicity and bioavailability studies (on mice and rats) or determination of pharmacokinetic properties.

## 5. Experimental section

### 5.1. Chemicals and instrumentation

All reagents and solvents were purchased from commercial sources (Sigma Aldrich, Activate Scientific, Alfa Aesar, Merck, Penta Chemicals and VWR) and they were used without any further purification. Low boiling point ( $\geq 90\%$  40-60°C) petroleum ether (PE) was used if not stated otherwise. Thin-layer chromatography (TLC) for reaction monitoring was performed on Merck aluminium sheets, silica gel 60 F<sub>254</sub>. Visualisation was performed either via UV (254 nm) or appropriate stain reagent solutions (alternatively in combination of both). Preparative column chromatography was performed on silica gel 60 (70-230 mesh, 63-200  $\mu\text{m}$ , 60 Å pore size). Melting points were determined on a Stuart SMP30 melting point apparatus and are uncorrected.

Nuclear magnetic resonance (NMR) spectra were acquired at 500/126/202 MHz (<sup>1</sup>H, <sup>13</sup>C and <sup>31</sup>P) on a Varian S500 spectrometer or at 300/75 MHz (<sup>1</sup>H and <sup>13</sup>C) on a Varian Gemini 300 spectrometer. Chemical shifts  $\delta$  are given in ppm and referenced to the signal center of solvent peaks (DMSO-*d*<sub>6</sub>:  $\delta$  2.50 ppm and 39.52 ppm for <sup>1</sup>H and <sup>13</sup>C, respectively; Chloroform-*d*:  $\delta$  7.26 ppm and 77.16 ppm for <sup>1</sup>H and <sup>13</sup>C, respectively), thus indirectly correlated to TMS standard ( $\delta$  0 ppm). Chemical shifts  $\delta$  for <sup>31</sup>P are given in ppm and referenced to the phosphoric acid standard ( $\delta$  0 ppm). Coupling constants are expressed in Hz. Spectra acquisitions were performed by assoc. prof. PharmDr. Jiří Kuneš, C.Sc. workgroup, Department of Inorganic and Organic Chemistry, Faculty of Pharmacy in Hradec Králové, Charles University in Prague.

High-resolution mass spectra (HRMS) were recorded by coupled LCMS system consisting of Dionex UltiMate 3000 analytical LC system and Q Exactive Plus hybrid quadrupole-orbitrap spectrometer. As an ion-source, heated electro-spray ionization (HESI) was utilised (setting: sheath gas flow rate 40, aux gas flow rate 10, sweep gas flow rate 2, spray voltage 3.2 kV, capillary temperature 350°C, aux gas temperature 300°C, S-lens RF level 50. Positive ions were monitored in the range of 100 – 1500 m/z with the resolution set to 140 000. Obtained mass spectra were processed in Xcalibur 3.0.63 software. Spectra assessments were performed by Mgr. *et* Mgr. Rafael Doležal, Ph.D. workgroup, Biomedical Research Centre, University Hospital in Hradec Králové.

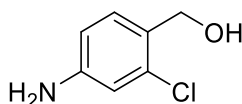
Elemental analyses (EA) were carried out on CE Instruments EA-1110 CHN (CE Instruments, Wigan, UK) and Micro Cube Elemental Analyzer (Elementar Analysensysteme GmbH, Hanau, Germany). Data acquisitions were performed by prof. PharmDr. Martin Doležal, Ph.D. workgroup, Department of Pharmaceutical Chemistry and Drug Control, Faculty of Pharmacy in Hradec Králové, Charles University in Prague.

## 5.2. Synthesis and characterisation data of intermediates and final compounds

Synthesis procedures and characterisation data for compounds **1-23** and their intermediates are included in attachment A2 [136].

Synthesis procedures and characterisation data for compounds **33-50** and their intermediates are included in attachment A3 [154].

### (4-Amino-2-chlorophenyl)methanol (**51**)



**51**

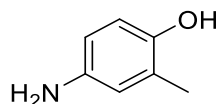
Lithium aluminium hydride (9 mmol, 0.34 g) was suspended in anhydrous THF (5 mL) at  $-5^{\circ}\text{C}$  and suspension was stirred 1 h at  $-5^{\circ}\text{C}$  under nitrogen atmosphere. Solution of 4-amino-2-chlorobenzoic acid (3 mmol, 0.51 g) in anhydrous THF (3 mL) was added dropwise over the 30 min time period [164]. The reaction mixture was allowed to reach RT and stirred overnight. The reaction was quenched with  $\text{H}_2\text{O}$ , alkalisied with saturated  $\text{NaHCO}_3$  solution and extracted to EtOAc ( $3 \times 25$  mL). The organic layers were combined, dried over anhydrous  $\text{Na}_2\text{SO}_4$  and solvent was removed under reduced pressure. The residue was purified by column chromatography ( $\text{CHCl}_3:\text{MeOH}$ , 500:1) to yield (4-amino-2-chlorophenyl)methanol as a beige solid (0.46 g, 98%).

$^1\text{H}$  NMR (500 MHz,  $\text{DMSO}-d_6$ )  $\delta$  7.11 (d,  $J = 8.2$  Hz, 1H), 6.57 (d,  $J = 2.2$  Hz, 1H), 6.49 (dd,  $J = 8.2, 2.2$  Hz, 1H), 5.26 (s, 2H), 4.95 (t,  $J = 5.5$  Hz, 1H), 4.37 (d,  $J = 5.5$  Hz, 2H).

### Procedure A (general conditions): Palladium on activated carbon catalysed hydrogenation (**52, 60-62, 109**)

A nitrobenzene/imine derivative was dissolved in EtOH and palladium on activated carbon (Pd/C, 10%, 0.05 eq) was added. The hydrogen atmosphere was introduced and the mixture was stirred at RT overnight [165]. The mixture was filtered through celite pad and solvent was removed under reduced pressure to yield corresponding final compound.

### 4-Amino-2-methylphenol (**52**)



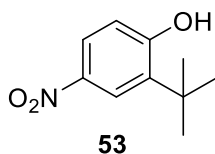
**52**

Beige solid, yield 99%, mp ND.

$^1\text{H}$  NMR (500 MHz,  $\text{DMSO}-d_6$ )  $\delta$  8.13 (s, 1H), 6.46 (d,  $J = 8.3$  Hz, 1H), 6.32 (d,  $J = 2.6$  Hz, 1H), 6.22 (dd,  $J = 8.3, 2.7$  Hz, 1H), 4.27 (br s, 2H), 2.00 (s, 3H).



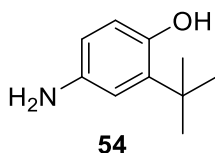
### 2-(*Tert*-butyl)-4-nitrophenol (53)



The solution of 2-(*tert*-butyl)phenol (3 mmol, 0.45 g) in glacial acetic acid (4 mL) was cooled to 5°C and the mixture of nitric acid (3 mmol, 0.19 mL, 70%) in glacial acetic acid (1 mL) was added drop-wise. Reaction mixture was allowed to reach RT and stirred for next 2 h [166]. Then, reaction mixture was poured to cooled H<sub>2</sub>O (50 mL) and precipitate was collected by suction filtration. The residue was purified by column chromatography (heptane:EtOAc, 25:1) to yield 2-(*tert*-butyl)-4-nitrophenol as a dark red solid (0.24 g, 41%).

<sup>1</sup>H NMR (500 MHz, Chloroform-*d*) δ 8.22 (d, *J* = 2.7 Hz, 1H), 8.01 (dd, *J* = 8.7, 2.7 Hz, 1H), 6.76 (d, *J* = 8.7 Hz, 1H), 5.91 (s, 1H), 1.44 (s, 9H).

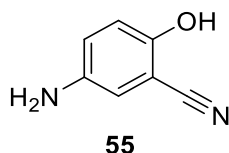
### 4-Amino-2-(*tert*-butyl)phenol (54)



Ammonium chloride (8 mmol, 0.43 g) and iron powder (20 mmol, 1.12 g) were added to the solution of 2-(*tert*-butyl)-4-nitrophenol (2 mmol, 0.40 g) in MeOH:H<sub>2</sub>O (5 mL, 1:1) and the reaction mixture was stirred at RT for next 2 h [167]. The mixture was diluted with THF, filtered through celite pad and solvent was removed under reduced pressure. Crude residue was purified by column chromatography (heptane:EtOAc, 3:1) to yield 4-amino-2-(*tert*-butyl)phenol as a beige solid (0.22 g, 67%).

<sup>1</sup>H NMR (300 MHz, Chloroform-*d*) δ 6.66 (d, *J* = 2.6 Hz, 1H), 6.50 (d, *J* = 8.2 Hz, 1H), 6.43 (dd, *J* = 8.2, 2.7 Hz, 1H), 1.38 (s, 9H).

### 5-Amino-2-hydroxybenzonitrile (55)

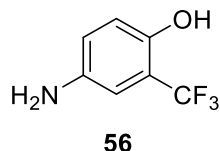


5-Amino-2-methoxybenzonitrile (2 mmol, 0.30 g) was suspended in anhydrous DCM (20 mL). Then, aluminium chloride (7 mmol, 0.93 g) was added and the reaction mixture was heated at reflux overnight. After the reaction was completed (monitored by TLC), water was slowly poured in and the reaction mixture was stirred for another 15 mins. Then the product was extracted to EtOAc (3 × 25 mL), organic layer was washed with brine, dried over anhydrous Na<sub>2</sub>SO<sub>4</sub> and

solvent was removed under reduced pressure. The crude product was purified by column chromatography (CHCl<sub>3</sub>:MeOH, 200:1) to obtain 5-amino-2-hydroxybenzonitrile as an orange solid (0.24 g, 88%) and used directly in next synthesis step.

HRMS (ESI) calcd for C<sub>7</sub>H<sub>7</sub>N<sub>2</sub>O [M+H]<sup>+</sup> 135.05529, found 135.05533.

#### 4-Amino-2-(trifluoromethyl)phenol (**56**)

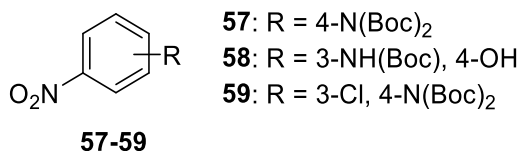


4-Methoxy-3-(trifluoromethyl)aniline (1.31 mmol, 0.25 g) was dissolved in glacial acetic acid (3.5 mL) and hydrobromic acid (3.5 mL, 40%). The reaction mixture was heated at reflux for next 20 h. The solution was neutralised with saturated NaHCO<sub>3</sub> solution. Aqueous layer was extracted with EtOAc (3 × 25 mL). Combined organic layers were washed with brine, dried over anhydrous Na<sub>2</sub>SO<sub>4</sub> and solvent was removed under reduced pressure. The crude residue was purified by column chromatography (CHCl<sub>3</sub>:MeOH, 30:1) to yield 4-amino-2-(trifluoromethyl)phenol as an off-white solid (65%).

<sup>1</sup>H NMR (500 MHz, DMSO-*d*<sub>6</sub>) δ 9.30 (s, 1H), 6.75 – 6.70 (m, 2H), 6.67 (dd, *J* = 8.6, 2.6 Hz, 1H), 4.95 (br s, 2H).

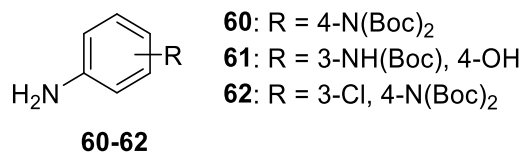
HRMS (ESI) calcd for C<sub>7</sub>H<sub>7</sub>F<sub>3</sub>NO [M+H]<sup>+</sup> 178.04742, found 178.04729.

#### Procedure B (general conditions): *N*-Boc-protection (**57-59**)



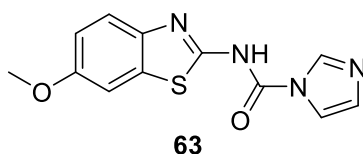
The mixture of an nitro-substituted aromatic amine (3 mmol) and DMAP (0.15 mmol) in anhydrous THF (15 mL) was cooled to 0°C and solution of *tert*-butyl-dicarbonate (6.15 mmol for **57** and **59**; 3.05 mmol for **58**) in anhydrous THF (5 mL) was added drop-wise. Reaction mixture was allowed to reach RT, stirred overnight and heated at 65°C for 2 h to complete the reaction [168]. Solvent was removed under reduced pressure, residue was diluted with EtOAc (75 mL), washed with citric acid (15%, 2 × 15 mL), water (15 mL) and brine (15 mL). Organic layer was dried over anhydrous Na<sub>2</sub>SO<sub>4</sub>, solvent removed under reduced pressure and crude residue was used without further purification.

### *N*-Boc-protected nitro-derivatives (60-62)



Procedure A (Pd/C catalysed hydrogenation) was used to obtain corresponding *N*-Boc-protected aniline derivative and crude product was used in next step without further purification.

### *N*-(6-Methoxybenzo[*d*]thiazol-2-yl)-1*H*-imidazole-1-carboxamide (63)

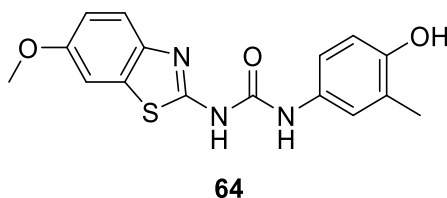


*N,N'*-Carbonyldiimidazole (12 mmol, 1.95 g) was added to a solution of 6-methoxybenzo[*d*]thiazol-2-amine (10 mmol, 1.80 g) in anhydrous DCM (50 mL) and the reaction was heated at reflux for 20 h. The reaction mixture was cooled down to 2-8°C, precipitate was collected by suction filtration and washed with cold DCM [154]. The crude product was dried under reduced pressure to yield *N*-(6-methoxybenzo[*d*]thiazol-2-yl)-1*H*-imidazole-1-carboxamide (**63**) as a white solid (2.72 g, 99%) and used in next reaction step without further purification.

### Procedure C (general conditions): 1-Aryl-3-(6-methoxybenzo[*d*]thiazol-2-yl)ureas (64-76)

An aromatic amine (1.1 mmol) was added to the suspension of *N*-(6-methoxybenzo[*d*]thiazol-2-yl)-1*H*-imidazole-1-carboxamide (1 mmol) in anhydrous acetonitrile (15 mL) and the reaction was heated at reflux for 20 h [154]. The reaction was cooled to RT, quenched with water (1 M HCl in presence of phenolic group) and the precipitate was collected by suction filtration. The crude product was recrystallised from Et<sub>2</sub>O:MeOH and dried to constant weight yielding corresponding 1-aryl-3-(6-methoxybenzo[*d*]thiazol-2-yl)ureas (**64-76**).

### 1-(4-Hydroxy-3-methylphenyl)-3-(6-methoxybenzo[*d*]thiazol-2-yl)urea (64)



Light-pink solid, yield 85%, mp 262-263°C.

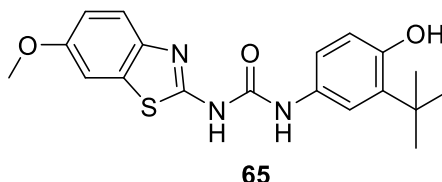
<sup>1</sup>H NMR (500 MHz, DMSO-*d*<sub>6</sub>) δ 10.55 (br s, 1H), 9.09 (s, 1H), 8.77 (s, 1H), 7.54 (d, *J* = 8.8 Hz, 1H), 7.50 (d, *J* = 2.6 Hz, 1H), 7.18 (d, *J* = 2.6 Hz, 1H), 7.10 (dd, *J* = 8.5, 2.7 Hz, 1H), 6.97 (dd, *J* = 8.8, 2.6 Hz, 1H), 6.73 (d, *J* = 8.5 Hz, 1H), 3.79 (s, 3H), 2.12 (s, 3H).

$^{13}\text{C}$  NMR (126 MHz,  $\text{DMSO-}d_6$ )  $\delta$  157.57, 155.61, 151.75, 151.47, 142.84, 132.53, 129.56, 124.11, 122.24, 120.13, 118.18, 114.64, 114.29, 104.87, 55.60, 16.12.

HRMS (ESI) calcd for  $\text{C}_{16}\text{H}_{16}\text{N}_3\text{O}_3\text{S}$   $[\text{M}+\text{H}]^+$  330.09069, found 330.09039.

Anal. Calcd for  $\text{C}_{16}\text{H}_{15}\text{N}_3\text{O}_3\text{S}$ : C, 58.35; H, 4.59; N, 12.76; S, 9.73. Found C, 58.05; H, 4.58; N, 12.70; S, 10.01.

### 1-(3-(*Tert*-butyl)-4-hydroxyphenyl)-3-(6-methoxybenzo[*d*]thiazol-2-yl)urea (65)



Beige solid, yield 73%, mp 259-260°C.

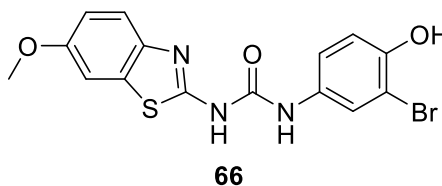
$^1\text{H}$  NMR (500 MHz,  $\text{DMSO-}d_6$ )  $\delta$  10.47 (br s, 1H), 9.18 (br s, 1H), 8.79 (s, 1H), 7.54 (d,  $J = 8.8$  Hz, 1H), 7.49 (d,  $J = 2.6$  Hz, 1H), 7.19 (d,  $J = 2.6$  Hz, 1H), 7.17 (dd,  $J = 8.4, 2.6$  Hz, 1H), 6.97 (dd,  $J = 8.8, 2.6$  Hz, 1H), 6.73 (d,  $J = 8.4$  Hz, 1H), 3.79 (s, 3H), 1.35 (s, 9H).

$^{13}\text{C}$  NMR (126 MHz,  $\text{DMSO-}d_6$ )  $\delta$  157.50, 155.61, 151.91, 151.84, 142.82, 135.53, 132.60, 129.43, 120.20, 118.58, 118.38, 116.13, 114.28, 104.90, 55.62, 34.35, 29.25.

HRMS (ESI) calcd for  $\text{C}_{19}\text{H}_{22}\text{N}_3\text{O}_3\text{S}$   $[\text{M}+\text{H}]^+$  372.13764, found 372.13730.

Anal. Calcd for  $\text{C}_{19}\text{H}_{21}\text{N}_3\text{O}_3\text{S}$ : C, 61.44; H, 5.70; N, 11.31; S, 8.63. Found C, 61.23; H, 5.52; N, 11.46; S, 8.94.

### 1-(3-Bromo-4-hydroxyphenyl)-3-(6-methoxybenzo[*d*]thiazol-2-yl)urea (66)



White solid, yield 82%, mp 246-247°C.

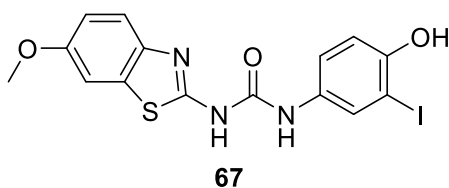
$^1\text{H}$  NMR (500 MHz,  $\text{DMSO-}d_6$ )  $\delta$  10.71 (br s, 1H), 9.99 (s, 1H), 8.97 (s, 1H), 7.75 (s, 1H), 7.54 (d,  $J = 8.4$  Hz, 1H), 7.50 (s, 1H), 7.22 (d,  $J = 8.6$  Hz, 1H), 6.97 (d,  $J = 8.5$  Hz, 1H), 6.92 (d,  $J = 8.6$  Hz, 1H), 3.79 (s, 3H).

$^{13}\text{C}$  NMR (126 MHz,  $\text{DMSO-}d_6$ )  $\delta$  157.84, 155.67, 152.21, 149.97, 142.25, 132.33, 131.04, 123.65, 120.14, 119.87, 116.28, 114.37, 108.86, 104.95, 55.61.

HRMS (ESI) calcd for  $\text{C}_{15}\text{H}_{13}\text{BrN}_3\text{O}_3\text{S}$   $[\text{M}+\text{H}]^+$  393.98555, found 393.98489.

Anal. Calcd for  $\text{C}_{15}\text{H}_{12}\text{BrN}_3\text{O}_3\text{S}$ : C, 45.70; H, 3.07; N, 10.66; S, 8.13. Found C, 45.73; H, 2.91; N, 10.70; S, 8.22.

**1-(4-Hydroxy-3-iodophenyl)-3-(6-methoxybenzo[d]thiazol-2-yl)urea (67)**



White solid, yield 85%, mp 241-242°C.

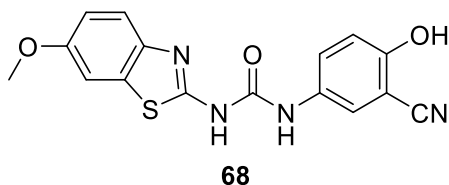
$^1\text{H}$  NMR (300 MHz, DMSO- $d_6$ )  $\delta$  10.07 (br s, 1H), 9.05 (s, 1H), 7.90 (d,  $J$  = 2.6 Hz, 1H), 7.54 (d,  $J$  = 8.8 Hz, 1H), 7.51 (d,  $J$  = 2.6 Hz, 1H), 7.25 (dd,  $J$  = 8.7, 2.6 Hz, 1H), 6.97 (dd,  $J$  = 8.8, 2.6 Hz, 1H), 6.85 (d,  $J$  = 8.7 Hz, 1H), 3.79 (s, 3H).

$^{13}\text{C}$  NMR (75 MHz, DMSO- $d_6$ )  $\delta$  157.72, 155.67, 152.67, 152.10, 142.15, 132.35, 131.29, 129.42, 120.99, 119.93, 114.75, 114.38, 104.93, 84.10, 55.62.

HRMS (ESI) calcd for  $\text{C}_{15}\text{H}_{13}\text{IN}_3\text{O}_3\text{S}$   $[\text{M}+\text{H}]^+$  441.97168, found 441.97049.

Anal. Calcd for  $\text{C}_{15}\text{H}_{12}\text{IN}_3\text{O}_3\text{S}$ : C, 40.83; H, 2.74; N, 9.52; S, 7.27. Found C, 40.49; H, 2.70; N, 9.19; S, 7.14.

**1-(3-Cyano-4-hydroxyphenyl)-3-(6-methoxybenzo[d]thiazol-2-yl)urea (68)**



Off-white solid, 98% yield, mp 277-279°C.

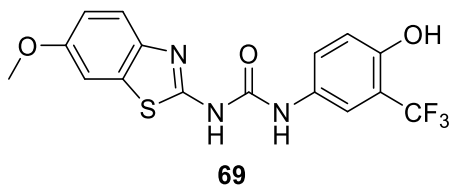
$^1\text{H}$  NMR (500 MHz, DMSO- $d_6$ ):  $\delta$  10.86 (s, 1H), 9.37 (s, 1H), 7.76 (d,  $J$  = 2.7 Hz, 1H), 7.56 – 7.52 (m, 2H), 7.51 (d,  $J$  = 2.6 Hz, 1H), 7.01 (d,  $J$  = 9.0 Hz, 1H), 6.98 (dd,  $J$  = 8.8, 2.6 Hz, 1H), 3.79 (s, 3H).

$^{13}\text{C}$  NMR (126 MHz, DMSO- $d_6$ ):  $\delta$  157.84, 156.05, 155.71, 152.44, 141.78, 132.24, 130.54, 126.52, 122.87, 119.79, 116.80, 116.73, 114.40, 105.00, 98.49, 55.61.

HRMS (ESI) calcd for  $\text{C}_{16}\text{H}_{13}\text{N}_4\text{O}_3\text{S}$   $[\text{M}+\text{H}]^+$  341.07029, found 341.07016.

Anal. Calcd for  $\text{C}_{16}\text{H}_{12}\text{N}_4\text{O}_3\text{S}$ : C, 56.46; H, 3.55; N, 16.46; S, 9.42. Found C, 56.67; H, 3.72; N, 16.29; S, 9.66.

**1-(4-Hydroxy-3-(trifluoromethyl)phenyl)-3-(6-methoxybenzo[d]thiazol-2-yl)urea (69)**



White solid, yield 64%, mp 260-262°C.

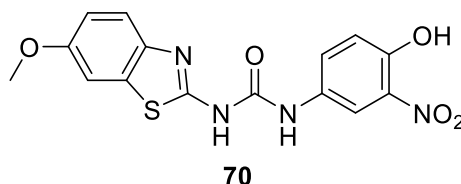
$^1\text{H}$  NMR (500 MHz, DMSO- $d_6$ )  $\delta$  10.35 (s, 1H), 9.74 (s, 1H), 7.74 (s, 1H), 7.55 (d,  $J = 9.0$  Hz, 1H), 7.51 (s, 1H), 7.47 (d,  $J = 9.1$  Hz, 1H), 7.03 (d,  $J = 8.9$  Hz, 1H), 6.98 (d,  $J = 9.1$  Hz, 1H), 3.79 (s, 3H).

$^{13}\text{C}$  NMR (126 MHz, DMSO- $d_6$ )  $\delta$  157.77, 155.77, 152.25, 151.45, 141.75, 132.25, 129.91, 124.99 (q,  $J = 273.1$  Hz), 124.82, 119.85, 117.49, 117.15 (q,  $J = 5.3$  Hz), 115.17 (q,  $J = 30.3$  Hz), 114.49, 105.01, 55.66.

HRMS (ESI) calcd for  $\text{C}_{16}\text{H}_{13}\text{F}_3\text{N}_3\text{O}_3\text{S}$   $[\text{M}+\text{H}]^+$  384.06242, found 384.06210.

Anal. Calcd for  $\text{C}_{16}\text{H}_{12}\text{F}_3\text{N}_3\text{O}_3\text{S}$ : C, 50.13; H, 3.16; N, 10.96; S, 8.36. Found C, 49.89; H, 3.01; N, 11.22; S, 8.39.

#### 1-(4-Hydroxy-3-nitrophenyl)-3-(6-methoxybenzo[*d*]thiazol-2-yl)urea (70)



Yellow solid, yield 99%, mp 263-264.5°C.

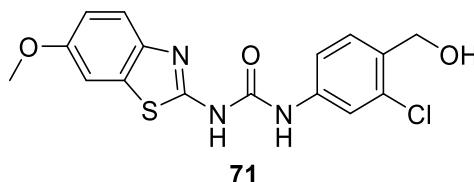
$^1\text{H}$  NMR (500 MHz, DMSO- $d_6$ )  $\delta$  10.90 (br s, 1H), 9.26 (s, 1H), 8.22 (d,  $J = 2.7$  Hz, 1H), 7.59 (dd,  $J = 9.0, 2.7$  Hz, 1H), 7.53 (d,  $J = 8.8$  Hz, 1H), 7.50 (d,  $J = 2.6$  Hz, 1H), 7.12 (d,  $J = 9.0$  Hz, 1H), 6.98 (dd,  $J = 8.8, 2.6$  Hz, 1H), 3.79 (s, 3H).

$^{13}\text{C}$  NMR (126 MHz, DMSO- $d_6$ )  $\delta$  158.16, 155.74, 152.69, 148.06, 135.86, 132.13, 130.51, 127.12, 119.61, 114.79, 114.45, 105.04, 55.63.

HRMS (ESI) calcd for  $\text{C}_{15}\text{H}_{13}\text{N}_4\text{O}_5\text{S}$   $[\text{M}+\text{H}]^+$  361.06012, found 361.05987.

Anal. Calcd for  $\text{C}_{15}\text{H}_{12}\text{N}_4\text{O}_5\text{S}$ : C, 50.00; H, 3.36; N, 15.55; S, 8.90. Found C, 49.81; H, 3.17; N, 15.46; S, 8.94.

#### 1-(3-Chloro-4-(hydroxymethyl)phenyl)-3-(6-methoxybenzo[*d*]thiazol-2-yl)urea (71)



Off-white solid, yield 92%, mp 229-230°C.

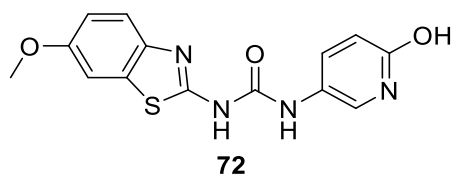
$^1\text{H}$  NMR (500 MHz,  $\text{DMSO-}d_6$ )  $\delta$  10.84 (br s, 1H), 9.26 (s, 1H), 7.72 (d,  $J = 2.2$  Hz, 1H), 7.55 (d,  $J = 8.7$  Hz, 1H), 7.51 (d,  $J = 2.6$  Hz, 1H), 7.47 (d,  $J = 8.4$  Hz, 1H), 7.38 (dd,  $J = 8.4$  Hz, 2.1 Hz, 1H), 6.98 (dd,  $J = 8.8, 2.6$  Hz, 1H), 5.29 (t,  $J = 5.6$  Hz, 1H), 4.53 (d,  $J = 5.2$  Hz, 2H), 3.80 (s, 3H).

$^{13}\text{C}$  NMR (126 MHz,  $\text{DMSO-}d_6$ )  $\delta$  157.75, 155.74, 152.27, 138.45, 133.63, 132.18, 131.19, 128.67, 127.18, 119.85, 118.56, 117.35, 114.44, 105.01, 59.99, 55.61.

HRMS (ESI) calcd for  $\text{C}_{16}\text{H}_{15}\text{ClN}_3\text{O}_3\text{S}$   $[\text{M}+\text{H}]^+$  364.05172, found 364.05103.

Anal. Calcd for  $\text{C}_{16}\text{H}_{14}\text{ClN}_3\text{O}_3\text{S}$ : C, 52.82; H, 3.88; N, 11.55; S, 8.81. Found C, 52.84; H, 3.73; N, 11.59; S, 9.11.

### 1-(6-Hydroxypyridin-3-yl)-3-(6-methoxybenzo[d]thiazol-2-yl)urea (72)



Light-brown solid, yield 82%, mp 272-273°C.

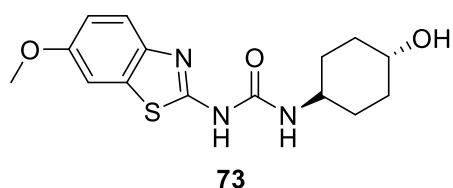
$^1\text{H}$  NMR (300 MHz,  $\text{DMSO-}d_6$ )  $\delta$  11.38 (br s, 1H), 9.08 (br s, 1H), 7.64 (s, 1H), 7.59 (d,  $J = 9.1$  Hz, 1H), 7.53 – 7.39 (m, 2H), 6.97 (dd,  $J = 9.2, 2.6$  Hz, 1H), 6.36 (d,  $J = 10.1$  Hz, 1H), 3.79 (s, 3H).

$^{13}\text{C}$  NMR (75 MHz,  $\text{DMSO-}d_6$ )  $\delta$  160.85, 158.50, 155.83, 153.21, 142.19, 138.04, 132.42, 127.92, 120.11, 119.28, 119.17, 114.49, 105.11, 55.78.

HRMS (ESI) calcd for  $\text{C}_{14}\text{H}_{13}\text{N}_4\text{O}_3\text{S}$   $[\text{M}+\text{H}]^+$  317.07029, found 317.07004.

Anal. Calcd for  $\text{C}_{14}\text{H}_{12}\text{N}_4\text{O}_3\text{S}$ : C, 53.16; H, 3.82; N, 17.71; S, 10.13. Found C, 52.86; H, 3.96; N, 17.52; S, 9.98.

### 1-((1S,4S)-4-hydroxycyclohexyl)-3-(6-methoxybenzo[d]thiazol-2-yl)urea (73)



White solid, yield 91%, mp 203-204°C.

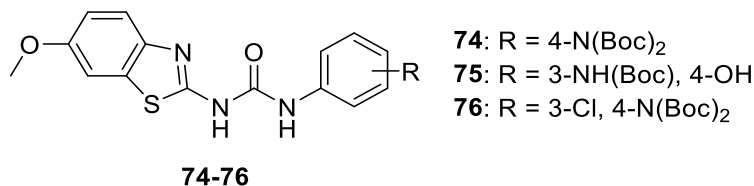
$^1\text{H}$  NMR (500 MHz,  $\text{DMSO-}d_6$ )  $\delta$  10.25 (br s, 1H), 7.49 (d,  $J = 8.8$  Hz, 1H), 7.47 (d,  $J = 2.6$  Hz, 1H), 6.94 (dd,  $J = 8.7, 2.6$  Hz, 1H), 6.60 (d,  $J = 7.7$  Hz, 1H), 4.54 (d,  $J = 4.3$  Hz, 1H), 3.78 (s, 3H), 3.50 – 3.39 (m, 2H), 1.92 – 1.74 (m, 4H), 1.31 – 1.15 (m, 4H).

$^{13}\text{C}$  NMR (126 MHz,  $\text{DMSO-}d_6$ )  $\delta$  157.71, 155.46, 153.00, 143.21, 132.57, 120.13, 114.07, 104.81, 67.77, 55.55, 47.98, 33.59, 30.41.

HRMS (ESI) calcd for  $\text{C}_{15}\text{H}_{20}\text{N}_3\text{O}_3\text{S}$   $[\text{M}+\text{H}]^+$  322.12199, found 322.12137.

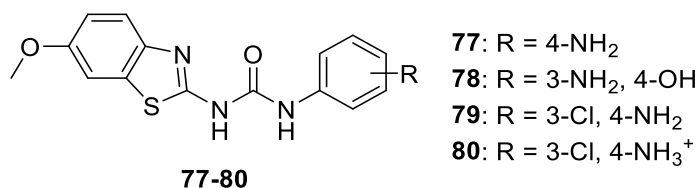
Anal. Calcd for C<sub>15</sub>H<sub>19</sub>N<sub>3</sub>O<sub>3</sub>S: C, 56.06; H, 5.96; N, 13.07; S, 9.98. Found C, 56.04; H, 5.79; N, 13.11; S, 10.26.

#### *N*-Boc-protected urea derivatives (74-76)



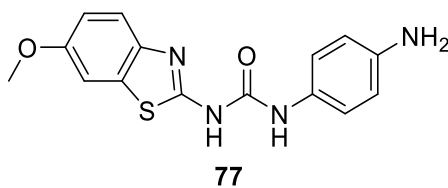
Compounds **74-76** were used in next step (*N*-Boc cleavage) without further analysis/purification.

#### Procedure D (general conditions): *N*-Boc-cleavage of *N*-Boc-protected derivatives (77-80)



*N*-Boc-protected urea derivative (**74-76**, 1 mmol) was stirred for 24 h in 4 M HCl-dioxane solution (10 mL) [168]. Reaction mixture was diluted with Et<sub>2</sub>O (50 mL) to achieve complete hydrochloride salt precipitation, which was collected by suction filtration. Solution of 1 M NaOH was added to the mixture of hydrochloride salt in H<sub>2</sub>O to achieve desired pH value and mixture was stirred for next 2 h. Final precipitate was collected by suction filtration, dried and recrystallised (Et<sub>2</sub>O:MeCN, 5:1) to yield corresponding urea derivatives (**77-80**).

#### 1-(4-Aminophenyl)-3-(6-methoxybenzo[d]thiazol-2-yl)urea (**77**)



White solid, yield 93%, mp 304-306°C (decomp).

<sup>1</sup>H NMR (500 MHz, DMSO-*d*<sub>6</sub>) δ 10.46 (br s, 1H), 8.63 (s, 1H), 7.54 (d, *J* = 8.8 Hz, 1H), 7.50 (d, *J* = 2.6 Hz, 1H), 7.15 – 7.10 (m, 2H), 6.96 (dd, *J* = 8.8, 2.6 Hz, 1H), 6.57 – 6.52 (m, 2H), 4.90 (s, 2H), 3.79 (s, 3H).

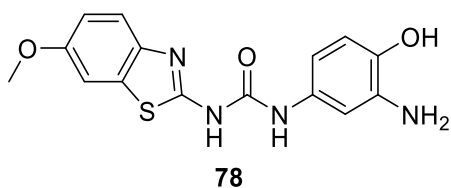
<sup>13</sup>C NMR (126 MHz, DMSO-*d*<sub>6</sub>) δ 157.58, 155.56, 151.75, 144.96, 142.74, 132.56, 127.01, 121.23, 120.12, 114.23, 114.05, 104.87, 55.58.

HRMS (ESI) calcd for C<sub>15</sub>H<sub>15</sub>N<sub>4</sub>O<sub>2</sub>S [M+H]<sup>+</sup> 315.09102, found 315.09058.

Anal. Calcd for C<sub>15</sub>H<sub>14</sub>N<sub>4</sub>O<sub>2</sub>S: C, 57.31; H, 4.49; N, 17.82; S, 10.20. Found C, 57.07; H, 4.34; N, 11.60; S, 10.54.



### 1-(3-Amino-4-hydroxyphenyl)-3-(6-methoxybenzo[d]thiazol-2-yl)urea (78)



Beige solid, yield 53%, mp 180-181°C.

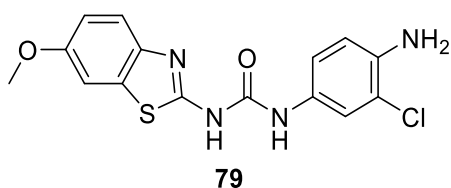
$^1\text{H}$  NMR (500 MHz, DMSO- $d_6$ )  $\delta$  10.41 (br s, 1H), 8.76 (br s, 1H), 8.65 (s, 1H), 7.53 (d,  $J$  = 8.8 Hz, 1H), 7.49 (d,  $J$  = 2.6 Hz, 1H), 6.96 (dd,  $J$  = 8.8, 2.6 Hz, 1H), 6.82 (d,  $J$  = 2.6 Hz, 1H), 6.57 (d,  $J$  = 8.3 Hz, 1H), 6.47 (dd,  $J$  = 8.3, 2.5 Hz, 1H), 4.61 (s, 2H), 3.79 (s, 3H).

$^{13}\text{C}$  NMR (126 MHz, DMSO- $d_6$ )  $\delta$  157.45, 155.57, 151.34, 143.00, 140.11, 136.90, 132.57, 130.42, 122.10, 120.22, 114.24, 107.26, 106.17, 104.84, 55.58.

HRMS (ESI) calcd for  $\text{C}_{15}\text{H}_{15}\text{N}_4\text{O}_3\text{S}$   $[\text{M}+\text{H}]^+$  331.08594, found 331.08527.

Anal. Calcd for  $\text{C}_{15}\text{H}_{14}\text{N}_4\text{O}_3\text{S}$ : C, 54.54; H, 4.27; N, 16.96; S, 9.70. Found C, 54.19; H, 4.30; N, 16.75; S, 9.51.

### 1-(4-Amino-3-chlorophenyl)-3-(6-methoxybenzo[d]thiazol-2-yl)urea (79)



Light-yellow solid, yield 78%, mp 310-311°C (decomp).

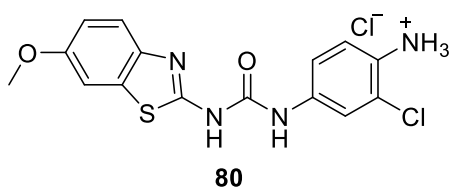
$^1\text{H}$  NMR (500 MHz, DMSO- $d_6$ )  $\delta$  10.60 (br s, 1H), 8.82 (s, 1H), 7.54 (d,  $J$  = 8.7 Hz, 1H), 7.50 (d,  $J$  = 2.6 Hz, 1H), 7.47 (d,  $J$  = 2.4 Hz, 1H), 7.06 (dd,  $J$  = 8.6, 2.4 Hz, 1H), 6.97 (dd,  $J$  = 8.8, 2.6 Hz, 1H), 6.78 (d,  $J$  = 8.6 Hz, 1H), 5.14 (s, 2H), 3.79 (s, 3H).

$^{13}\text{C}$  NMR (126 MHz, DMSO- $d_6$ )  $\delta$  157.69, 155.61, 151.90, 140.78, 132.42, 128.05, 120.50, 120.23, 119.97, 116.77, 115.48, 114.29, 104.91, 55.59.

HRMS (ESI) calcd for  $\text{C}_{15}\text{H}_{14}\text{ClN}_4\text{O}_2\text{S}$   $[\text{M}+\text{H}]^+$  349.05205, found 349.05154.

Anal. Calcd for  $\text{C}_{15}\text{H}_{13}\text{ClN}_4\text{O}_2\text{S}$ : C, 51.65; H, 3.76; N, 16.06; S, 9.19. Found C, 51.94; H, 3.74; N, 15.98; S, 8.94.

### 2-Chloro-4-(3-(6-methoxybenzo[d]thiazol-2-yl)ureido)benzenaminium chloride (80)



Portion of yield was collected in form of hydrochloride prior to 1 M NaOH addition.

White solid, yield 99%, mp 320-322°C (decomp).

$^1\text{H}$  NMR (300 MHz, DMSO- $d_6$ )  $\delta$  10.54 (s, 1H), 10.11 (br s, 3H), 7.84 (d,  $J = 2.3$  Hz, 1H), 7.57 (d,  $J = 2.3$  Hz, 1H), 7.55 – 7.50 (m, 2H), 7.44 (dd,  $J = 8.7, 2.3$  Hz, 1H), 6.99 (dd,  $J = 8.8, 2.6$  Hz, 1H), 3.79 (s, 3H).

$^{13}\text{C}$  NMR (75 MHz, DMSO- $d_6$ )  $\delta$  157.52, 155.84, 152.42, 141.58, 138.66, 132.24, 126.55, 125.32, 124.63, 119.90, 119.19, 118.06, 114.60, 105.03, 55.68.

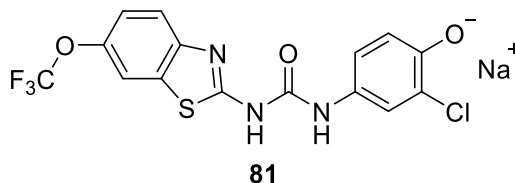
HRMS (ESI) calcd for  $\text{C}_{15}\text{H}_{14}\text{ClN}_4\text{O}_2\text{S}$   $[\text{M}+\text{H}]^+$  349.05205, found 349.05112.

Anal. Calcd for  $\text{C}_{15}\text{H}_{14}\text{Cl}_2\text{N}_4\text{O}_2\text{S}$ : C, 46.76; H, 3.66; N, 14.54; S, 8.32. Found C, 46.38; H, 3.54; N, 14.20; S, 8.12.

### Procedure E (general conditions): Sodium phenolates (81-82)

Phenolic compound (1 mmol) was dissolved in THF, NaOH (3 mmol, 0.12 g) was added and mixture was stirred for 10 minutes. The excess of NaOH was filtered off and solvent was removed under reduced pressure to yield corresponding sodium phenolate.

#### Sodium 2-chloro-4-(3-(6-(trifluoromethoxy)benzo[*d*]thiazol-2-yl)ureido)phenolate (81)

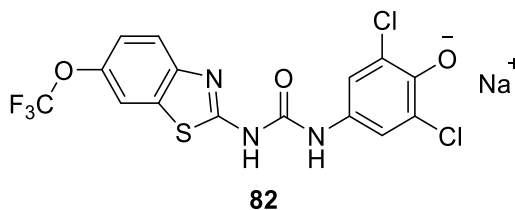


Light brown solid, yield 94%, mp ND.

$^1\text{H}$  NMR (500 MHz, DMSO- $d_6$ )  $\delta$  7.91 (s, 1H), 7.47 (s, 1H), 7.45 (d,  $J = 1.6$  Hz, 1H), 7.16 (d,  $J = 8.7$  Hz, 1H), 6.97 (dd,  $J = 8.6, 1.6$  Hz, 1H), 6.90 (d,  $J = 8.5$  Hz, 1H), 6.39 (d,  $J = 8.4$  Hz, 1H).

HRMS (ESI) calcd for  $\text{C}_{15}\text{H}_{10}\text{ClF}_3\text{N}_3\text{O}_3\text{S}$   $[\text{M}+\text{H}]^+$  404.00780, found 404.00775.

#### Sodium 2,6-dichloro-4-(3-(6-(trifluoromethoxy)benzo[*d*]thiazol-2-yl)ureido)phenolate (82)



Light brown solid, yield 95%, mp ND.

$^1\text{H}$  NMR (500 MHz, DMSO- $d_6$ )  $\delta$  7.81 (s, 1H), 7.43 (d,  $J = 2.5$  Hz, 1H), 7.22 (s, 2H), 7.15 (d,  $J = 8.7$  Hz, 1H), 6.96 (dd,  $J = 8.6, 2.5$  Hz, 1H).

HRMS (ESI) calcd for  $\text{C}_{15}\text{H}_9\text{Cl}_2\text{F}_3\text{N}_3\text{O}_3\text{S}$   $[\text{M}+\text{H}]^+$  437.96883, found 437.96884.

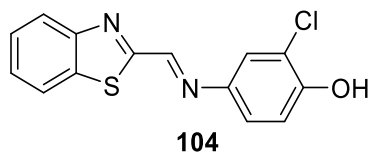
## Compounds 83-103

Compounds **83-103** were prepared by graduate student Mgr. Matěj Chříbek, thus experimental data for selected compounds are included in his Master thesis [155].

### Procedure F (general conditions): Schiff bases synthesis (104-108)

Equimolar amounts of amine and aldehyde were dissolved in toluene (10 mL) and heated at reflux for 48 h. Solvent was removed under reduced pressure and the crude residue was recrystallised (PE:Et<sub>2</sub>O) to yield corresponding product as an yellow solid.

#### (E)-4-((Benzo[d]thiazol-2-ylmethylene)amino)-2-chlorophenol (104)



Yellow solid, yield 95%, mp 242-243°C.

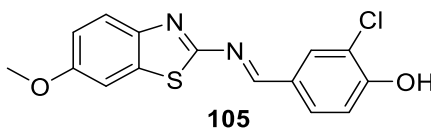
<sup>1</sup>H NMR (500 MHz, DMSO-*d*<sub>6</sub>) δ 10.62 (s, 1H), 8.99 (s, 1H), 8.19 – 8.15 (m, 1H), 8.14 – 8.10 (m, 1H), 7.65 (d, *J* = 2.6 Hz, 1H), 7.61 – 7.53 (m, 2H), 7.41 (dd, *J* = 8.6, 2.6 Hz, 1H), 7.06 (d, *J* = 8.6 Hz, 1H).

<sup>13</sup>C NMR (126 MHz, DMSO-*d*<sub>6</sub>) δ 167.46, 153.55, 153.50, 151.59, 140.62, 134.54, 126.95, 126.78, 123.82, 123.40, 123.10, 122.65, 120.41, 116.82.

HRMS (ESI) calcd for C<sub>14</sub>H<sub>10</sub>ClN<sub>2</sub>OS [M+H]<sup>+</sup> 289.01969, found 289.0195.

Anal. Calcd for C<sub>14</sub>H<sub>9</sub>ClN<sub>2</sub>OS: C, 58.24; H, 3.14; N, 9.70; S, 11.10. Found C, 58.25; H, 3.09; N, 9.61; S, 11.42.

#### (E)-2-Chloro-4-(((6-methoxybenzo[d]thiazol-2-yl)imino)methyl)phenol (105)



Yellow solid, yield 84%, mp 260.5-261.5°C.

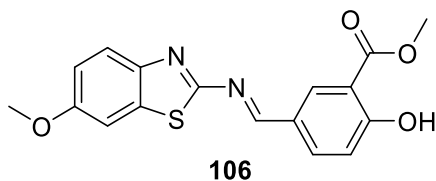
<sup>1</sup>H NMR (500 MHz, DMSO-*d*<sub>6</sub>) δ 11.34 (s, 1H), 8.99 (s, 1H), 8.07 (d, *J* = 2.1 Hz, 1H), 7.90 (dd, *J* = 8.5, 2.1 Hz, 1H), 7.80 (d, *J* = 8.8 Hz, 1H), 7.64 (d, *J* = 2.6 Hz, 1H), 7.14 (d, *J* = 8.5 Hz, 1H), 7.10 (dd, *J* = 8.9, 2.6 Hz, 1H), 3.84 (s, 3H).

<sup>13</sup>C NMR (126 MHz, DMSO-*d*<sub>6</sub>) δ 168.94, 164.36, 157.82, 157.18, 145.55, 135.28, 131.85, 130.29, 127.05, 123.08, 120.64, 117.06, 115.64, 105.09, 55.70.

HRMS (ESI) calcd for C<sub>15</sub>H<sub>12</sub>ClN<sub>2</sub>O<sub>2</sub>S [M+H]<sup>+</sup> 319.03025, found 319.0302.

Anal. Calcd for C<sub>15</sub>H<sub>11</sub>ClN<sub>2</sub>O<sub>2</sub>S: C, 56.52; H, 3.48; N, 8.79; S, 10.06. Found C, 56.43; H, 3.31; N, 8.70; S, 10.31.

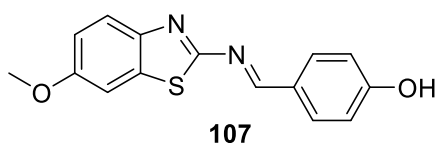
**Methyl (*E*)-2-hydroxy-5-(((6-methoxybenzo[*d*]thiazol-2-yl)imino)methyl)benzoate (106)**



Yellow solid, yield 80%, mp ND.

$^1\text{H}$  NMR (500 MHz, DMSO- $d_6$ )  $\delta$  11.14 (s, 1H), 9.08 (s, 1H), 8.50 (d,  $J = 2.2$  Hz, 1H), 8.19 (dd,  $J = 8.7, 2.2$  Hz, 1H), 7.81 (d,  $J = 8.9$  Hz, 1H), 7.65 (d,  $J = 2.6$  Hz, 1H), 7.17 (d,  $J = 8.6$  Hz, 1H), 7.10 (dd,  $J = 8.9, 2.7$  Hz, 1H), 3.93 (s, 3H), 3.84 (s, 3H).

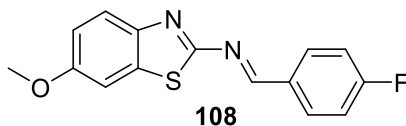
**(*E*)-4-(((6-Methoxybenzo[*d*]thiazol-2-yl)imino)methyl)phenol (107)**



Yellow solid, yield 93%, mp ND.

$^1\text{H}$  NMR (500 MHz, DMSO- $d_6$ )  $\delta$  10.55 (s, 1H), 8.97 (s, 1H), 7.93 (d,  $J = 8.7$  Hz, 2H), 7.78 (d,  $J = 8.9$  Hz, 1H), 7.62 (d,  $J = 2.6$  Hz, 1H), 7.08 (dd,  $J = 8.9, 2.6$  Hz, 1H), 6.94 (d,  $J = 8.6$  Hz, 2H), 3.83 (s, 3H).

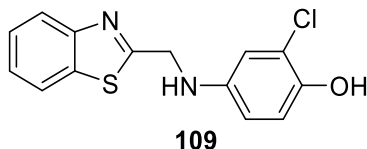
**(*E*)-1-(4-Fluorophenyl)-*N*-(6-methoxybenzo[*d*]thiazol-2-yl)methanimine (108)**



Yellow solid, yield 88%, mp ND.

$^1\text{H}$  NMR (500 MHz, DMSO- $d_6$ )  $\delta$  9.15 (s, 1H), 8.20 – 8.12 (m, 2H), 7.83 (d,  $J = 8.9$  Hz, 1H), 7.67 (d,  $J = 2.4$  Hz, 1H), 7.47 – 7.40 (m, 2H), 7.12 (dd,  $J = 8.9, 2.6$  Hz, 1H), 3.84 (s, 3H).

**4-((Benzo[*d*]thiazol-2-ylmethyl)amino)-2-chlorophenol (109)**



Adopted procedure A with compound **104** suspended in MeOH (15 mL) was used. Crude residue was recrystallised (Et<sub>2</sub>O:EtOH) to obtain 4-((benzo[*d*]thiazol-2-ylmethyl)amino)-2-chlorophenol.

White solid, yield 69%, mp 188.5-189.5°C.

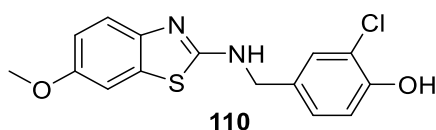
$^1\text{H}$  NMR (500 MHz,  $\text{DMSO-}d_6$ )  $\delta$  9.10 (s, 1H), 8.02 (d,  $J = 7.8$  Hz, 1H), 7.94 (d,  $J = 8.1$  Hz, 1H), 7.51 – 7.45 (m, 1H), 7.42 – 7.36 (m, 1H), 6.73 (d,  $J = 8.7$  Hz, 1H), 6.62 (d,  $J = 2.8$  Hz, 1H), 6.47 (dd,  $J = 8.7, 2.8$  Hz, 1H), 6.40 (t,  $J = 6.1$  Hz, 1H), 4.62 (d,  $J = 6.1$  Hz, 2H).

$^{13}\text{C}$  NMR (126 MHz,  $\text{DMSO-}d_6$ )  $\delta$  174.86, 153.13, 144.46, 141.51, 134.53, 125.95, 124.76, 122.25 (two non-equivalent carbons), 120.00, 117.47, 113.54, 112.62, 46.38.

HRMS (ESI) calcd for  $\text{C}_{14}\text{H}_{12}\text{ClN}_2\text{OS}$   $[\text{M}+\text{H}]^+$  291.03534, found 291.0349.

Anal. Calcd for  $\text{C}_{14}\text{H}_{11}\text{ClN}_2\text{OS}$ : C, 57.83; H, 3.81; N, 9.63; S, 11.03. Found C, 57.59; H, 3.66; N, 9.52; S, 11.35.

### 2-Chloro-4-(((6-methoxybenzo[*d*]thiazol-2-yl)amino)methyl)phenol (110)



A Schiff base (**105**, 1 mmol, 0.32 g) and  $\text{NaBH}_4$  (1.1 mmol, 42 mg) were added to anhydrous MeOH (5 mL) and the mixture was stirred at RT overnight. The mixture was diluted with  $\text{H}_2\text{O}$  and extracted with EtOAc ( $3 \times 15$  mL), dried over anhydrous  $\text{Na}_2\text{SO}_4$  and solvent was removed under reduced pressure. The crude residue was recrystallised ( $\text{Et}_2\text{O}:\text{EtOH}$ ) to yield 2-chloro-4-(((6-methoxybenzo[*d*]thiazol-2-yl)amino)methyl)phenol as a white solid.

White solid, yield 83%, mp 163.5-164.5°C.

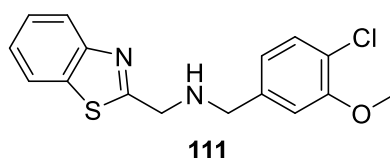
$^1\text{H}$  NMR (500 MHz,  $\text{DMSO-}d_6$ )  $\delta$  10.08 (s, 1H), 8.18 (t,  $J = 5.7$  Hz, 1H), 7.33 (d,  $J = 2.1$  Hz, 1H), 7.31 (d,  $J = 2.7$  Hz, 1H), 7.29 (d,  $J = 8.7$  Hz, 1H), 7.14 (dd,  $J = 8.4, 2.2$  Hz, 1H), 6.92 (d,  $J = 8.3$  Hz, 1H), 6.82 (dd,  $J = 8.7, 2.6$  Hz, 1H), 4.43 (d,  $J = 5.4$  Hz, 2H), 3.73 (s, 3H).

$^{13}\text{C}$  NMR (126 MHz,  $\text{DMSO-}d_6$ )  $\delta$  164.48, 154.36, 152.04, 146.46, 131.40, 130.82, 128.87, 127.30, 119.35, 118.42, 116.48, 112.97, 105.60, 55.54, 46.24.

HRMS (ESI) calcd for  $\text{C}_{15}\text{H}_{14}\text{ClN}_2\text{O}_2\text{S}$   $[\text{M}+\text{H}]^+$  321.04590, found 321.0454.

Anal. Calcd for  $\text{C}_{15}\text{H}_{13}\text{ClN}_2\text{O}_2\text{S}$ : C, 56.16; H, 4.08; N, 8.73; S, 9.99. Found C, 56.14; H, 3.97; N, 8.79; S, 10.22.

### 1-(Benzo[*d*]thiazol-2-yl)-*N*-(3-chloro-4-methoxyphenyl)methanamine (111)

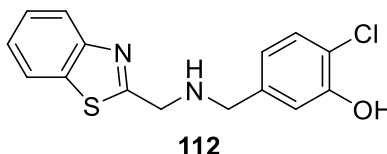


2-(Bromomethyl)benzo[*d*]thiazole (1.75 mmol, 0.34 g), (3-chloro-4-methoxyphenyl)methanamine (2.94 mmol, 0.51 g) and *N,N*-diisopropylethylamine (2.94 mmol, 0.38 g, 0.51 mL) were dissolved in DCM (15 mL) and mixture was stirred at RT for next 24 h. Solvent was removed

under reduced pressure and residue was purified by column chromatography (PE:CHCl<sub>3</sub>, 1:1) to yield 1-(benzo[*d*]thiazol-2-yl)-*N*-(3-chloro-4-methoxybenzyl)methanamine as a light yellow oil (0.54 g, 96%).

<sup>1</sup>H NMR (500 MHz, Chloroform-*d*) δ 7.99 – 7.95 (m, 1H), 7.91 – 7.87 (m, 1H), 7.49 – 7.44 (m, 1H), 7.42 (d, *J* = 2.1 Hz, 1H), 7.40 – 7.35 (m, 1H), 7.23 (dd, *J* = 8.4, 2.1 Hz, 1H), 6.90 (d, *J* = 8.4 Hz, 1H), 4.23 (s, 2H), 3.90 (s, 3H), 3.84 (s, 2H).

#### 4-(((Benzo[*d*]thiazol-2-ylmethyl)amino)methyl)-2-chlorophenol (112)



1-(Benzo[*d*]thiazol-2-yl)-*N*-(3-chloro-4-methoxybenzyl)methanamine (**111**, 1.69 mmol, 0.54 g) was dissolved in anhydrous DCE (10 mL) and nitrogen atmosphere was introduced. Aluminium chloride (5.07 mmol, 0.68 g) was added portion-wise and mixture was heated at 60°C overnight. The reaction mixture was cooled down to RT, quenched with H<sub>2</sub>O, partitioned between H<sub>2</sub>O:EtOAc and extracted with EtOAc (3 × 25 mL). The organic layers were combined, dried over anhydrous Na<sub>2</sub>SO<sub>4</sub> and solvent was removed under reduced pressure. The residue was purified by column chromatography (PE:EtOAc, 2:1) to yield 4-(((benzo[*d*]thiazol-2-ylmethyl)amino)methyl)-2-chlorophenol as a white solid (0.23 g, 45%).

White solid, yield 45%, mp 120-121°C.

<sup>1</sup>H NMR (500 MHz, Chloroform-*d*) δ 8.00 – 7.95 (m, 1H), 7.90 – 7.86 (m, 1H), 7.49 – 7.44 (m, 1H), 7.40 – 7.36 (m, 1H), 7.35 (d, *J* = 2.1 Hz, 1H), 7.13 (dd, *J* = 8.3, 2.1 Hz, 1H), 6.94 (d, *J* = 8.3 Hz, 1H), 4.23 (s, 2H), 3.82 (s, 2H).

<sup>13</sup>C NMR (126 MHz, Chloroform-*d*) δ 173.26, 153.36, 150.94, 135.10, 132.71, 129.03, 128.39, 126.14, 125.06, 122.83, 121.91, 120.18, 116.43, 52.38, 50.68.

HRMS (ESI) calcd for C<sub>15</sub>H<sub>14</sub>ClN<sub>2</sub>OS [M+H]<sup>+</sup> 305.05099, found 305.05084.

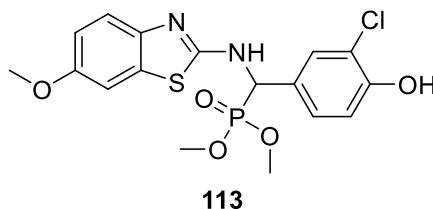
Anal. Calcd for C<sub>15</sub>H<sub>13</sub>ClN<sub>2</sub>OS: C, 59.11; H, 4.30; N, 9.19; S, 10.52. Found C, 59.15; H, 4.37; N, 9.11; S, 10.61.

#### Procedure G (general conditions): Dimethyl (aryl((6-methoxybenzo[*d*]thiazol-2-yl)amino)methyl) phosphonates (113-116)

A Schiff base (**105-108**, 1 mmol) was suspended in THF (5 mL) followed by immediate addition of dimethyl phosphite (1.1 mmol) and 1,1,3,3-tetramethylguanidine (1.1 mmol) [169]. The mixture was heated at 65°C for next 12 h, then solvent was removed under reduced pressure and

residue was purified by column chromatography (CHCl<sub>3</sub>:MeOH). The crude product was recrystallised (PE:Et<sub>2</sub>O) to yield corresponding phosphonate.

**Dimethyl ((3-chloro-4-hydroxyphenyl)((6-methoxybenzo[d]thiazol-2-yl)amino)methyl) phosphonate (113)**



White solid, yield 65%, mp 198-199°C.

<sup>1</sup>H NMR (500 MHz, DMSO-*d*<sub>6</sub>) δ 10.28 (s, 1H), 8.77 (dd, *J* = 9.7, 3.1 Hz, 1H), 7.50 (t, *J* = 2.1 Hz, 1H), 7.32 (d, *J* = 2.7 Hz, 1H), 7.31 (d, *J* = 8.8 Hz, 1H), 7.27 (dt, *J* = 8.5, 2.1 Hz, 1H), 6.95 (d, *J* = 8.4 Hz, 1H), 6.82 (dd, *J* = 8.7, 2.6 Hz, 1H), 5.57 (dd, *J* = 21.0, 9.6 Hz, 1H), 3.73 (s, 3H), 3.66 (d, *J* = 10.6 Hz, 3H), 3.55 (d, *J* = 10.6 Hz, 3H).

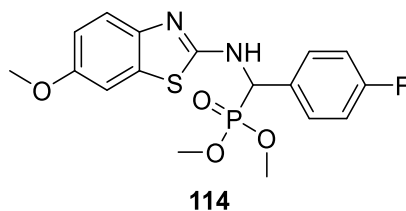
<sup>13</sup>C NMR (126 MHz, DMSO-*d*<sub>6</sub>) δ 163.76 (d, *J* = 10.1 Hz), 154.82, 152.90 (d, *J* = 2.4 Hz), 145.72, 132.01, 129.40 (d, *J* = 5.4 Hz), 128.12 (d, *J* = 5.9 Hz), 127.58, 119.66 (d, *J* = 2.2 Hz), 118.94, 116.52, 113.25, 105.76, 55.71, 53.66 (d, *J* = 6.8 Hz), 53.41 (d, *J* = 7.0 Hz), 52.95 (d, *J* = 155.3 Hz).

<sup>31</sup>P NMR (202 MHz, DMSO-*d*<sub>6</sub>) δ 23.71.

HRMS (ESI) calcd for C<sub>17</sub>H<sub>19</sub>ClN<sub>2</sub>O<sub>5</sub>PS [M+H]<sup>+</sup> 429.04353, found 429.0425.

Anal. Calcd for C<sub>17</sub>H<sub>18</sub>ClN<sub>2</sub>O<sub>5</sub>PS: C, 47.62; H, 4.23; N, 6.53; S, 7.48. Found C, 47.93; H, 4.45; N, 6.24; S, 7.44.

**Dimethyl ((4-fluorophenyl)((6-methoxybenzo[d]thiazol-2-yl)amino)methyl) phosphonate (114)**  
[156]



White solid, yield 65%, mp 173-174°C.

<sup>1</sup>H NMR (500 MHz, DMSO-*d*<sub>6</sub>) δ 9.48 (s, 1H), 8.76 (dd, *J* = 9.7, 2.9 Hz, 1H), 7.33 – 7.27 (m, 4H), 6.82 (dd, *J* = 8.7, 2.7 Hz, 1H), 6.75 (d, *J* = 8.4 Hz, 2H), 5.54 (dd, *J* = 20.9, 9.7 Hz, 1H), 3.72 (s, 3H), 3.64 (d, *J* = 10.5 Hz, 3H), 3.50 (d, *J* = 10.5 Hz, 3H).

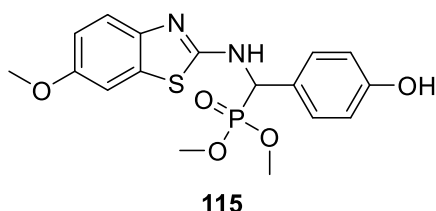
<sup>13</sup>C NMR (126 MHz, DMSO-*d*<sub>6</sub>) δ 163.62 (d, *J* = 10.0 Hz), 161.69 (dd, *J* = 244.1, 2.9 Hz), 154.67, 145.52, 132.10 (d, *J* = 2.9 Hz), 131.87, 130.02 (dd, *J* = 8.3, 5.5 Hz), 118.79, 115.18 (dd, *J* = 21.6, 1.7 Hz), 113.09, 105.58, 53.53 (d, *J* = 6.8 Hz), 53.25 (d, *J* = 6.8 Hz), 53.12 (d, *J* = 154.1 Hz).

$^{31}\text{P}$  NMR (202 MHz,  $\text{DMSO-}d_6$ )  $\delta$  23.56 (d,  $J = 4.5$  Hz).

HRMS (ESI) calcd for  $\text{C}_{17}\text{H}_{19}\text{FN}_2\text{O}_4\text{PS}$   $[\text{M}+\text{H}]^+$  397.07817, found 397.07755.

Anal. Calcd for  $\text{C}_{17}\text{H}_{18}\text{FN}_2\text{O}_4\text{PS}$ : C, 51.51; H, 4.58; N, 7.07; S, 8.09. Found C, 51.29; H, 4.67; N, 7.29; S, 8.31.

**Dimethyl ((4-hydroxyphenyl)((6-methoxybenzo[*d*]thiazol-2-yl)amino)methyl) phosphonate (115) [156]**



White solid, yield 76%, mp 217-218°C.

$^1\text{H}$  NMR (500 MHz,  $\text{DMSO-}d_6$ )  $\delta$  9.48 (s, 1H), 8.76 (dd,  $J = 9.7, 2.9$  Hz, 1H), 7.33 – 7.28 (m, 4H), 6.82 (dd,  $J = 8.7, 2.7$  Hz, 1H), 6.75 (d,  $J = 8.4$  Hz, 2H), 5.54 (dd,  $J = 20.9, 9.7$  Hz, 1H), 3.72 (s, 3H), 3.64 (d,  $J = 10.5$  Hz, 3H), 3.50 (d,  $J = 10.5$  Hz, 3H).

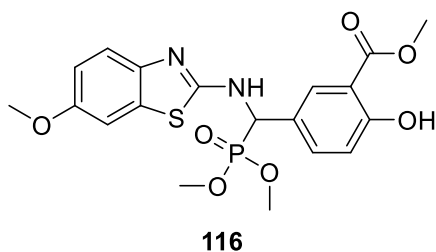
$^{13}\text{C}$  NMR (126 MHz,  $\text{DMSO-}d_6$ )  $\delta$  163.70 (d,  $J = 10.0$  Hz), 157.06 (d,  $J = 2.4$  Hz), 154.57, 145.64, 131.82, 129.31 (d,  $J = 5.7$  Hz), 125.77, 118.68, 115.08, 113.01, 105.57, 55.53, 53.33 (d,  $J = 6.9$  Hz), 53.28 (d,  $J = 155.2$  Hz), 53.14 (d,  $J = 6.9$  Hz).

$^{31}\text{P}$  NMR (202 MHz,  $\text{DMSO-}d_6$ )  $\delta$  24.25.

HRMS (ESI) calcd for  $\text{C}_{17}\text{H}_{20}\text{N}_2\text{O}_5\text{PS}$   $[\text{M}+\text{H}]^+$  395.08251, found 395.08215.

Anal. Calcd for  $\text{C}_{17}\text{H}_{19}\text{N}_2\text{O}_5\text{PS}$ : C, 51.77; H, 4.86; N, 7.10; S, 8.13. Found C, 51.63; H, 4.88; N, 7.12; S, 8.14.

**Methyl 5-((dimethoxyphosphoryl)((6-methoxybenzo[*d*]thiazol-2-yl)amino)methyl)-2-hydroxybenzoate (116) [156]**



White solid, yield 73%, mp 180-181°C.

$^1\text{H}$  NMR (500 MHz,  $\text{DMSO-}d_6$ )  $\delta$  10.53 (s, 1H), 8.90 (dd,  $J = 9.6, 3.5$  Hz, 1H), 7.95 (t,  $J = 2.3$  Hz, 1H), 7.65 (dt,  $J = 8.7, 2.1$  Hz, 1H), 7.32 (d,  $J = 2.7$  Hz, 1H), 7.30 (d,  $J = 8.7$  Hz, 1H), 7.01 (d,  $J = 8.6$  Hz, 1H), 6.82 (dd,  $J = 8.8, 2.7$  Hz, 1H), 5.63 (dd,  $J = 21.3, 9.4$  Hz, 1H), 3.91 (s, 3H), 3.72 (s, 3H), 3.67 (d,  $J = 10.6$  Hz, 3H), 3.55 (d,  $J = 10.6$  Hz, 3H).



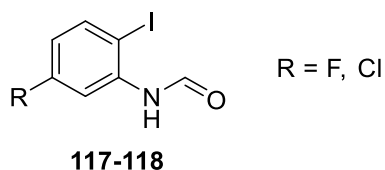
$^{13}\text{C}$  NMR (126 MHz,  $\text{DMSO-}d_6$ )  $\delta$  168.86, 163.61 (d,  $J = 10.1$  Hz), 159.53 (d,  $J = 2.0$  Hz), 154.65, 145.52, 135.35 (d,  $J = 5.1$  Hz), 131.88, 129.33 (d,  $J = 6.0$  Hz), 126.83, 118.79, 117.49, 105.58, 113.07, 113.03 (d,  $J = 1.9$  Hz), 55.53, 53.55 (d,  $J = 7.1$  Hz), 53.26 (d,  $J = 6.8$  Hz), 52.90 (d,  $J = 155.2$  Hz), 52.53.

$^{31}\text{P}$  NMR (202 MHz,  $\text{DMSO-}d_6$ )  $\delta$  23.67.

HRMS (ESI) calcd for  $\text{C}_{19}\text{H}_{22}\text{N}_2\text{O}_7\text{PS}$   $[\text{M}+\text{H}]^+$  453.08798, found 453.08701.

Anal. Calcd for  $\text{C}_{19}\text{H}_{21}\text{N}_2\text{O}_7\text{PS}$ : C, 50.44; H, 4.68; N, 6.19; S, 7.09. Found C, 50.46; H, 4.69; N, 6.20; S, 7.27.

#### Procedure H (general conditions): *N*-(5-halogen-2-iodophenyl)formamides (117-118)

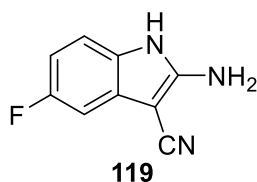


5-Halogen-2-iodoaniline (2 mmol) was dissolved in toluene (5 mL), formic acid (4 mmol) was added and reaction was heated at reflux overnight [170, 171]. Reaction mixture was cooled down, precipitate was collected by suction filtration, washed with PE and dried under reduced pressure to yield *N*-(5-halogen-2-iodophenyl)formamide. Crude product was used in next reaction step without further purification.

#### Procedure I (general conditions): 2-Amino-5-halogen-1*H*-indole-3-carboxylic acid derivatives (119-122)

*N*-(5-halogen-2-iodophenyl)formamide (2 mmol) and 2-cyanoacetic acid derivative (4 mmol, malononitrile or ethyl 2-cyanoacetate) were dissolved in DMSO (4 mL). Potassium carbonate (8 mmol, 1.11 g) and copper(I) iodate (0.2 mmol, 38 mg) were added and reaction was heated at 120°C for 1.5 h. Reaction was quenched with 1 M HCl, diluted with  $\text{H}_2\text{O}$  (15 mL) and extracted with EtOAc ( $3 \times 30$  mL). Organic layers was washed with brine (20 mL), dried over anhydrous  $\text{Na}_2\text{SO}_4$  and solvent was removed under reduced pressure. Crude product was purified by column chromatography (PE:EtOAc) to yield 2-amino-5-halogen-1*H*-indole-3-carboxylic acid derivative (119-122) [172, 173].

#### 2-Amino-5-fluoro-1*H*-indole-3-carbonitrile (119)



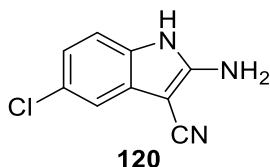
Light-brown oil, yield 70%, mp ND.

$^1\text{H}$  NMR (500 MHz, DMSO- $d_6$ )  $\delta$  10.68 (s, 1H), 7.04 (dd,  $J$  = 8.6, 4.6 Hz, 1H), 6.83 (d,  $J$  = 2.5 Hz, 1H), 6.81 (br s, 2H), 6.65 (m, 1H).

$^{13}\text{C}$  NMR (126 MHz, DMSO- $d_6$ )  $\delta$  158.04 (d,  $J$  = 232.8 Hz), 154.87, 129.35 (d,  $J$  = 10.9 Hz), 128.56, 117.24, 110.81 (d,  $J$  = 9.7 Hz), 106.31 (d,  $J$  = 24.8 Hz), 101.04 (d,  $J$  = 25.5 Hz), 62.36 (d,  $J$  = 3.4 Hz).

HRMS (ESI) calcd for  $\text{C}_9\text{H}_7\text{FN}_3$   $[\text{M}+\text{H}]^+$  176.06185, found 176.06169.

### 2-Amino-5-chloro-1H-indole-3-carbonitrile (120) [172]



Light-brown solid, yield 44%, mp 210-211°C (Lit. 209-212°C [172]).

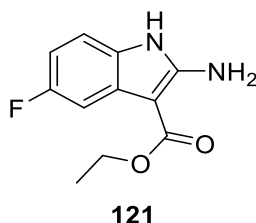
$^1\text{H}$  NMR (300 MHz, DMSO- $d_6$ )  $\delta$  10.84 (s, 1H), 7.11 (d,  $J$  = 8.6 Hz, 1H), 7.07 (d,  $J$  = 2.1 Hz, 1H), 6.94 (br s, 2H), 6.89 (dd,  $J$  = 8.5, 2.1 Hz, 1H).

$^{13}\text{C}$  NMR (75 MHz, DMSO- $d_6$ )  $\delta$  154.63, 130.83, 129.90, 125.05, 119.20, 117.08, 114.20, 111.43, 61.63.

HRMS (ESI) calcd for  $\text{C}_9\text{H}_7\text{ClN}_3$   $[\text{M}+\text{H}]^+$  192.03230, found 192.03236.

Anal. Calcd for  $\text{C}_9\text{H}_6\text{ClN}_3$ : C, 56.41; H, 3.16; N, 21.93. Found C, 56.79; H, 3.53; N, 22.13.

### Ethyl 2-amino-5-fluoro-1H-indole-3-carboxylate (121) [174]



Light-brown solid, yield 43%, mp 185-186°C.

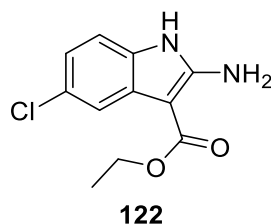
$^1\text{H}$  NMR (500 MHz, DMSO- $d_6$ )  $\delta$  10.67 (s, 1H), 7.22 (dd,  $J$  = 10.2, 2.2 Hz, 1H), 7.07 (dd,  $J$  = 8.5, 4.7 Hz, 1H), 6.76 (br s, 2H), 6.69 – 6.63 (m, 1H), 4.22 (q,  $J$  = 7.1 Hz, 2H), 1.32 (t,  $J$  = 7.1 Hz, 3H).

$^{13}\text{C}$  NMR (126 MHz, DMSO- $d_6$ )  $\delta$  165.44, 158.04 (d,  $J$  = 231.0 Hz), 154.44, 129.04, 127.79 (d,  $J$  = 10.8 Hz), 110.14 (d,  $J$  = 9.8 Hz), 105.76 (d,  $J$  = 24.9 Hz), 103.64 (d,  $J$  = 25.7 Hz), 84.07 (d,  $J$  = 3.2 Hz), 58.13, 14.67.

HRMS (ESI) calcd for  $\text{C}_{11}\text{H}_{12}\text{FN}_2\text{O}_2$   $[\text{M}+\text{H}]^+$  223.08773, found 223.08785.

Anal. Calcd for  $\text{C}_{11}\text{H}_{11}\text{FN}_2\text{O}_2$ : C, 59.46; H, 4.99; N, 12.61. Found C, 59.72; H, 5.27; N, 12.37.

**Ethyl 2-amino-5-chloro-1*H*-indole-3-carboxylate (122)** [172]



Light-brown solid, yield 42%, mp 190-191°C (Lit. 191-193°C [172]).

<sup>1</sup>H NMR (300 MHz, DMSO-*d*<sub>6</sub>) δ 10.77 (s, 1H), 7.47 (s, 1H), 7.10 (d, *J* = 8.6 Hz, 1H), 6.87 (d, *J* = 8.6 Hz, 1H), 6.82 (br s, 2H), 4.23 (q, *J* = 7.0 Hz, 2H), 1.31 (t, *J* = 7.0 Hz, 3H).

<sup>13</sup>C NMR (75 MHz, DMSO-*d*<sub>6</sub>) δ 165.38, 154.19, 131.32, 128.27, 124.87, 118.75, 116.96, 110.94, 83.41, 58.23, 14.74.

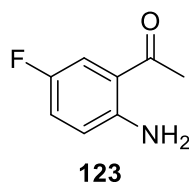
MS (ESI) calcd for C<sub>11</sub>H<sub>12</sub>ClN<sub>2</sub>O<sub>2</sub> [M+H]<sup>+</sup> 239.05818, found 239.05829.

Anal. Calcd for C<sub>11</sub>H<sub>11</sub>ClN<sub>2</sub>O<sub>2</sub>: C, 55.36; H, 4.65; N, 11.74. Found C, 55.69; H, 4.36; N, 11.47.

**Procedure J (general conditions): 1-(2-Amino-5-halogenphenyl)ethan-1-ones (123-125)**

1-(5-Halogen-2-nitrophenyl)ethan-1-ones were subjected to procedure A to obtain corresponding 1-(2-amino-5-halogenphenyl)ethan-1-ones as yellow oils, which gradually solidified over the prolonged time.

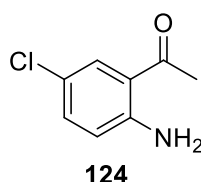
**1-(2-Amino-5-fluorophenyl)ethan-1-one (123)**



Yellow solid, yield 99%, mp ND.

<sup>1</sup>H NMR (500 MHz, Chloroform-*d*) δ 7.37 (dd, *J* = 9.8, 2.9 Hz, 1H), 7.05 (ddd, *J* = 9.0, 7.6, 2.9 Hz, 1H), 6.61 (dd, *J* = 9.0, 4.6 Hz, 1H), 6.11 (br s, 2H), 2.55 (s, 3H).

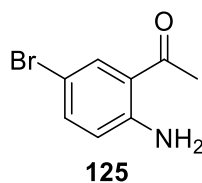
**1-(2-Amino-5-chlorophenyl)ethan-1-one (124)**



Yellow solid, yield 99%, mp ND.

<sup>1</sup>H NMR (500 MHz, Chloroform-*d*) δ 7.66 (d, *J* = 2.4 Hz, 1H), 7.21 (dd, *J* = 8.8, 2.4 Hz, 1H), 6.60 (d, *J* = 8.8 Hz, 1H), 2.56 (s, 3H).

### 1-(2-Amino-5-bromophenyl)ethan-1-one (125)



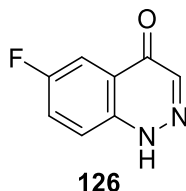
Yellow solid, yield 99%, mp ND.

$^1\text{H}$  NMR (500 MHz, Chloroform-*d*)  $\delta$  7.80 (d,  $J = 2.3$  Hz, 1H), 7.32 (dd,  $J = 8.8, 2.3$  Hz, 1H), 6.55 (d,  $J = 8.8$  Hz, 1H), 6.29 (br s, 2H), 2.56 (s, 3H).

### Procedure K (general conditions): 6-Halogencinnolin-4(1H)-one (126-128)

1-(2-Amino-5-halogenphenyl)ethan-1-one (2 mmol) was dissolved in 6 M HCl and cooled to 0°C. Solution of sodium nitrate (2.2 mmol, 0.15 g) in H<sub>2</sub>O (1-2 mL) was added drop-wise to the reaction mixture (over the course of 15 min), reaction was allowed to reach RT, stirred overnight and then heated at reflux for next 6 h [175]. Reaction mixture was extracted with EtOAc (3  $\times$  40 mL), dried over anhydrous Na<sub>2</sub>SO<sub>4</sub> and solvent was removed under reduced pressure. Crude product was purified by column chromatography (CHCl<sub>3</sub>:MeOH) to yield corresponding 6-halogencinnolin-4(1H)-one (126-128).

### 6-Fluorocinnolin-4(1H)-one (126) [176]



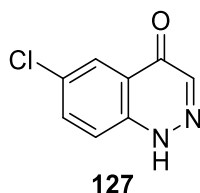
Beige solid, yield 61%, mp 264.5 – 265.5°C (Lit. 267°C [176]).

$^1\text{H}$  NMR (500 MHz, DMSO-*d*<sub>6</sub>)  $\delta$  13.64 (br s, 1H), 7.73 (s, 1H), 7.72 – 7.64 (m, 3H).

$^{13}\text{C}$  NMR (126 MHz, DMSO-*d*<sub>6</sub>)  $\delta$  169.65 (d,  $J = 2.9$  Hz), 158.84 (d,  $J = 245.6$  Hz), 138.91, 138.06, 123.91 (d,  $J = 7.2$  Hz), 123.33 (d,  $J = 26.2$  Hz), 119.94 (d,  $J = 8.3$  Hz), 107.58 (d,  $J = 22.1$  Hz).

HRMS (ESI) calcd for C<sub>8</sub>H<sub>6</sub>FN<sub>2</sub>O [M+H]<sup>+</sup> 165.04587, found 165.04565.

### 6-Chlorocinnolin-4(1H)-one (127) [176]

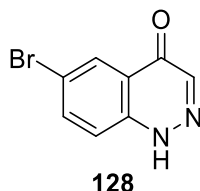


Beige solid, yield 47%, mp ND.

$^1\text{H}$  NMR (500 MHz,  $\text{DMSO-}d_6$ )  $\delta$  13.67 (br s, 1H), 7.97 (d,  $J = 2.4$  Hz, 1H), 7.83 (dd,  $J = 9.0, 2.4$  Hz, 1H), 7.79 (s, 1H), 7.64 (d,  $J = 9.0$  Hz, 1H).

HRMS (ESI) calcd for  $\text{C}_8\text{H}_6\text{ClN}_2\text{O}$   $[\text{M}+\text{H}]^+$  181.01632, found 181.01611.

#### 6-Bromocinnolin-4(1H)-one (128) [175, 176]



Beige solid, yield 45%, mp ND.

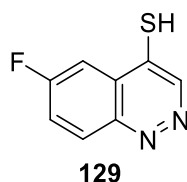
$^1\text{H}$  NMR (500 MHz,  $\text{DMSO-}d_6$ )  $\delta$  13.65 (br s, 1H), 8.10 (d,  $J = 2.0$  Hz, 1H), 7.92 (dd,  $J = 9.0, 2.0$  Hz, 1H), 7.81 (s, 1H), 7.56 (d,  $J = 9.0$  Hz, 1H).

HRMS (ESI) calcd for  $\text{C}_8\text{H}_6\text{BrN}_2\text{O}$   $[\text{M}+\text{H}]^+$  224.96580, found 224.96543.

#### Procedure L (general conditions): 6-Halogencinnoline-4-thiols (129-131)

6-Halogencinnolin-4(1H)-one was dissolved in anhydrous toluene and Lawesson's reagent was added. Nitrogen atmosphere was introduced and reaction mixture was heated at  $100^\circ\text{C}$  until the disappearance of starting material (TLC,  $\sim 3$  h) [177]. Solvent was removed under reduced pressure and crude residue was purified by column chromatography (PE:DCM:EtOAc, 5:2:1) to yield corresponding 6-fluorocinnoline-4-thiol.

#### 6-Fluorocinnoline-4-thiol (129) [176]



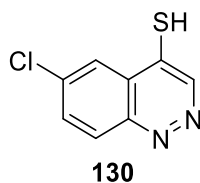
Orange solid, yield 94%, mp  $175\text{--}176^\circ\text{C}$  (Lit.  $179\text{--}180^\circ\text{C}$  [176]).

$^1\text{H}$  NMR (500 MHz,  $\text{DMSO-}d_6$ )  $\delta$  8.49 (s, 1H), 8.01 (dd,  $J = 9.6, 2.6$  Hz, 1H), 7.86 – 7.74 (m, 2H).

$^{13}\text{C}$  NMR (126 MHz,  $\text{DMSO-}d_6$ )  $\delta$  185.42, 160.97 (d,  $J = 248.2$  Hz), 148.83, 133.71, 133.64, 124.46 (d,  $J = 26.9$  Hz), 121.60 (d,  $J = 8.2$  Hz), 110.02 (d,  $J = 23.6$  Hz).

HRMS (ESI) calcd for  $\text{C}_8\text{H}_6\text{FN}_2\text{S}$   $[\text{M}+\text{H}]^+$  181.02302, found 181.02283.

**6-Chlorocinnoline-4-thiol (130)** [176]



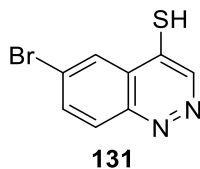
Dark-red solid, yield 92%, mp 178-179°C (Lit. 181-182°C [176]).

$^1\text{H}$  NMR (500 MHz, DMSO- $d_6$ )  $\delta$  8.51 (s, 1H), 8.32 (d,  $J$  = 2.4 Hz, 1H), 7.90 (dd,  $J$  = 9.0, 2.4 Hz, 1H), 7.73 (d,  $J$  = 9.0 Hz, 1H).

$^{13}\text{C}$  NMR (126 MHz, DMSO- $d_6$ )  $\delta$  185.44, 149.84, 135.18, 134.86, 133.16, 132.53, 125.05, 120.64.

HRMS (ESI) calcd for  $\text{C}_8\text{H}_6\text{ClN}_2\text{S}$   $[\text{M}+\text{H}]^+$  196.99347, found 196.99342.

**6-Bromocinnoline-4-thiol (131)** [176]



Dark-red solid, yield 91%, mp 185°C (Lit. 187-189°C [176]).

$^1\text{H}$  NMR (500 MHz, DMSO- $d_6$ )  $\delta$  8.51 (s, 1H), 8.45 (d,  $J$  = 2.2 Hz, 1H), 7.99 (dd,  $J$  = 9.0, 2.2 Hz, 1H), 7.63 (d,  $J$  = 9.0 Hz, 1H).

$^{13}\text{C}$  NMR (126 MHz, DMSO- $d_6$ )  $\delta$  185.32, 149.94, 137.37, 135.37, 133.54, 128.30, 120.89, 120.55.

HRMS (ESI) calcd for  $\text{C}_8\text{H}_6\text{BrN}_2\text{S}$   $[\text{M}+\text{H}]^+$  240.94296, found 240.94285.

### **5.3. Biological evaluation of final compounds**

All experimental procedures are included in attachments A2-A4 [136, 154, 162]. Please find below list of performed experiments along with contributing workgroups.

#### **ABAD activity assay**

Experiments were performed in cooperation with prof. Frank Gunn-Moore workgroup, University of St. Andrews, United Kingdom.

Author contributed to *in vitro* evaluation (ABAD experiments) and CHANA probe synthesis during his research stay at University of St. Andrews.

#### **MAO and HRP assays**

Experiments were performed in cooperation with Dr. Rona R. Ramsay workgroup, University of St. Andrews, United Kingdom.

Author contributed to *in vitro* evaluation (HRP, MAO) during his research stay at University of St. Andrews.

#### **Cytotoxicity assays**

Experiments were performed in cooperation with PharmDr. Ondřej Soukup, Ph.D. workgroup, University Hospital Hradec Králové, Czech Republic.

#### **Elog $P$ and Elog $D$ determination**

Experiments were performed in cooperation with assoc. prof. PharmDr. Kamil Musílek, Ph.D. workgroup, University of Hradec Králové, Czech Republic.

#### **PAMPA assay**

Experiments were performed in cooperation with PharmDr. Ondřej Soukup, Ph.D. and Mgr. *et* Mgr. Rafael Doležal, Ph.D. workgroups, University Hospital Hradec Králové, Czech Republic.

## 6. Abstract (English)

Charles University in Prague, Faculty of Pharmacy in Hradec Králové

**Department:** Department of Pharmaceutical Chemistry and Drug Control

**Candidate:** Mgr. Lukáš Hroch

**Supervisor:** assoc. prof. PharmDr. Kamil Musílek, Ph.D.

**Title of dissertation:** Inhibitors of mitochondrial enzymes as potential therapeutics for Alzheimer's disease

There were about 50 million people living with dementia in 2015. It is expected that number of people living with dementia will reach 130 million by the year of 2050. Alzheimer's disease (AD) is one of the most common causes of dementia and it is estimated to account for about 60-80% of overall cases. Current symptomatic treatment only alleviates symptoms and delays progression of the disease. However, there is no effective treatment, which would address the underlying cause of AD. The extracellular depositions of insoluble amyloid beta peptide (A $\beta$ ) were thought to be a causative factor and main target for a long time. Yet, targeted treatment towards the reduction of extracellular A $\beta$  depositions failed to show expected therapeutic merit. Later on, it has been shown that development of AD starts much earlier than any A $\beta$  plaques or symptoms could be observed. With growing evidence of soluble A $\beta$  in intracellular regions, main attention moved to investigations of A $\beta$  within the cells. A $\beta$  interacts with variety of cellular structures and proteins, including those in cellular compartments such as mitochondria.

Presented work is focused on mitochondrial enzymes, which are affected by A $\beta$  and could be potential therapeutic targets for AD treatment. Among those enzymes, A $\beta$ -binding alcohol dehydrogenase (ABAD), also known as 17 $\beta$ -hydroxysteroid dehydrogenase type 10 (17 $\beta$ -HSD10), showed the most favourable potential and it is the enzyme of focus herein. The introductory part covers biological aspects of AD with gradual focus on selected enzymes, while chemistry review is dedicated to aspects around discussed structural scaffolds. Experimental work details the design, synthesis and evaluation of small molecules targeting ABAD. Structural scaffolds were derived from frentizole, fragment database hits or other enzyme scaffolds with partial intent to introduce multi-target-directed ligand strategies.

About 90 final compounds were designed, prepared and evaluated for their ability to inhibit ABAD enzyme. Synthesised diverse pool of compounds provided valuable initial data set to established basic structure and activity relationships and it yielded several potential hits for future development. Moreover, selected compounds are subjects of further *in vitro* / *in vivo* studies to assess their desirable pharmacological properties.



## 7. Abstrakt (Czech)

Univerzita Karlova v Praze, Farmaceutická fakulta v Hradci Králové

**Katedra:** Katedra farmaceutické chemie a kontroly léčiv

**Kandidát:** Mgr. Lukáš Hroch

**Školitel:** doc. PharmDr. Kamil Musílek, Ph.D.

**Název disertační práce:** Inhibitory mitochondriálních enzymů jako potenciální léčiva Alzheimerovy nemoci

V roce 2015 bylo postiženo demencí přes 50 milionů lidí po celém světě. Je odhadováno, že k roku 2050, číslo lidí postižených demencí vzroste až k 130 milionům. Alzheimerova nemoc (AD) patří mezi nejčastější příčiny demence s podílem až 60-80% na všech případech. Současná symptomatická léčba pouze mírní projevy nemoci a zpomaluje její progresi. Bohužel žádná efektivní léčba, které by cílila na příčinu onemocnění, není stále k dispozici. Dlouho se domnívalo, že příčinou AD jsou extracelulární depozita amyloid-beta peptidu (A $\beta$ ). Cílená léčba, která redukovala depozita A $\beta$ , ale nepřinesla očekávané zlepšení symptomů a kýžené výsledky. S postupem času se zjistilo, že rozvoj AD začíná mnohem dříve, než se projeví první symptomy či možnost pozorovat depozita A $\beta$  plaků. Proto se výzkum více začal zaměřovat na intracelulárně lokalizovaný A $\beta$  a jeho toxický efekt na buněčné struktury. Postupně se začalo objevovat více a více studií, které popisují přítomnost A $\beta$  v buňce (včetně buněčných organel jako jsou mitochondrie) a jeho negativní roli v ovlivnění různých fyziologických procesů.

Práce je zaměřena na mitochondriální enzymy, které jsou negativně ovlivněny A $\beta$ , a proto reprezentují potenciální cíle v léčbě AD. Mezi tyto enzymy patří A $\beta$ -vázající alkoholdehydrogenasa (ABAD), známá také jako 17 $\beta$ -hydroxysteroid dehydrogenasa (17 $\beta$ -HSD10). Prezentovaná práce je zaměřena právě na tento enzym ABAD. Zatímco úvodní část práce je zaměřena na problematiku vývoje AD s postupným zaměřením na vybrané mitochondriální enzymy, přehledový článek se soustředí na vybrané potenciálně účinné farmakofory benzothiazolů centrální nervové soustavy. Experimentální část práce popisuje návrh, přípravu a hodnocení malých molekul, které cílí na enzym ABAD. Strukturní předlohy jsou odvozeny od struktury frentizolu, chemických struktur vybraných z databází nebo kombinují předlohy pro další enzymy s částečným navázáním na „multi-target-directed“ strategii, kde jedna molekula ovlivňuje více biologických cílů.

Kolem 90 sloučenin bylo navrženo, připraveno a otestováno na inhibici aktivity enzymu ABAD. Připravený set sloučenin poskytl důležitá data, pro vyhodnocení vztahu mezi strukturou a účinkem s tím, že bylo popsáno několik účinných inhibitorů ABAD pro další studie. Účinné sloučeniny jsou dále hodnoceny a testovány na další vhodné cíle pomocí vybraných *in vitro* / *in vivo* metodik.

## 8. Outputs

### 8.1. Publications

#### Publications directly related to the project

- 1) HROCH, L., P. GUEST, O. BENEK, O. SOUKUP, J. JANOCKOVA, R. DOLEZAL, K. KUCA, L. AITKEN, T. K. SMITH, F. GUNN-MOORE, D. ZALA, R. R. RAMSAY and K. MUSILEK. Synthesis and evaluation of frentizole-based indolyl thiourea analogues as MAO/ABAD inhibitors for Alzheimer's disease treatment. *Bioorganic and Medicinal Chemistry*. 2017, vol. 25, no. 3, pp. 1143–1152. IF<sub>2016</sub> = 2.923.
- 2) BENEK, O., L. HROCH, L. AITKEN, R. DOLEZAL, P. GUEST, M. BENKOVA, O. SOUKUP, K. MUSIL, K. KUCA, T. K. SMITH, F. GUNN-MOORE and K. MUSILEK. 6-benzothiazolyl ureas, thioureas and guanidines are potent inhibitors of ABAD/17 $\beta$ -HSD10 and potential drugs for Alzheimer's disease treatment: Design, synthesis and in vitro evaluation. *Medicinal Chemistry*. 2017, vol. 13, no. 4, pp. 345–358. IF<sub>2016</sub> = 1.458.
- 3) HROCH, L., O. BENEK, P. GUEST, L. AITKEN, O. SOUKUP, J. JANOCKOVA, K. MUSIL, V. DOHNAL, R. DOLEZAL, K. KUCA, T. K. SMITH, F. GUNN-MOORE and K. MUSILEK. Design, synthesis and in vitro evaluation of benzothiazole-based ureas as potential ABAD/17 $\beta$ -HSD10 modulators for Alzheimer's disease treatment. *Bioorganic and Medicinal Chemistry Letters*. 2016, vol. 26, no. 15, pp. 3675–3678. IF<sub>2016</sub> = 2.486.
- 4) BENEK, O., O. SOUKUP, M. PASDIOROVA, L. HROCH, V. SEP SOVA, P. JOST, M. HRABINOVA, D. JUN, K. KUCA, D. ZALA, R. R. RAMSAY, J. MARCO-CONTELLES and K. MUSILEK. Design, Synthesis and in vitro Evaluation of Indolotacrine Analogues as Multitarget-Directed Ligands for the Treatment of Alzheimer's Disease. *ChemMedChem*. 2016, vol. 11, no. 12, pp. 1264–1269. IF<sub>2016</sub> = 2.980.
- 5) BENEK, O., L. AITKEN, L. HROCH, K. KUCA, F. GUNN-MOORE and K. MUSILEK. A Direct Interaction Between Mitochondrial Proteins and Amyloid- $\beta$  Peptide and its Significance for the Progression and Treatment of Alzheimer's Disease. *Current Medicinal Chemistry*. 2015, vol. 22, no. 9, pp. 1056–1085. IF<sub>2016</sub> = 3.455.
- 6) HROCH, L., L. AITKEN, O. BENEK, M. DOLEZAL, K. KUCA, F. GUNN-MOORE and K. MUSILEK. Benzothiazoles - Scaffold Of Interest For CNS Targeted Drugs. *Current Medicinal Chemistry*. 2015, vol. 22, no. 6, pp. 730–747. IF<sub>2016</sub> = 3.455.

## Other publications

- 7) LOVERIDGE, E. J., L. HROCH, R. L. HUGHES, T. WILLIAMS, R. L. DAVIES, A. ANGELASTRO, L. Y. P. LUK, G. MAGLIA and R. K. ALLEMANN. Reduction of Folate by Dihydrofolate Reductase from *Thermotoga Maritima*. *Biochemistry*. 2017, vol. 56, no. 13, pp. 1879–1886. IF<sub>2016</sub> = 2.876.
- 8) HROCH, L., M. HRUSKOVA, J. SCHMITZ, G. SCHNAKENBURG and M. GÜTSCHOW. 3,5,5-Trisubstituted Hydantoins From Activated Cbz-Aminomalonic Acids. *Synthesis*. 2012, vol. 44, no. 12, pp. 1907–1912. IF<sub>2016</sub> = 2.652.

## 8.2. Conference communications

- List of conference proceedings with underlined presenting author

### Talks directly related to the project

- 1) HROCH, L., O. BENEK, L. AITKEN, J. MARCO-CONTELLES, R. R. RAMSAY, F. GUNN-MOORE and K. MUSILEK. New Indole Derivatives as Inhibitors of Monoamine Oxidases. COST CM1103 ESR Conference, Computational Chemistry for Neurological Targets, Belgrade (Serbia), May 6–8, 2015.
- 2) HROCH, L., O. BENEK, L. AITKEN, F. GUNN-MOORE and K. MUSILEK. Novel ABAD Modulators for Modifying Treatment of Alzheimer's disease. 5<sup>th</sup> Postgraduate and 3<sup>rd</sup> Postdoctoral conference, Hradec Kralove (Czech Republic), February 3–4, 2015, Abstract Book.
- 3) BENEK, O., L. HROCH, P. GUEST, L. AITKEN, M. PASDIOROVA, O. SOUKUP, K. KUCA, F. GUNN-MOORE and K. MUSILEK. ABAD Modulators for AD Modifying Treatment – Design, Synthesis and In vitro Screening. 49<sup>th</sup> Advances in Organic, Bioorganic and Pharmaceutical Chemistry – Liblice 2014, Lazne Belohrad (Czech Republic), November 7–9, 2014, Abstract book.
- 4) BENEK, O., L. HROCH, P. GUEST, L. AITKEN, M. PASDIOROVA, O. SOUKUP, K. KUCA, F. GUNN-MOORE and K. MUSILEK. ABAD Modulators for AD Modifying Treatment – Design, Synthesis and In vitro Screening. 5<sup>th</sup> Targeting Mitochondria, Berlin (Germany), October 29–31, 2014, Abstract book.
- 5) MUSILEK, K., O. BENEK, L. HROCH, P. GUEST, L. AITKEN, O. SOUKUP, K. KUCA, R. R. RAMSAY and F. GUNN-MOORE. Benzothiazoles - Scaffold of interest for CNS targeted drugs. Neuropathology and Neuropharmacology of monoaminergic systems, Bordeaux (France), October 8–10, 2014, Abstract book.
- 6) HROCH, L., O. BENEK, P. GUEST, F. GUNN-MOORE and K. MUSILEK. Modulators of A $\beta$ -ABAD Interaction for Treatment of Alzheimer's disease. 4<sup>th</sup> Postgraduate and 2<sup>nd</sup>

Postdoctoral conference, Hradec Kralove (Czech Republic), January 28–29, 2014, Abstract Book.

- 7) HROCH, L., O. BENEK, P. GUEST, L. AITKEN, F. GUNN-MOORE and K. MUSILEK. Modulators of ABAD-A $\beta$  interaction for treatment of Alzheimer's disease. COST CM1103 Training School, Istanbul (Turkey), September 9–14, 2013.

#### **Posters directly related to the project**

- 1) BENEK, O., L. HROCH, K. KUCA, F. GUNN-MOORE, D. I. PEREZ, A. MARTINEZ and K. MUSILEK. 1-(Benzo[d]thiazol-2-yl)-3-phenylureas as novel casein kinase 1 inhibitors for treatment of neurodegenerative disorders. The 13<sup>th</sup> International Conference on Alzheimer's and Parkinson's Diseases and Related Neurological Disorders, Vienna (Austria), March 29 – April 2, 2017
- 2) BENEK, O., L. HROCH, O. SOUKUP, J. HROUDOVA, P. GUEST, L. AITKEN, K. KUCA, F. GUNN-MOORE, J. RABOCH, Z. FISAR and K. MUSILEK. ABAD (17 $\beta$ -HSD10) inhibitors designed for AD modifying treatment and their impact on key mitochondrial enzymes. The 13th International Conference on Alzheimer's and Parkinson's Diseases and Related Neurological Disorders, Vienna (Austria), March 29 – April 2, 2017.
- 3) HROCH, L., L. AITKEN, O. BENEK, O. SOUKUP, J. JANOCKOVA, K. MUSIL, V. DOHNAL, R. DOLEZAL, K. KUCA, P. GUEST, T. K. SMITH, F. GUNN-MOORE and K. MUSILEK. Design, synthesis and in vitro evaluation of riluzole-based ureas as potential ABAD modulators for Alzheimer's disease treatment. 24<sup>th</sup> International Symposium on Medicinal Chemistry, Manchester (United Kingdom), August 28 – September 1, 2016.
- 4) BENEK, O., L. HROCH, P. GUEST, L. AITKEN, T. K. SMITH, F. GUNN-MOORE, K. KUCA and K. MUSILEK. Design, synthesis and evaluation of novel ABAD inhibitors for treatment of Alzheimer's disease. 24<sup>th</sup> International Symposium on Medicinal Chemistry, Manchester (UK), August 28 – September 1, 2016.
- 5) BENEK, O., P. GUEST, L. AITKEN, L. HROCH, T. K. SMITH, O. SOUKUP, K. MUSIL, V. DOHNAL, D. JUN, K. KUCA, F. GUNN-MOORE and K. MUSILEK. Modulators of mitochondrial enzymes involved in neurodegenerative diseases. 45. konference Syntéza a analýza léčiv, Hradec Králové (Czech Republic), June 22–24, 2016, Abstract book.
- 6) BENEK, O., L. HROCH, P. GUEST, L. AITKEN, M. PASDIOROVA, O. SOUKUP, K. KUCA, F. GUNN-MOORE and K. MUSILEK. ABAD Modulators targeted to AD Mitochondrial Dysfunction – Design, Synthesis and In vitro Screening. The 12<sup>th</sup> International Conference on Alzheimer's and Parkinson's Diseases and Related Neurological Disorders, Nice (France), March 18–22, 2015.

- 7) HROCH, L., O. BENEK, K. KUČA, P. GUEST, L. AITKEN, F. GUNN-MOORE and K. MUSILEK. Design, Synthesis and Evaluation of Novel ABAD Modulators for Treatment of Alzheimer's Disease. 23<sup>th</sup> International Symposium on Medicinal Chemistry, Lisbon (Portugal), September 7–11, 2014, ChemMedChem, M008, p. 201.
- 8) MUSILEK, K., O. BENEK, L. HROCH, P. GUEST, T. KUCERA, L. AITKEN, K. KUČA and F. GUNN-MOORE. ABAD modulators for AD modifying treatment – synthesis, in vitro screening and molecular modelling. 23<sup>th</sup> International Symposium on Medicinal Chemistry, Lisbon (Portugal), September 7–11, 2014, ChemMedChem, M019, p. 209.
- 9) HROCH, L., O. BENEK, P. GUEST, L. AITKEN, F. GUNN-MOORE and K. MUSILEK. Novel ABAD and A $\beta$ -ABAD Interaction Modulators for Treatment of Alzheimer's Disease. 4<sup>th</sup> Meeting of the Paul Ehrlich MedChem Euro-PhD Network, Hradec Kralove (Czech Republic), June 20–22, 2014, Abstract Book, P-28.
- 10) BENEK, O., L. HROCH, P. GUEST, L. AITKEN, T. K. SMITH, O. SOUKUP, K. KUČA, R. RAMSAY, F. GUNN-MOORE and K. MUSILEK. Design, synthesis and evaluation of ABAD modulators. WG1-2 COST meeting, Smolenice (Slovakia), April 22–24, 2014, Abstract book.
- 11) HROCH, L., O. BENEK, P. GUEST, L. AITKEN, F. GUNN-MOORE and K. MUSILEK. Novel indole-based modulators of A $\beta$ -ABAD interaction for treatment of Alzheimer's disease. COST CM1103 Training School, Istanbul (Turkey), September 9–13, 2013.
- 12) BENEK, O., L. HROCH, K. KUČA, P. GUEST, L. AITKEN, F. GUNN-MOORE and K. MUSILEK. Synthesis and evaluation of benzothiazolylurea analogues as inhibitors of ABAD-A $\beta$  interaction for treatment of Alzheimer's disease. COST CM1103 Training School, Istanbul (Turkey), September 9–13, 2013, Abstract book.
- 13) HROCH, L., O. BENEK, J. KORABECNY, F. GUNN-MOORE and K. MUSILEK. Modulatory ABAD jako potenciální léčiva Alzheimerovy nemoci. 42. konference Syntéza a analýza léčiv, Hradec Králové (Czech Republic), September 2–5, 2013, Abstract Book.

#### **Other posters**

- 14) HROCH, L., Y. LI, J. PARRY and M. MACKA. Miniaturisation of data acquisition electronics and implementation of LED-based multi-wavelength detection for a portable capillary liquid chromatography system. 24<sup>th</sup> Annual RACI Research and Development Topics, Sydney (Australia), December 5–7, 2016.
- 15) HROCH, L., Y. LI, J. PARRY and M. MACKA. Miniaturisation of data acquisition electronics and implementation of LED-based multi-wavelength detection for a portable capillary liquid chromatography system. ACROSS International Symposium on Advances in Separation Science, Hobart (Australia), November 30 – December 2, 2016.

## 9. References

- [1] ALZHEIMER, A. Über eine eigenartige Erkrankung der Hirnrinde. *Allgemeine Zeitschrift für Psychiatrie und phychish-Gerichtliche Medizin*. 1907, vol. 64, no. 1, pp. 146–148.
- [2] O'BRIEN, C. Science History: Auguste D. and Alzheimer's Disease. *Science*. 1996, vol. 273, no. 5271, p. 28. ISSN 0036-8075. DOI 10.1126/science.273.5271.28
- [3] KRAEPELIN, E. *Psychiatrie. Ein Lehrbuch für Studierende und Aerzte*. Leipzig: Germany:Barth, 1899.
- [4] KATZMAN, R. The prevalence and malignancy of alzheimer disease: A major killer. *Archives of Neurology*. 1976, vol. 33, no. 4, pp. 217–218. ISSN 0003-9942. DOI 10.1001/archneur.1976.00500040001001
- [5] ALZHEIMER'S ASSOCIATION. 2017 Alzheimer's disease facts and figures. *Alzheimer's & Dementia*. 2017, vol. 3, no. 1, pp. 325–373.
- [6] BLENNOW, K., M. J. DE LEON and H. ZETTERBERG. Alzheimer's disease. *Lancet*. 2006, vol. 368, no. 9533, pp. 387–403. ISSN 01406736. DOI 10.1016/S0140-6736(06)69113-7
- [7] MACCIONI, R. B., G. FARÍAS, I. MORALES and L. NAVARRETE. The Revitalized Tau Hypothesis on Alzheimer's Disease. *Archives of Medical Research*. 2010, vol. 41, no. 3, pp. 226–231. ISSN 01884409. DOI 10.1016/j.arcmed.2010.03.007
- [8] MCKHANN, G., D. DRACHMAN, M. FOLSTEIN, R. KATZMAN, D. PRICE and E. M. STADLAN. Clinical diagnosis of Alzheimer's disease: Report of the NINCDS-ADRDA Work Group\* under the auspices of Department of Health and Human Services Task Force on Alzheimer's Disease. *Neurology*. 1984, vol. 34, no. 7, pp. 939–939. ISSN 0028-3878. DOI 10.1212/WNL.34.7.939
- [9] PRICE, D. L. and S. S. SISODIA. Mutant Genes in Familial Alzheimer's Disease and Transgenic Models. *Processing*. 1998, vol. 21, no. 1, pp. 479–505. ISSN 0147-006X. DOI 10.1146/annurev.neuro.21.1.479
- [10] ANAND, R., K. D. GILL and A. A. MAHDI. Therapeutics of Alzheimer's disease: Past, present and future. *Neuropharmacology*. 2014, vol. 76, no. 1, pp. 27–50. ISSN 00283908. DOI 10.1016/j.neuropharm.2013.07.004
- [11] DALE, H. H. the Action of Certain Esters and Ethers of Choline, and Their Relation To Muscarine. *Journal of Pharmacology and Experimental Therapeutics*. 1914, vol. 6, no. 2, pp. 147–190. ISSN 1521-0103.
- [12] DALE, H. H. and H. W. DUDLEY. The presence of histamine and acetylcholine in the spleen of the ox and the horse. *The Journal of physiology*. 1929, vol. 68, no. 2, pp. 97–123. ISSN 0022-3751. DOI 10.1113/jphysiol.1929.sp002598
- [13] LOEWI, O. Über humerole Übertragbarkeit der Herznervenwirkung. I. Mitteilung. *Pflügers Archiv. European Journal of Physiology*. 1921, vol. 189, no. 1, pp. 239–242. ISSN 0031-6768. DOI 10.1007/BF01738910
- [14] CONTESTABILE, A. The history of the cholinergic hypothesis. *Behavioural Brain Research*. 2011, vol. 221, no. 2, pp. 334–340. ISSN 01664328. DOI 10.1016/j.bbr.2009.12.044
- [15] BOWEN, D. M., C. B. SMITH, P. WHITE and A. N. DAVISON. Neurotransmitter-related enzymes and indices of hypoxia in senile dementia and other abiotrophies. *Brain*. 1976, vol. 99, no. 3, pp. 459–496. ISSN 00068950. DOI 10.1093/brain/99.3.459
- [16] DAVIES, P. and A. J. F. MALONEY. Selective Loss of Central Cholinergic Neurons in Alzheimer's Disease. *The Lancet*. 1976, vol. 308, no. 8000, p. 1403. ISSN 01406736. DOI 10.1016/S0140-6736(76)91936-X
- [17] PERRY, E. K., P. H. GIBSON, G. BLESSED, R. H. PERRY and B. E. TOMLINSON. Neurotransmitter enzyme abnormalities in senile dementia. *Journal of the Neurological Sciences*. 1977, vol. 34, no. 2, pp. 247–265. ISSN 0022510X. DOI 10.1016/0022-510X(77)90073-9
- [18] WILCOCK, G. K., M. M. ESIRI, D. M. BOWEN and C. C. T. SMITH. Alzheimer's disease. Correlation of cortical choline acetyltransferase activity with the severity of dementia and histological abnormalities. *Journal of the Neurological Sciences*. 1982, vol. 57, nos. 2–3, pp. 407–417. ISSN 0022510X. DOI 10.1016/0022-510X(82)90045-4

- [19] WHITEHOUSE, P. J., D. L. PRICE, A. W. CLARK, J. T. COYLE and M. R. DELONG. Alzheimer disease: Evidence for selective loss of cholinergic neurons in the nucleus basalis. *Annals of Neurology*. 1981, vol. 10, no. 2, pp. 122–126. ISSN 15318249. DOI 10.1002/ana.410100203
- [20] RYLETT, R. J., M. J. BALL and E. H. COLHOUN. Evidence for high affinity choline transport in synaptosomes prepared from hippocampus and neocortex of patients with Alzheimer's disease. *Brain Research*. 1983, vol. 289, nos. 1–2, pp. 169–175. ISSN 00068993. DOI 10.1016/0006-8993(83)90017-3
- [21] BARTUS, R., R. DEAN, B. BEER and A. LIPPA. The cholinergic hypothesis of geriatric memory dysfunction. *Science*. 1982, vol. 217, no. 4558, pp. 408–414. ISSN 0036-8075. DOI 10.1126/science.7046051
- [22] CUMMINGS, J. L. and D. KAUFER. Neuropsychiatric aspects of Alzheimer's disease: The cholinergic hypothesis revisited. *Neurology*. 1996, vol. 47, no. 4, pp. 876–883. ISSN 0028-3878. DOI 10.1212/WNL.47.4.876
- [23] FRANCIS, P. T., A. M. PALMER, M. SNAPE and G. K. WILCOCK. The cholinergic hypothesis of Alzheimer's disease: a review of progress. *Journal of neurology, neurosurgery, and psychiatry*. 1999, vol. 66, no. 2, pp. 137–147. ISSN 0022-3050. DOI 10.1136/JNNP.66.2.137
- [24] KOSIK, K., C. JOACHIM and D. SELKOE. Microtubule-associated protein  $\tau$  (tau) is a major antigenic component of paired helical filaments in Alzheimer disease. *Alzheimer Disease & Associated Disorders*. 1987, vol. 1, no. 3, p. 203. ISSN 0893-0341. DOI 10.1097/00002093-198701030-00022
- [25] GRUNDKE-IQBAL, I., K. IQBAL, Y. C. TUNG, M. QUINLAN, H. M. WISNIEWSKI and L. I. BINDER. Abnormal phosphorylation of the microtubule-associated protein  $\tau$  (tau) in Alzheimer cytoskeletal pathology. *Proceedings of the National Academy of Sciences*. 1986, vol. 83, no. 13, pp. 4913–4917. ISSN 0027-8424. DOI 10.1073/pnas.83.13.4913
- [26] BRION, J. P. Neurofibrillary tangles and Alzheimer's disease. *European Neurology*. 1998, vol. 40, no. 3, pp. 130–140. ISSN 00143022. DOI 10.1159/000007969
- [27] BRETTEVILLE, A. and E. PLANEL. Tau Aggregates: Toxic, Inert, or Protective Species? *Journal of Alzheimer's Disease*. 2008, vol. 14, no. 4, pp. 431–436. ISSN 18758908. DOI 10.3233/JAD-2008-14411
- [28] MERAZ-RÍOS, M. A., K. I. LIRA-DE LEÓN, V. CAMPOS-PEÑA, M. A. DE ANDA-HERNÁNDEZ and R. MENA-LÓPEZ. Tau oligomers and aggregation in Alzheimer's disease. *Journal of Neurochemistry*. 2010, vol. 112, no. 6, pp. 1353–1367. ISSN 00223042. DOI 10.1111/j.1471-4159.2009.06511.x
- [29] KÖPKE, E., Y. C. TUNG, S. SHAIKH, A. D. C. ALONSO, K. IQBAL and I. GRUNDKE-IQBAL. Microtubule-associated protein tau: Abnormal phosphorylation of a non-paired helical filament pool in Alzheimer disease. *Journal of Biological Chemistry*. 1993, vol. 268, no. 32, pp. 24374–24384. ISSN 00219258. DOI 10.1016/j.bbrc.2011.11.056
- [30] MANDELKOW, E., M. VON BERGEN, J. BIERNAT and E. M. MANDELKOW. Structural principles of tau and the paired helical filaments of Alzheimer's disease. *Brain Pathology*. 2007, vol. 17, no. 1, pp. 83–90. ISSN 10156305. DOI 10.1111/j.1750-3639.2007.00053.x
- [31] MAZANETZ, M. P. and P. M. FISCHER. Untangling tau hyperphosphorylation in drug design for neurodegenerative diseases. *Nature Reviews Drug Discovery*. 2007, vol. 6, no. 6, pp. 464–479. ISSN 1474-1776. DOI 10.1038/nrd2111
- [32] HARDY, J. and G. HIGGINS. Alzheimer's disease: the amyloid cascade hypothesis. *Science*. 1992, vol. 256, no. 5054, pp. 184–185. ISSN 0036-8075. DOI 10.1126/science.1566067
- [33] HARDY, J. The Amyloid Hypothesis of Alzheimer's Disease: Progress and Problems on the Road to Therapeutics. *Science*. 2002, vol. 297, no. 5580, pp. 353–356. ISSN 00368075. DOI 10.1126/science.1072994
- [34] HUYNH, R. A. and C. MOHAN. Alzheimer's Disease: Biomarkers in the Genome, Blood, and Cerebrospinal Fluid. *Frontiers in Neurology*. 2017, vol. 8, no. 1, pp. 1–15. ISSN 16642295. DOI 10.3389/fneur.2017.00102
- [35] TAYLOR, J. P., J. HARDY and K. H. FISCHBECK. Toxic Proteins in Neurodegenerative Disease. *Science*.

- 2002, vol. 296, no. 5575, pp. 1991–1995. ISSN 0036-8075. DOI 10.1126/science.1067122
- [36] BITAN, G., M. D. KIRKITADZE, A. LOMAKIN, S. S. VOLLERS, G. B. BENEDEK and D. B. TEPLow. Amyloid  $\beta$ -protein ( $A\beta$ ) assembly:  $A\beta$ 40 and  $A\beta$ 42 oligomerize through distinct pathways. *Proceedings of the National Academy of Sciences*. 2003, vol. 100, no. 1, pp. 330–335. ISSN 0027-8424. DOI 10.1073/pnas.222681699
- [37] HROCH, L., L. AITKEN, O. BENEK, M. DOLEZAL, K. KUCA, F. GUNN-MOORE and K. MUSILEK. Benzothiazoles - Scaffold of Interest for CNS Targeted Drugs. *Current Medicinal Chemistry*. 2015, vol. 22, no. 6, pp. 730–747. ISSN 1875533X. DOI 10.2174/0929867322666141212120631
- [38] BATEMAN, R. J., C. XIONG, T. L. S. BENZINGER, A. M. FAGAN, A. GOATE, N. C. FOX, D. S. MARCUS, N. J. CAIRNS, X. XIE, T. M. BLAZEY, D. M. HOLTZMAN, A. SANTACRUZ, V. BUCKLES, A. OLIVER, K. MOULDER, P. S. AISEN, B. GHETTI, W. E. KLUNK, E. MCDADE, R. N. MARTINS, C. L. MASTERS, R. MAYEUX, J. M. RINGMAN, M. N. ROSSOR, P. R. SCHOFIELD, R. A. SPERLING, S. SALLOWAY and J. C. MORRIS. Clinical and Biomarker Changes in Dominantly Inherited Alzheimer's Disease. *New England Journal of Medicine*. 2012, vol. 367, no. 9, pp. 795–804. ISSN 0028-4793. DOI 10.1056/NEJMoa1202753
- [39] JACK, C. R. and D. M. HOLTZMAN. Biomarker Modeling of Alzheimer's Disease. *Neuron*. 2013, vol. 80, no. 6, pp. 1347–1358. ISSN 10974199. DOI 10.1016/j.neuron.2013.12.003
- [40] SELKOE, D. J. and J. HARDY. The amyloid hypothesis of Alzheimer's disease at 25 years. *EMBO Molecular Medicine*. 2016, vol. 8, no. 6, pp. 595–608. ISSN 1757-4676. DOI 10.15252/emmm.201606210
- [41] LLEÓ, A., S. M. GREENBERG and J. H. GROWDON. Current Pharmacotherapy for Alzheimer's Disease. *Annual Review of Medicine*. 2006, vol. 57, no. 1, Annual Review of Medicine, pp. 513–533. ISSN 0066-4219. DOI 10.1146/annurev.med.57.121304.131442
- [42] WILKINSON, D., P. FRANCIS, E. SCHWAM and J. PAYNE-PARRISH. Cholinesterase Inhibitors Used in the Treatment of Alzheimer's Disease. *Drugs & Aging*. 2004, vol. 21, no. 7, pp. 453–478. ISSN 1170-229X. DOI 10.2165/00002512-200421070-00004
- [43] WATKINS, P. B., H. J. ZIMMERMAN, M. J. KNAPP, S. I. GRACON and K. W. LEWIS. Hepatotoxic effects of tacrine administration in patients with Alzheimer's disease. *JAMA: the journal of the American Medical Association*. 1994, vol. 271, no. 13, pp. 992–998. ISSN 00987484. DOI 10.1001/jama.271.13.992
- [44] MICHAELIS, E. K. Molecular biology of glutamate receptors in the central nervous system and their role in excitotoxicity, oxidative stress and aging. *Progress in Neurobiology*. 1998, vol. 54, no. 4, pp. 369–415. ISSN 03010082. DOI 10.1016/S0301-0082(97)00055-5
- [45] REVETT, T. J., G. B. BAKER, J. JHAMANDAS and S. KAR. Glutamate system, amyloid  $\beta$  peptides and tau protein: Functional interrelationships and relevance to Alzheimer disease pathology. *Journal of Psychiatry and Neuroscience*. 2013, vol. 38, no. 1, pp. 6–23. ISSN 14882434. DOI 10.1503/jpn.110190
- [46] WU, W. L. and L. ZHANG.  $\gamma$ -Secretase inhibitors for the treatment of Alzheimer's disease. *Drug Development Research*. 2009, vol. 70, no. 2, pp. 94–100. ISSN 02724391. DOI 10.1002/ddr.20288
- [47] WOLFE, M. S.  $\gamma$ -Secretase inhibitors and modulators for Alzheimer's disease. *Journal of Neurochemistry*. 2012, vol. 120, no. 1, pp. 89–98. ISSN 00223042. DOI 10.1111/j.1471-4159.2011.07501.x
- [48] BERGMANS, B. A. and B. DE STROOPER.  $\gamma$ -Secretases: From Cell Biology To Therapeutic Strategies. *The Lancet Neurology*. 2010, vol. 9, no. 2, pp. 215–226. ISSN 14744422. DOI 10.1016/S1474-4422(09)70332-1
- [49] PANZA, F., V. FRISARDI, B. P. IMBIMBO, C. CAPURSO, G. LOGROSCINO, D. SANCARLO, D. SERIPA, G. VENDEMIALE, A. PILOTTO and V. SOLFRIZZI. REVIEW:  $\gamma$ -Secretase Inhibitors for the Treatment of Alzheimer's Disease: The Current State. *CNS Neuroscience & Therapeutics*. 2010, vol. 16, no. 5, pp. 272–284. ISSN 17555930. DOI 10.1111/j.1755-5949.2010.00164.x
- [50] DE STROOPER, B. Lessons from a failed  $\gamma$ -secretase Alzheimer trial. *Cell*. 2014, vol. 159, no. 4, pp. 721–726.



- [51] BATEMAN, R. J., P. S. AISEN, B. DE STROOPER, N. C. FOX, C. A. LEMERE, J. M. RINGMAN, S. SALLOWAY, R. A. SPERLING, M. WINDISCH and C. XIONG. Autosomal-dominant Alzheimer's disease: a review and proposal for the prevention of Alzheimer's disease. *Alzheimer's Research & Therapy*. 2010, vol. 3, no. 1, p. 1. ISSN 1758-9193. DOI 10.1186/alzrt59
- [52] LING, Y., K. MORGAN and N. KALSHEKER. Amyloid precursor protein (APP) and the biology of proteolytic processing: relevance to Alzheimer's disease. *The International Journal of Biochemistry & Cell Biology*. 2003, vol. 35, no. 11, pp. 1505–1535. ISSN 13572725. DOI 10.1016/S1357-2725(03)00133-X
- [53] SHERRINGTON, R., E. I. ROGAEV, Y. LIANG, E. A. ROGAEVA, G. LEVESQUE, M. IKEDA, H. CHI, C. LIN, G. LI, K. HOLMAN, T. TSUDA, L. MAR, J.-F. FONCIN, A. C. BRUNI, M. P. MONTESI, S. SORBI, I. RAINERO, L. PINESSI, L. NEE, I. CHUMAKOV, D. POLLEN, A. BROOKES, P. SANSEAU, R. J. POLINSKY, W. WASCO, H. DA SILVA, A. R., J. L. HAINES, M. A. PERICAK-VANCE, R. E. TANZI, A. D. ROSES, P. E. FRASER, J. M. ROMMENS and P. H. ST GEORGE-HYSLOP. Cloning of a gene bearing missense mutations in early-onset familial Alzheimer's disease. *Nature*. 1995, vol. 375, no. 6534, pp. 754–760. ISSN 0028-0836. DOI 10.1038/375754a0
- [54] LEVY-LAHAD, E., W. WASCO, P. POORKAJ, D. ROMANO, J. OSHIMA, W. PETTINGELL, C. YU, P. JONDRO, S. SCHMIDT, K. WANG and e. AL. Candidate gene for the chromosome 1 familial Alzheimer's disease locus. *Science*. 1995, vol. 269, no. 5226, pp. 973–977. ISSN 0036-8075. DOI 10.1126/science.7638622
- [55] AMEMORI, T., P. JENDELOVA, J. RUZICKA, L. M. URDZIKOVA and E. SYKOVA. Alzheimer's disease: Mechanism and approach to cell therapy. *International Journal of Molecular Sciences*. 2015, vol. 16, no. 11, pp. 26417–26451. ISSN 14220067. DOI 10.3390/ijms161125961
- [56] GOATE, A., M. C. CHARTIER-HARLIN, M. MULLAN, J. BROWN, F. CRAWFORD, L. FIDANI, L. GIUFFRA, A. HAYNES, N. IRVING, L. JAMES, R. MANT, P. NEWTON, K. ROOKE, P. ROQUES, C. TALBOT, M. PERICAK-VANCE, A. ROSES, R. WILLIAMSON, M. ROSSOR, M. OWEN and J. HARDY. Segregation of a missense mutation in the amyloid precursor protein gene with familial Alzheimer's disease. *Nature*. 1991, vol. 349, no. 6311, pp. 704–706. ISSN 0028-0836. DOI 10.1038/349704a0
- [57] HARVEY, R. J. The prevalence and causes of dementia in people under the age of 65 years. *Journal of Neurology, Neurosurgery & Psychiatry*. 2003, vol. 74, no. 9, pp. 1206–1209. ISSN 0022-3050. DOI 10.1136/jnnp.74.9.1206
- [58] MATTSON, M. P. Pathways towards and away from Alzheimer's disease. *Nature*. 2004, vol. 431, no. 7004, pp. 107–107. ISSN 0028-0836. DOI 10.1038/nature02940
- [59] MAHLEY, R. W., K. H. WEISGRABER and Y. HUANG. Apolipoprotein E: structure determines function, from atherosclerosis to Alzheimer's disease to AIDS. *Journal of Lipid Research*. 2009, vol. 50, no. Suppl, pp. S183–S188. ISSN 0022-2275. DOI 10.1194/jlr.R800069-JLR200
- [60] CEDAZO-MÍNGUEZ, A. and R. F. COWBURN. Apolipoprotein E: a major piece in the Alzheimer's disease puzzle. *Journal of Cellular and Molecular Medicine*. 2001, vol. 5, no. 3, pp. 254–266. ISSN 1582-1838. DOI 10.1111/j.1582-4934.2001.tb00159.x
- [61] CEDAZO-MÍNGUEZ, A. Apolipoprotein E and Alzheimer's disease: molecular mechanisms and therapeutic opportunities. *Journal of Cellular and Molecular Medicine*. 2007, vol. 11, no. 6, pp. 1227–1238. ISSN 15821838. DOI 10.1111/j.1582-4934.2007.00130.x
- [62] SMITH, J. D. Apolipoprotein E4: an allele associated with many diseases. *Annals of Medicine*. 2000, vol. 32, no. 2, pp. 118–127. ISSN 0785-3890. DOI 10.3109/07853890009011761
- [63] CORDER, E., A. SAUNDERS, W. STRITTMATTER, D. SCHMECHEL, P. GASKELL, G. SMALL, A. ROSES, J. HAINES and M. PERICAK-VANCE. Gene dose of apolipoprotein E type 4 allele and the risk of Alzheimer's disease in late onset families. *Science*. 1993, vol. 261, no. 5123, pp. 921–923. ISSN 0036-8075.

DOI 10.1126/science.8346443

- [64] POIRIER, J., P. BERTRAND, J. POIRIER, S. KOGAN, S. GAUTHIER, J. POIRIER, S. GAUTHIER, J. DAVIGNON, D. BOUTHILLIER and J. DAVIGNON. Apolipoprotein E polymorphism and Alzheimer's disease. *The Lancet*. 1993, vol. 342, no. 8873, pp. 697–699. ISSN 01406736. DOI 10.1016/0140-6736(93)91705-Q
- [65] WISNIEWSKI, T., E. M. CASTAÑO, A. GOLABEK, T. VOGEL and B. FRANGIONE. Acceleration of Alzheimer's fibril formation by apolipoprotein E in vitro. *The American Journal of Pathology*. 1994, vol. 145, no. 5, pp. 1030–1035. ISSN 0002-9440.
- [66] JIANG, Q., C. Y. D. LEE, S. MANDREKAR, B. WILKINSON, P. CRAMER, N. ZELCER, K. MANN, B. LAMB, T. M. WILLSON, J. L. COLLINS, J. C. RICHARDSON, J. D. SMITH, T. A. COMERY, D. RIDDELL, D. M. HOLTZMAN, P. TONONNOZ and G. E. LANDRETH. ApoE Promotes the Proteolytic Degradation of A $\beta$ . *Neuron*. 2008, vol. 58, no. 5, pp. 681–693. ISSN 08966273. DOI 10.1016/j.neuron.2008.04.010
- [67] ROSES, A. D. A model for susceptibility polymorphisms for complex diseases: apolipoprotein E and Alzheimer disease. *Neurogenetics*. 1997, vol. 1, no. 1, pp. 3–11. ISSN 1364-6745. DOI 10.1007/s100480050001
- [68] TANZI, R. E. and L. BERTRAM. New frontiers in Alzheimer's disease genetics. *Neuron*. 2001, vol. 32, no. 2, pp. 181–184. ISSN 08966273. DOI 10.1016/S0896-6273(01)00476-7
- [69] KANG, J., H. LEMAIRE, A. UNTERBECK, J. SALBAUM, C. MASTERS, K. GRZESCHIK, G. MULTHAUP, K. BEYREUTHER and B. MÜLLER-HILL. The precursor of Alzheimer's disease amyloid A4 protein resembles a cell-surface receptor. *Alzheimer Disease & Associated Disorders*. 1987, vol. 1, no. 3, pp. 206–207. ISSN 0893-0341. DOI 10.1097/00002093-198701030-00032
- [70] BAYER, T. A., R. CAPPAL, C. L. MASTERS, K. BEYREUTHER and G. MULTHAUP. It all sticks together--the APP-related family of proteins and Alzheimer's disease. *Molecular psychiatry*. 1999, vol. 4, no. 6, pp. 524–528. ISSN 1359-4184. DOI 10.1038/sj.mp.4000552
- [71] O'BRIEN, R. J. and P. C. WONG. Amyloid Precursor Protein Processing and Alzheimer's Disease. *Annual Review of Neuroscience*. 2011, vol. 34, no. 1, pp. 185–204. ISSN 0147-006X. DOI 10.1146/annurev-neuro-061010-113613
- [72] VARDY, E. R. L. C., A. J. CATTO and N. M. HOOPER. Proteolytic mechanisms in amyloid- $\beta$  metabolism: Therapeutic implications for Alzheimer's disease. *Trends in Molecular Medicine*. 2005, vol. 11, no. 10, pp. 464–472. ISSN 14714914. DOI 10.1016/j.molmed.2005.08.004
- [73] NUNAN, J. and D. H. SMALL. Regulation of APP cleavage by  $\alpha$ -,  $\beta$ - and  $\gamma$ -secretases. *FEBS Letters*. 2000, vol. 483, no. 1, pp. 6–10. ISSN 00145793. DOI 10.1016/S0014-5793(00)02076-7
- [74] HAASS, C. and D. J. SELKOE. Soluble protein oligomers in neurodegeneration: lessons from the Alzheimer's amyloid  $\beta$ -peptide. *Nature Reviews Molecular Cell Biology*. 2007, vol. 8, no. 2, pp. 101–112. ISSN 1471-0072. DOI 10.1038/nrm2101
- [75] KUMMER, M. P. and M. T. HENEKA. Truncated and modified amyloid-beta species. *Alzheimer's Research & Therapy*. 2014, vol. 6, no. 3, p. 28. ISSN 1758-9193. DOI 10.1186/alzrt258
- [76] BIBL, M., M. GALLUS, V. WELGE, S. LEHMANN, K. SPARBIER, H. ESSELMANN and J. WILTFANG. Characterization of cerebrospinal fluid aminoterminally truncated and oxidized amyloid- $\beta$  peptides. *Proteomics - Clinical Applications*. 2012, vol. 6, nos. 3–4, pp. 163–169. ISSN 18628346. DOI 10.1002/prca.201100082
- [77] BURDICK, D., B. SOREGHAN, M. KWON, J. KOSMOSKI, M. KNAUER, A. HENSCHEN, J. YATES, C. COTMAN and C. GLABE. Assembly and aggregation properties of synthetic Alzheimer's A4/ $\beta$  amyloid peptide analogs. *Journal of Biological Chemistry*. 1992, vol. 267, no. 1, pp. 546–554. ISSN 00219258.
- [78] TEPLow, D. B. Structural and kinetic features of amyloid  $\beta$ -protein fibrillogenesis. *Amyloid*. 1998, vol. 5, no. 2, pp. 121–142. ISSN 1350-6129. DOI 10.3109/13506129808995290
- [79] CAUGHEY, B. and P. T. LANSBURY. PROTOFIBRILS, PORES, FIBRILS, AND

- NEURODEGENERATION: Separating the Responsible Protein Aggregates from The Innocent Bystanders. *Annual Review of Neuroscience*. 2003, vol. 26, no. 1, pp. 267–298. ISSN 0147-006X. DOI 10.1146/annurev.neuro.26.010302.081142
- [80] WALSH, D. M., I. KLYUBIN, J. V. FADEEVA, W. K. CULLEN, R. ANWYL, M. S. WOLFE, M. J. ROWAN and D. J. SELKOE. Naturally secreted oligomers of amyloid  $\beta$  protein potently inhibit hippocampal long-term potentiation in vivo. *Nature*. 2002, vol. 416, no. 6880, pp. 535–539. ISSN 00280836. DOI 10.1038/416535a
- [81] CLEARY, J. P., D. M. WALSH, J. J. HOFMEISTER, G. M. SHANKAR, M. A. KUSKOWSKI, D. J. SELKOE and K. H. ASHE. Natural oligomers of the amyloid- $\beta$  protein specifically disrupt cognitive function. *Nature Neuroscience*. 2005, vol. 8, no. 1, pp. 79–84. ISSN 1097-6256. DOI 10.1038/nm1372
- [82] SCHEUNER, D., C. ECKMAN, M. JENSEN, X. SONG, M. CITRON, N. SUZUKI, T. D. BIRD, J. HARDY, M. HUTTON, W. KUKULL, E. LARSON, L. LEVY-LAHAD, M. VIITANEN, E. PESKIND, P. POORKAJ, G. SCHELLENBERG, R. TANZI, W. WASCO, L. LANNFELT, D. SELKOE and S. YOUNKIN. Secreted amyloid  $\beta$ -protein similar to that in the senile plaques of Alzheimer's disease is increased in vivo by the presenilin 1 and 2 and APP mutations linked to familial Alzheimer's disease. *Nature Medicine*. 1996, vol. 2, no. 8, pp. 864–870. ISSN 1078-8956. DOI 10.1038/nm0896-864
- [83] FAGAN, A. M., M. A. MINTUN, R. H. MACH, S. Y. LEE, C. S. DENCE, A. R. SHAH, G. N. LAROSSA, M. L. SPINNER, W. E. KLUNK, C. A. MATHIS, S. T. DEKOSKY, J. C. MORRIS and D. M. HOLTZMAN. Inverse relation between in vivo amyloid imaging load and cerebrospinal fluid A $\beta$ 42 in humans. *Annals of Neurology*. 2006, vol. 59, no. 3, pp. 512–519. ISSN 03645134. DOI 10.1002/ana.20730
- [84] BAYER, T. A. and WIRTHS O. Intracellular accumulation of amyloid-beta – a predictor for synaptic dysfunction and neuron loss in Alzheimer's disease. *Frontiers in Aging Neuroscience*. 2010, vol. 2, no. 1, p. 10. ISSN 16634365. DOI 10.3389/fnagi.2010.00008
- [85] GOURAS, G. K., J. TSAI, J. NASLUND, B. VINCENT, M. EDGAR, F. CHECLER, J. P. GREENFIELD, V. HAROUTUNIAN, J. D. BUXBAUM, H. XU, P. GREENGARD and N. R. RELKIN. Intraneuronal A $\beta$ 42 Accumulation in Human Brain. *The American Journal of Pathology*. 2000, vol. 156, no. 1, pp. 15–20. ISSN 00029440. DOI 10.1016/S0002-9440(10)64700-1
- [86] TAKAHASHI, R. H., T. A. MILNER, F. LI, E. E. NAM, M. A. EDGAR, H. YAMAGUCHI, M. F. BEAL, H. XU, P. GREENGARD and G. K. GOURAS. Intraneuronal Alzheimer A $\beta$ 42 Accumulates in Multivesicular Bodies and Is Associated with Synaptic Pathology. *The American Journal of Pathology*. 2002, vol. 161, no. 5, pp. 1869–1879. ISSN 00029440. DOI 10.1016/S0002-9440(10)64463-X
- [87] LAFERLA, F. M., K. N. GREEN and S. ODDO. Intracellular amyloid- $\beta$  in Alzheimer's disease. *Nature Reviews Neuroscience*. 2007, vol. 8, no. 7, pp. 499–509. ISSN 1471-003X. DOI 10.1038/nrn2168
- [88] PENKE, B., A. M. TÓTH, I. FÖLDI, M. SZUCS and T. JANÁKY. Intraneuronal  $\beta$ -amyloid and its interactions with proteins and subcellular organelles. *Electrophoresis*. 2012, vol. 33, no. 24, pp. 3608–3616. ISSN 01730835. DOI 10.1002/elps.201200297
- [89] MUIRHEAD, K. E. A., E. BORGER, L. AITKEN, S. J. CONWAY and F. J. GUNN-MOORE. The consequences of mitochondrial amyloid  $\beta$ -peptide in Alzheimer's disease. *Biochemical Journal*. 2010, vol. 426, no. 3, pp. 255–270. ISSN 0264-6021. DOI 10.1042/BJ20091941
- [90] BI, X., C. M. GALL, J. ZHOU and G. LYNCH. Uptake and pathogenic effects of amyloid beta peptide 1-42 are enhanced by integrin antagonists and blocked by NMDA receptor antagonists. *Neuroscience*. 2002, vol. 112, no. 4, pp. 827–840. ISSN 03064522. DOI 10.1016/S0306-4522(02)00132-X
- [91] BEAL, M. F. Mitochondria take center stage in aging and neurodegeneration. *Annals of Neurology*. 2005, vol. 58, no. 4, pp. 495–505. ISSN 03645134. DOI 10.1002/ana.20624
- [92] PETROZZI, L., G. RICCI, N. J. GIGLIOLI, G. SICILIANO and M. MANCUSO. Mitochondria and Neurodegeneration. *Bioscience Reports*. 2007, vol. 27, nos. 1–3, pp. 87–104. ISSN 0144-8463. DOI

- 10.1007/s10540-007-9038-z
- [93] TILLEMENT, L., L. LECANU and V. PAPADOPOULOS. Alzheimer's disease: Effects of  $\beta$ -amyloid on mitochondria. *Mitochondrion*. 2011, vol. 11, no. 1, pp. 13–21. ISSN 15677249. DOI 10.1016/j.mito.2010.08.009
- [94] HANSSON PETERSEN, C. A., N. ALIKHANI, H. BEHBAHANI, B. WIEHAGER, P. F. PAVLOV, I. ALAFUZOFF, V. LEINONEN, A. ITO, B. WINBLAD, E. GLASER and M. ANKARCORONA. The amyloid  $\beta$ -peptide is imported into mitochondria via the TOM import machinery and localized to mitochondrial cristae. *Proceedings of the National Academy of Sciences*. 2008, vol. 105, no. 35, pp. 13145–13150. ISSN 0027-8424. DOI 10.1073/pnas.0806192105
- [95] ANANDATHEERTHAVARADA, H. K. and L. DEVI. Mitochondrial translocation of amyloid precursor protein and its cleaved products: relevance to mitochondrial dysfunction in Alzheimer's disease. *Reviews in the neurosciences*. 2007, vol. 18, no. 5, pp. 343–354. ISSN 2191-0200. DOI 10.1515/revneuro.2007.18.5.343
- [96] PINHO, C. M., P. F. TEIXEIRA and E. GLASER. Mitochondrial import and degradation of amyloid- $\beta$  peptide. *Biochimica et Biophysica Acta - Bioenergetics*. 2014, vol. 1837, no. 7, pp. 1069–1074. ISSN 18792650. DOI 10.1016/j.bbabi.2014.02.007
- [97] DE BRITO, O. M. and L. SCORRANO. An intimate liaison: spatial organization of the endoplasmic reticulum–mitochondria relationship. *The EMBO Journal*. 2010, vol. 29, no. 16, pp. 2715–2723. ISSN 0261-4189. DOI 10.1038/emboj.2010.177
- [98] BENEK, O., L. AITKEN, L. HROCH, K. KUČA, F. GUNN-MOORE and K. MUSILEK. A Direct interaction between mitochondrial proteins and amyloid-beta peptide and its significance for the progression and treatment of Alzheimer's disease. *Current Medicinal Chemistry*. 2015, vol. 22, no. 9, pp. 1056–1085. ISSN 0929-8673. DOI 10.2174/0929867322666150114163051
- [99] YAN, S. D., J. FU, C. SOTO, X. CHEN, H. ZHU, F. AL-MOHANNA, K. COLLISON, a ZHU, E. STERN, T. SAIDO, M. TOHYAMA, S. OGAWA, a ROHER and D. STERN. An intracellular protein that binds amyloid-beta peptide and mediates neurotoxicity in Alzheimer's disease. *Nature*. 1997, vol. 389, no. 6652, pp. 689–695. ISSN 0028-0836. DOI 10.1038/39522
- [100] FURUTA, S., A. KOBAYASHI, S. MIYAZAWA and T. HASHIMOTO. Cloning and expression of cDNA for a newly identified isozyme of bovine liver 3-hydroxyacyl-CoA dehydrogenase and its import into mitochondria. *Biochimica et Biophysica Acta - Gene Structure and Expression*. 1997, vol. 1350, no. 3, pp. 317–324. ISSN 01674781. DOI 10.1016/S0167-4781(96)00171-6
- [101] HE, X. Y., H. SCHULZ and S. Y. YANG. A human brain L-3-hydroxyacyl-coenzyme a dehydrogenase is identical to an amyloid  $\beta$ -peptide-binding protein involved in Alzheimer's disease. *Journal of Biological Chemistry*. 1998, vol. 273, no. 17, pp. 10741–10746. ISSN 00219258. DOI 10.1074/jbc.273.17.10741
- [102] HE, X. Y., G. MERZ, P. MEHTA, H. SCHULZ and S. Y. YANG. Human brain short chain L-3-hydroxyacyl coenzyme A dehydrogenase is a single-domain multifunctional enzyme. Characterization of a novel 17 $\beta$ -hydroxysteroid dehydrogenase. *Journal of Biological Chemistry*. 1999, vol. 274, no. 21, pp. 15014–15019. ISSN 00219258. DOI 10.1074/jbc.274.21.15014
- [103] OPPERMANN, U. C. T., S. SALIM, L. O. TJERNBERG, L. TERENIUS and H. JÖRNVALL. Binding of amyloid  $\beta$ -peptide to mitochondrial hydroxyacyl-CoA dehydrogenase (ERAB): Regulation of an SDR enzyme activity with implications for apoptosis in Alzheimer's disease. *FEBS Letters*. 1999, vol. 451, no. 3, pp. 238–242. ISSN 00145793. DOI 10.1016/S0014-5793(99)00586-4
- [104] HE, X. Y., G. MERZ, Y. Z. YANG, P. MEHTA, H. SCHULZ and S. Y. YANG. Characterization and localization of human type10 17 $\beta$ -hydroxysteroid dehydrogenase. *European journal of biochemistry / FEBS*. 2001, vol. 268, no. 18, pp. 4899–4907. ISSN 0014-2956. DOI 10.1046/j.0014-2956.2001.02421.2421.x
- [105] YANG, S. Y., X. Y. HE and H. SCHULZ. Multiple functions of type 10 17 $\beta$ -hydroxysteroid dehydrogenase. *Trends in Endocrinology and Metabolism*. 2005, vol. 16, no. 4, pp. 167–175. ISSN 10432760. DOI

- 10.1016/j.tem.2005.03.006
- [106] LUO, M. J., L. F. MAO and H. SCHULZ. Short-Chain 3-Hydroxy-2-methylacetyl-CoA Dehydrogenase from Rat Liver: Purification and Characterization of a Novel Enzyme of Isoleucine Metabolism. *Archives of Biochemistry and Biophysics*. 1995, vol. 321, no. 1, pp. 214–220. ISSN 00039861. DOI 10.1006/abbi.1995.1388
- [107] KOBAYASHI, A., L. L. JIANG and T. HASHIMOTO. Two mitochondrial 3-hydroxyacyl-CoA dehydrogenases in bovine liver. *Journal of biochemistry*. 1996, vol. 119, no. 4, pp. 775–82. ISSN 0021-924X. DOI 10.1093/oxfordjournals.jbchem.a021307
- [108] YAN, S. Du, Y. SHI, A. ZHU, J. FU, H. ZHU, Y. ZHU, L. GIBSON, E. STERN, K. COLLISON, F. AL-MOHANNA, S. OGAWA, A. ROHER, S. G. CLARKE and D. M. STERN. Role of ERAB/L-3-hydroxyacyl-coenzyme A dehydrogenase type II activity in A $\beta$ -induced cytotoxicity. *Journal of Biological Chemistry*. 1999, vol. 274, no. 4, pp. 2145–2156. ISSN 00219258. DOI 10.1074/jbc.274.4.2145
- [109] OFMAN, R., J. P. N. RUITER, M. FEENSTRA, M. DURAN, B. T. POLL-THE, J. ZSCHOCKE, R. ENSENAUER, W. LEHNERT, J. O. SASS, W. SPERL and R. J. A. WANDERS. 2-Methyl-3-hydroxybutyryl-CoA dehydrogenase deficiency is caused by mutations in the HADH2 gene. *American journal of human genetics*. 2003, vol. 72, no. 5, pp. 1300–1307. ISSN 0002-9297. DOI 10.1086/375116
- [110] MILLER, A. P. and H. F. WILLARD. Chromosomal basis of X chromosome inactivation: Identification of a multigene domain in Xp11.21-p11.22 that escapes X inactivation. *Proceedings of the National Academy of Sciences*. 1998, vol. 95, no. 15, pp. 8709–8714. ISSN 0027-8424. DOI 10.1073/pnas.95.15.8709
- [111] POWELL, A. J., J. A. READ, M. J. BANFIELD, F. GUNN-MOORE, S. S. YAN, J. W. LUSTBADER, A. R. STERN, D. M. STERN and R. L. BRADY. Recognition of structurally diverse substrates by type II 3-hydroxyacyl-CoA dehydrogenase (HADH II)/Amyloid- $\beta$  binding alcohol dehydrogenase (ABAD). *Journal of Molecular Biology*. 2000, vol. 303, no. 2, pp. 311–327. ISSN 00222836. DOI 10.1006/jmbi.2000.4139
- [112] LUSTBADER, J. W., M. CIRILLI, C. LIN, H. W. XU, K. TAKUMA, N. WANG, C. CASPERSEN, X. CHEN, S. POLLAK, M. CHANEY, F. TRINCHESE, S. LIU, F. GUNN-MOORE, L. F. LUE, D. G. WALKER, P. KUPPUSAMY, Z. L. ZEWIER, O. ARANCIO, D. STERN, S. S. YAN and H. WU. ABAD Directly Links A $\beta$  to Mitochondrial Toxicity in Alzheimer's Disease. *Science*. 2004, vol. 304, no. 5669, pp. 448–452. ISSN 0036-8075. DOI 10.1126/science.1091230
- [113] KISSINGER, C. R., P. A. REJTO, L. A. PELLETIER, J. A. THOMSON, R. E. SHOWALTER, M. A. ABREO, C. S. AGREE, S. MARGOSIAK, J. J. MENG, R. M. AUST, D. VANDERPOOL, B. LI, A. TEMPCZYK-RUSSELL and J. E. VILAFRANCA. Crystal structure of human ABAD/HSD10 with a bound inhibitor: Implications for design of Alzheimer's disease therapeutics. *Journal of Molecular Biology*. 2004, vol. 342, no. 3, pp. 943–952. ISSN 00222836. DOI 10.1016/j.jmb.2004.07.071
- [114] ROSSMAN, M. G., A. LILJAS, C. I. BRÄNDÉN and L. J. BANASZAK. 2 Evolutionary and Structural Relationships among Dehydrogenases. *Enzymes*. 1975, vol. 11, no. 1, pp. 61–102. ISSN 18746047. DOI 10.1016/S1874-6047(08)60210-3
- [115] BRETON, R., D. HOUSSET, C. MAZZA and J. C. FONTECILLA-CAMPS. The structure of a complex of human 17 $\beta$ -hydroxysteroid dehydrogenase with estradiol and NADP<sup>+</sup> identifies two principal targets for the design of inhibitors. *Structure*. 1996, vol. 4, no. 8, pp. 905–915. ISSN 09692126. DOI 10.1016/S0969-2126(96)00098-6
- [116] HE, X. Y., Y. Z. YANG, H. SCHULZ and S. Y. YANG. Intrinsic alcohol dehydrogenase and hydroxysteroid dehydrogenase activities of human mitochondrial short-chain L-3-hydroxyacyl-CoA dehydrogenase. *The Biochemical journal*. 2000, vol. 345, no. 1, pp. 139–143. ISSN 0264-6021. DOI 10.1042/0264-6021:3450139
- [117] ENSENAUER, R., H. NIEDERHOFF, J. P. N. RUITER, R. J. A. WANDERS, K. OTFRIED SCHWAB, M. BRANDIS and W. LEHNERT. Clinical variability in 3-hydroxy-2-methylbutyryl-CoA dehydrogenase deficiency. *Annals of Neurology*. 2002, vol. 51, no. 5, pp. 656–659. ISSN 03645134. DOI 10.1002/ana.10169

- [118] SASS, J. O., R. FORSTNER and W. SPERL. 2-Methyl-3-hydroxybutyryl-CoA dehydrogenase deficiency: Impaired catabolism of isoleucine presenting as neurodegenerative disease. *Brain and Development*. 2004, vol. 26, no. 1, pp. 12–14. ISSN 03877604. DOI 10.1016/S0387-7604(03)00071-8
- [119] HOLZMANN, J., P. FRANK, E. LÖFFLER, K. L. BENNETT, C. GERNER and W. ROSSMANITH. RNase P without RNA: Identification and Functional Reconstitution of the Human Mitochondrial tRNA Processing Enzyme. *Cell*. 2008, vol. 135, no. 3, pp. 462–474. ISSN 00928674. DOI 10.1016/j.cell.2008.09.013
- [120] BOYNTON, T. O. and L. J. SHIMKETS. Myxococcus CsgA, Drosophila sniffer, and human HSD10 are cardiolipin phospholipases. *Genes and Development*. 2015, vol. 29, no. 18, pp. 1903–1914. ISSN 15495477. DOI 10.1101/gad.268482.115
- [121] XIE, Y., S. DENG, Z. CHEN, S. S. YAN and D. W. LANDRY. Identification of small-molecule inhibitors of the A $\beta$ -ABAD interaction. *Bioorganic and Medicinal Chemistry Letters*. 2006, vol. 16, no. 17, pp. 4657–4660. ISSN 0960894X. DOI 10.1016/j.bmcl.2006.05.099
- [122] YAN, Y., Y. LIU, M. SORCI, G. BELFORT, J. W. LUSTBADER, S. S. YAN and C. WANG. Surface Plasmon Resonance and Nuclear Magnetic Resonance Studies of ABAD–A $\beta$  Interaction. *Biochemistry*. 2007, vol. 46, no. 7, pp. 1724–1731. ISSN 0006-2960. DOI 10.1021/bi061314n
- [123] BORGER, E., L. AITKEN, K. E. A. MUIRHEAD, Z. E. ALLEN, J. A. AINGE, S. J. CONWAY and F. J. GUNN-MOORE. Mitochondrial  $\beta$ -amyloid in Alzheimer's disease. *Biochemical Society Transactions*. 2011, vol. 39, no. 4, pp. 868–873. ISSN 0300-5127. DOI 10.1042/BST0390868
- [124] SAYRE, L. M., D. A. ZELASKO, P. L. R. HARRIS, G. PERRY, R. G. SALOMON and M. A. SMITH. 4-Hydroxynonenal-Derived Advanced Lipid Peroxidation End Products Are Increased in Alzheimer's Disease. *Journal of Neurochemistry*. 1997, vol. 68, no. 5, pp. 2092–2097. ISSN 1471-4159. DOI 10.1046/j.1471-4159.1997.68052092.x
- [125] MURAKAMI, Y., I. OHSAWA, T. KASAHARA and S. OHTA. Cytoprotective role of mitochondrial amyloid  $\beta$  peptide-binding alcohol dehydrogenase against a cytotoxic aldehyde. *Neurobiology of Aging*. 2009, vol. 30, no. 2, pp. 325–329. ISSN 01974580. DOI 10.1016/j.neurobiolaging.2007.07.002
- [126] HE, X. Y., G. Y. WEN, G. MERZ, D. LIN, Y. Z. YANG, P. MEHTA, H. SCHULZ and S. Y. YANG. Abundant type 10 17 $\beta$ -hydroxysteroid dehydrogenase in the hippocampus of mouse Alzheimer's disease model. *Molecular Brain Research*. 2002, vol. 99, no. 1, pp. 46–53. ISSN 0169328X. DOI 10.1016/S0169-328X(02)00102-X
- [127] YAO, J., M. TAYLOR, F. DAVEY, Y. REN, J. AITON, P. COOTE, F. FANG, J. X. CHEN, S. Du YAN and F. J. GUNN-MOORE. Interaction of amyloid binding alcohol dehydrogenase/A $\beta$  mediates up-regulation of peroxiredoxin II in the brains of Alzheimer's disease patients and a transgenic Alzheimer's disease mouse model. *Molecular and Cellular Neuroscience*. 2007, vol. 35, no. 2, pp. 377–382. ISSN 10447431. DOI 10.1016/j.mcn.2007.03.013
- [128] RAMJAUN, A. R., A. ANGERS, V. LEGENDRE-GUILLEMIN, X. K. TONG and P. S. MCPHERSON. Endophilin Regulates JNK Activation through Its Interaction with the Germinal Center Kinase-like Kinase. *Journal of Biological Chemistry*. 2001, vol. 276, no. 31, pp. 28913–28919. ISSN 00219258. DOI 10.1074/jbc.M103198200
- [129] REN, Y., W. X. HONG, F. DAVEY, M. TAYLOR, J. AITON, P. COOTE, F. FANG, J. YAO, D. CHEN, J. X. CHEN, D. Y. SHI and F. J. GUNN-MOORE. Endophilin I expression is increased in the brains of Alzheimer disease patients. *Journal of Biological Chemistry*. 2008, vol. 283, no. 9, pp. 5685–5691. ISSN 00219258. DOI 10.1074/jbc.M707932200
- [130] MILTON, N. G., N. P. MAYOR and J. RAWLINSON. Identification of amyloid-beta binding sites using an antisense peptide approach. *Neuroreport*. 2001, vol. 12, no. 11, pp. 2561–2566. ISSN 0959-4965.
- [131] YAO, J., H. DU, S. YAN, F. FANG, C. WANG, L. F. LUE, L. GUO, D. CHEN, D. M. STERN, F. J. GUNN MOORE, J. XI CHEN, O. ARANCIO and S. S. YAN. Inhibition of Amyloid- $\beta$  (A $\beta$ ) Peptide-Binding Alcohol

- Dehydrogenase-A $\beta$  Interaction Reduces A $\beta$  Accumulation and Improves Mitochondrial Function in a Mouse Model of Alzheimer's Disease. *Journal of Neuroscience*. 2011, vol. 31, no. 6, pp. 2313–2320. ISSN 0270-6474. DOI 10.1523/JNEUROSCI.4717-10.2011
- [132] HE, X. Y., Y. Z. YANG, D. M. PEEHL, A. LAUDERDALE, H. SCHULZ and S. Y. YANG. Oxidative 3 $\alpha$ -hydroxysteroid dehydrogenase activity of human type 10 17 $\beta$ -hydroxysteroid dehydrogenase. *The Journal of Steroid Biochemistry and Molecular Biology*. 2003, vol. 87, nos. 2–3, pp. 191–198. ISSN 09600760. DOI 10.1016/j.jsbmb.2003.07.007
- [133] AYAN, D., R. MALTAIS and D. POIRIER. Identification of a 17 $\beta$ -Hydroxysteroid Dehydrogenase Type10 Steroidal Inhibitor: A Tool to Investigate the Role of Type10 in Alzheimer's Disease and Prostate Cancer. *ChemMedChem*. 2012, vol. 7, no. 7, pp. 1181–1184. ISSN 18607179. DOI 10.1002/cmdc.201200129
- [134] LIM, Y.-A., A. GRIMM, M. GIESE, A. G. MENSAH-NYAGAN, J. E. VILAFRANCA, L. M. ITTNER, A. ECKERT and J. GÖTZ. Inhibition of the Mitochondrial Enzyme ABAD Restores the Amyloid- $\beta$ -Mediated Dereglulation of Estradiol. *PLoS ONE*. 2011, vol. 6, no. 12, p. e28887. DOI 10.1371/journal.pone.0028887
- [135] VALASANI, K. R., Q. SUN, G. HU, J. LI, F. DU, Y. GUO, E. A. CARLSON and X. G. and S. S. YAN. Identification of Human ABAD Inhibitors for Rescuing A $\beta$ -Mediated Mitochondrial Dysfunction. *Current Alzheimer Research*. 2014, vol. 11, no. 2, pp. 128–136. ISSN 1875-5828. DOI 10.2174/1567205011666140130150108
- [136] HROCH, L., P. GUEST, O. BENEK, O. SOUKUP, J. JANOCKOVA, R. DOLEZAL, K. KUCA, L. AITKEN, T. K. SMITH, F. GUNN-MOORE, D. ZALA, R. R. RAMSAY and K. MUSILEK. Synthesis and evaluation of frentizole-based indolyl thiourea analogues as MAO/ABAD inhibitors for Alzheimer's disease treatment. *Bioorganic and Medicinal Chemistry*. 2017, vol. 25, no. 3, pp. 1143–1152. ISSN 14643391. DOI 10.1016/j.bmc.2016.12.029
- [137] CAVALLI, A., M. L. BOLOGNESI, A. MÌNARINI, M. ROSINI, V. TUMIATTI, M. RECANATINI and C. MELCHIORRE. Multi-target-directed ligands to combat neurodegenerative diseases. *Journal of Medicinal Chemistry*. 2008, vol. 51, no. 3, pp. 347–372. ISSN 00222623. DOI 10.1021/jm7009364
- [138] YOUDIM, M. B. H. and J. J. BUCCAFUSCO. Multi-functional drugs for various CNS targets in the treatment of neurodegenerative disorders. *Trends in Pharmacological Sciences*. 2005, vol. 26, no. 1, pp. 27–35. ISSN 01656147. DOI 10.1016/j.tips.2004.11.007
- [139] LUO, W., Y. P. LI, Y. HE, S. L. HUANG, J. H. TAN, T. M. OU, D. LI, L. Q. GU and Z. S. HUANG. Design, synthesis and evaluation of novel tacrine-multialkoxybenzene hybrids as dual inhibitors for cholinesterases and amyloid beta aggregation. *Bioorganic and Medicinal Chemistry*. 2011, vol. 19, no. 2, pp. 763–770. ISSN 09680896. DOI 10.1016/j.bmc.2010.12.022
- [140] FANG, L., D. APPENROTH, M. DECKER, M. KIEHNTOPF, C. ROEGLER, T. DEUFEL, C. FLECK, S. PENG, Y. ZHANG and J. LEHMANN. Synthesis and biological evaluation of NO-donor-tacrine hybrids as hepatoprotective anti-Alzheimer drug candidates. *Journal of Medicinal Chemistry*. 2008, vol. 51, no. 4, pp. 713–716. ISSN 00222623. DOI 10.1021/jm701491k
- [141] MARCO-CONTELLES, J., R. LEÓN, C. DE LOS RÍOS, A. GUGLIETTA, J. TERCENIO, M. G. LÓPEZ, A. G. GARCÍA and M. VILLARROYA. Novel multipotent tacrine-dihydropyridine hybrids with improved acetylcholinesterase inhibitory and neuroprotective activities as potential drugs for the treatment of Alzheimer's disease. *Journal of Medicinal Chemistry*. 2006, vol. 49, no. 26, pp. 7607–7610. ISSN 00222623. DOI 10.1021/jm061047j
- [142] BOLEA, I., J. JUÁREZ-JIMÉNEZ, C. DE LOS RÍOS, M. CHIOUA, R. POUPLANA, F. J. LUQUE, M. UNZETA, J. MARCO-CONTELLES and A. SAMADI. Synthesis, biological evaluation, and molecular modeling of donepezil and N-[(5-(Benzyloxy)-1-methyl-1H-indol-2-yl)methyl]-N-methylprop-2-yn-1-amine hybrids as new multipotent cholinesterase/monoamine oxidase inhibitors for the treatment of Alzheimer's

- disease. *Journal of Medicinal Chemistry*. 2011, vol. 54, no. 24, pp. 8251–8270. ISSN 00222623. DOI 10.1021/jm200853t
- [143] STERLING, J., Y. HERZIG, T. GOREN, N. FINKELSTEIN, D. LERNER, W. GOLDENBERG, I. MISKOLCZI, S. MOLNAR, F. RANTAL, T. TAMAS, G. TOTH, A. ZAGYVA, A. ZEKANY, G. LAVIAN, A. GROSS, R. FRIEDMAN, M. RAZIN, W. HUANG, B. KRAIS, M. CHOREV, M. B. YODIM and M. WEINSTOCK. Novel dual inhibitors of AChE and MAO derived from hydroxy aminoindan and phenethylamine as potential treatment for Alzheimer's disease. *Journal of Medicinal Chemistry*. 2002, vol. 45, no. 24, pp. 5260–5279. ISSN 00222623. DOI 10.1021/jm020120c
- [144] YODIM, M. B. H., D. EDMONDSON and K. F. TIPTON. The therapeutic potential of monoamine oxidase inhibitors. *Nature Reviews Neuroscience*. 2006, vol. 7, no. 4, pp. 295–309. ISSN 1471-003X. DOI 10.1038/nrn1883
- [145] DRINGENBERG, H. C. Alzheimer's disease: More than a "cholinergic disorder" - Evidence that cholinergic-monoaminergic interactions contribute to EEG slowing and dementia. *Behavioural Brain Research*. 2000, vol. 115, no. 2, pp. 235–249. ISSN 01664328. DOI 10.1016/S0166-4328(00)00261-8
- [146] SHIH, J. C., K. CHEN and M. J. RIDD. MONOAMINE OXIDASE: From Genes to Behavior. *Annual Review of Neuroscience*. 1999, vol. 22, no. 1, pp. 197–217. ISSN 0147-006X. DOI 10.1146/annurev.neuro.22.1.197
- [147] R. RAMSAY, R. Monoamine Oxidases: The Biochemistry of the Proteins As Targets in Medicinal Chemistry and Drug Discovery. *Current Topics in Medicinal Chemistry*. 2013, vol. 12, no. 20, pp. 2189–2209. ISSN 15680266. DOI 10.2174/1568026611212200007
- [148] SPARKS, D. L., V. M. WOELTZ and W. R. MARKESBERY. Alterations in brain monoamine oxidase activity in aging, Alzheimer's disease, and Pick's disease. *Archives of neurology*. 1991, vol. 48, no. 7, pp. 718–721. ISSN 0003-9942. DOI 10.1001/archneur.1991.00530190064017
- [149] JOSSAN, S. S., P. G. GILLBERG, C. G. GOTTFRIES, I. KARLSSON and L. ORELAND. Monoamine oxidase B in brains from patients with Alzheimer's disease: A biochemical and autoradiographical study. *Neuroscience*. 1991, vol. 45, no. 1, pp. 1–12. ISSN 03064522. DOI 10.1016/0306-4522(91)90098-9
- [150] EMILSSON, L., P. SAETRE, J. BALCIUNIENE, A. CASTENSSON, N. CAIRNS and E. E. JAZIN. Increased monoamine oxidase messenger RNA expression levels in frontal cortex of Alzheimer's disease patients. *Neuroscience Letters*. 2002, vol. 326, no. 1, pp. 56–60. ISSN 03043940. DOI 10.1016/S0304-3940(02)00307-5
- [151] KENNEDY, B. P., M. G. ZIEGLER, M. ALFORD, L. a HANSEN, L. J. THAL and E. MASLIAH. Early and persistent alterations in prefrontal cortex MAO A and B in Alzheimer's disease. *Journal of Neural Transmission*. 2003, vol. 110, no. 7, pp. 789–801. ISSN 0300-9564. DOI 10.1007/s00702-003-0828-6
- [152] BURKE, W. J., S. W. LI, C. A. SCHMITT, P. XIA, H. D. CHUNG and K. N. GILLESPIE. Accumulation of 3,4-dihydroxyphenylglycolaldehyde, the neurotoxic monoamine oxidase A metabolite of norepinephrine, in locus ceruleus cell bodies in Alzheimer's disease: Mechanism of neuron death. *Brain Research*. 1999, vol. 816, no. 2, pp. 633–637. ISSN 00068993. DOI 10.1016/S0006-8993(98)01211-6
- [153] YANA, M. H., X. WANG and X. ZHU. Mitochondrial defects and oxidative stress in Alzheimer disease and Parkinson disease. *Free Radical Biology and Medicine*. 2013, vol. 62, no. 1, pp. 90–101. ISSN 08915849. DOI 10.1016/j.freeradbiomed.2012.11.014
- [154] HROCH, L., O. BENEK, P. GUEST, L. AITKEN, O. SOUKUP, J. JANOCKOVA, K. MUSIL, V. DOHNAL, R. DOLEZAL, K. KUCA, T. K. SMITH, F. GUNN-MOORE and K. MUSILEK. Design, synthesis and in vitro evaluation of benzothiazole-based ureas as potential ABAD/17 $\beta$ -HSD10 modulators for Alzheimer's disease treatment. *Bioorganic and Medicinal Chemistry Letters*. 2016, vol. 26, no. 15, pp. 3675–3678. ISSN 14643405. DOI 10.1016/j.bmcl.2016.05.087
- [155] CHRIBEK, M. *Preparation of phenyl derived benzothiazoles as potential ABAD modulators*. Hradec Králové, 2016. Charles University in Prague, Faculty of Pharmacy in Hradec Kralove, Department of Pharmaceutical



Chemistry and Drug Control.

- [156] VALASANI, K. R., G. HU, M. O. CHANEY and S. S. YAN. Structure-Based Design and Synthesis of Benzothiazole Phosphonate Analogues with Inhibitors of Human Aβ for Treatment of Alzheimer's Disease. *Chemical Biology and Drug Design*. 2013, vol. 81, no. 2, pp. 238–249. ISSN 17470277. DOI 10.1111/cbdd.12068
- [157] BENEK, O. *Preparation and evaluation of potential drugs inhibiting mitochondrial enzymes*. Hradec Králové, 2016. University of Defence in Brno, Faculty of Military Health Sciences in Hradec Kralove, Department of Toxicology and Military Pharmacy.
- [158] PAJOUHESH, H. and G. R. LENZ. Medicinal chemical properties of successful central nervous system drugs. *NeuroRX*. 2005, vol. 2, no. 4, pp. 541–553. ISSN 1545-5343. DOI 10.1602/neurorx.2.4.541
- [159] LIPINSKI, C. A., F. LOMBARDO, B. W. DOMINY and P. J. FEENEY. Experimental and computational approaches to estimate solubility and permeability in drug discovery and development settings. *Advanced Drug Delivery Reviews*. 1997, vol. 23, nos. 1–3, pp. 3–25. ISSN 0169409X. DOI 10.1016/S0169-409X(96)00423-1
- [160] WAGER, T. T., X. HOU, P. R. VERHOEST and A. VILLALOBOS. Moving beyond rules: The development of a central nervous system multiparameter optimization (CNS MPO) approach to enable alignment of druglike properties. *ACS Chemical Neuroscience*. 2010, vol. 1, no. 6, pp. 435–449. ISSN 19487193. DOI 10.1021/cn100008c
- [161] JUÁREZ-JIMÉNEZ, J., E. MENDES, C. GALDEANO, C. MARTINS, D. B. SILVA, J. MARCO-CONTELLES, M. DO CARMO CARREIRAS, F. J. LUQUE and R. R. RAMSAY. Exploring the structural basis of the selective inhibition of monoamine oxidase A by dicarbonitrile aminoheterocycles: Role of Asn181 and Ile335 validated by spectroscopic and computational studies. *Biochimica et Biophysica Acta - Proteins and Proteomics*. 2014, vol. 1844, no. 2, pp. 389–397. ISSN 15709639. DOI 10.1016/j.bbapap.2013.11.003
- [162] BENEK, O., O. SOUKUP, M. PASDIOROVA, L. HROCH, V. SEPSOVA, P. JOST, M. HRABINOVA, D. JUN, K. KUCA, D. ZALA, R. R. RAMSAY, J. MARCO-CONTELLES and K. MUSILEK. Design, Synthesis and in vitro Evaluation of Indolotacrine Analogues as Multitarget-Directed Ligands for the Treatment of Alzheimer's Disease. *ChemMedChem*. 2016, vol. 11, no. 12, pp. 1264–1269. ISSN 18607187. DOI 10.1002/cmdc.201500383
- [163] GUEST, P. *The identification and characterisation of novel inhibitors of the 17β-HSD10 enzyme for the treatment of Alzheimer's disease*. St. Andrews, 2016. University of St. Andrews.
- [164] BOUNAUD, P. Y., S. HOPKINS, E. JEFFERSON, M. WILSON, M. WONG and T. KANOUNI. Pyrazolothiazole Protein Kinase Modulators. U.S. Patent 11/560,460. 2007.
- [165] MÉNARD, D., I. NICULESCU-DUVAZ, H. P. DIJKSTRA, D. NICULESCU-DUVAZ, B. M. J. M. SUIJKERBUIJK, A. ZAMBON, A. NOURRY, E. ROMAN, L. DAVIES, H. A. MANNE, F. FRIEDLOS, R. KIRK, S. WHITTAKER, A. GILL, R. D. TAYLOR, R. MARAIS and C. J. SPRINGER. Novel potent BRAF inhibitors: Toward 1 nM compounds through optimization of the central phenyl ring. *Journal of Medicinal Chemistry*. 2009, vol. 52, no. 13, pp. 3881–3891. ISSN 00222623. DOI 10.1021/jm900242c
- [166] NIZOVTSSEV, A. V., A. SCHEURER, B. KOSOG, F. W. HEINEMANN and K. MEYER. Synthesis of differently substituted tacn-based ligands: Towards the control of solubility and electronic and steric properties of uranium coordination complexes. *European Journal of Inorganic Chemistry*. 2013, vol. 2013, no. 14, pp. 2538–2548. ISSN 14341948. DOI 10.1002/ejic.201201549
- [167] JIN, Y., Z. Y. ZHOU, W. TIAN, Q. YU and Y. Q. LONG. 4'-Alkoxy substitution enhancing the anti-mitotic effect of 5-(3',4',5'-substituted)anilino-4-hydroxy-8-nitroquinazolines as a novel class of anti-microtubule agents. *Bioorganic and Medicinal Chemistry Letters*. 2006, vol. 16, no. 22, pp. 5864–5869. ISSN 0960894X. DOI 10.1016/j.bmcl.2006.08.058
- [168] ENGERS, D. W., J. R. FIELD, U. LE, Y. ZHOU, J. D. BOLINGER, R. ZAMORANO, A. L. BLOBAUM, C. K.

- JONES, S. JADHAV, C. D. WEAVER, P. J. CONN, C. W. LINDSLEY, C. M. NISWENDER and C. R. HOPKINS. Discovery, Synthesis, and Structure–Activity Relationship Development of a Series of *N*-(4-Acetamido)phenylpicolinamides as Positive Allosteric Modulators of Metabotropic Glutamate Receptor 4 (mGlu<sub>4</sub>) with CNS Exposure in Rats. *Journal of Medicinal Chemistry*. 2011, vol. 54, no. 4, pp. 1106–1110. ISSN 0022-2623. DOI 10.1021/jm101271s
- [169] REDDY, S. S., V. K. RAO, B. S. KRISHNA, C. S. REDDY, P. V. RAO and C. N. RAJU. Synthesis, Antimicrobial, and Antioxidant Activity of New  $\alpha$ -Aminophosphonates. *Phosphorus, sulfur, and silicon and the related elements*. 2011, vol. 186, no. 7, pp. 1411–1421. ISSN 10426507. DOI 10.1080/10426507.2010.514682
- [170] KOBAYASHI, K., K. YONEDA, K. MIYAMOTO, O. MORIKAWA and H. KONISHI. A convenient synthesis of quinolines by reactions of *o*-isocyano- $\beta$ -methoxystyrenes with nucleophiles. *Tetrahedron*. 2004, vol. 60, no. 50, pp. 11639–11645. ISSN 00404020. DOI 10.1016/j.tet.2004.09.069
- [171] JUNG, S. H., J. H. AHN, S. K. PARK and J. CHOI. A Practical and Convenient Procedure for the *N*-Formylation of Amines Using Formic Acid. *Bull. Korean Chem. Soc.* 2002, vol. 23, no. 1, pp. 149–150. ISSN 02532964. DOI 10.5012/bkcs.2002.23.1.149
- [172] KOBAYASHI, K., T. KOMATSU, Y. YOKOI and H. KONISHI. Synthesis of 2-aminoindole-3-carboxylic acid derivatives by the copper(I) iodide catalyzed reaction of *N*-(2-iodophenyl)formamides with malononitrile or cyanoacetates. *Synthesis*. 2011, vol. 2011, no. 5, pp. 764–768. ISSN 00397881. DOI 10.1055/s-0030-1258422
- [173] YANG, X., H. FU, R. QIAO, Y. JIANG and Y. ZHAO. A simple copper-catalyzed cascade synthesis of 2-amino-1*H*-indole-3-carboxylate derivatives. *Advanced Synthesis and Catalysis*. 2010, vol. 352, no. 6, pp. 1035–1038. ISSN 16154150. DOI 10.1002/adsc.200900887
- [174] ARIGELA, R. K., R. KUMAR, S. SAMALA, S. GUPTA and B. KUNDU. Diversity-Oriented Synthesis of Polycyclic Indoles: Brønsted or Lewis Acid Catalyzed Three-Component Reaction for the Synthesis of  $\alpha$ -Carbolines and Pyrimidoindoles. *European Journal of Organic Chemistry*. 2014, vol. 2014, no. 27, pp. 6057–6066. ISSN 10990690. DOI 10.1002/ejoc.201402633
- [175] WOODS, K. W., J. P. FISCHER, A. CLAIBORNE, T. LI, S. A. THOMAS, G. D. ZHU, R. B. DIEBOLD, X. LIU, Y. SHI, V. KLINGHOFER, E. K. HAN, R. GUAN, S. R. MAGNONE, E. F. JOHNSON, J. J. BOUSKA, A. M. OLSON, R. de JONG, T. OLTERS DORF, Y. LUO, S. H. ROSENBERG, V. L. GIRANDA and Q. LI. Synthesis and SAR of indazole-pyridine based protein kinase B/Akt inhibitors. *Bioorganic and Medicinal Chemistry*. 2006, vol. 14, no. 20, pp. 6832–6846. ISSN 09680896. DOI 10.1016/j.bmc.2006.06.047
- [176] CASTLE, R. N., R. R. SHOUP, K. ADACHI and D. L. ALDOUS. Cinnoline chemistry. IX. 5-, 6-, 7- and 8-halogen substituted 4-mercaptocinnolines and related compounds. *Journal of Heterocyclic Chemistry*. 1964, vol. 1, no. 2, pp. 98–106. ISSN 0022152X. DOI 10.1002/jhet.5570010210
- [177] ZHANG, X., X. JIANG, K. ZHANG, L. MAO, J. LUO, C. CHI, H. S. O. CHAN and J. WU. Synthesis, Self-Assembly, and Charge Transporting Property of Contorted Tetrabenzocoronenes. *Journal of Organic Chemistry*. 2010, vol. 75, no. 23, pp. 8069–8077. ISSN 00223263. DOI 10.1021/jo101701k

## 10. Attachments

- A1** HROCH, L., L. AITKEN, O. BENEK, M. DOLEZAL, K. KUCA, F. GUNN-MOORE and K. MUSILEK. Benzothiazoles - Scaffold Of Interest For CNS Targeted Drugs. *Current Medicinal Chemistry*. 2015, vol. 22, no. 6, pp. 730–747. IF<sub>2016</sub> = 3.455.
- A2** HROCH, L., P. GUEST, O. BENEK, O. SOUKUP, J. JANOCKOVA, R. DOLEZAL, K. KUCA, L. AITKEN, T. K. SMITH, F. GUNN-MOORE, D. ZALA, R. R. RAMSAY and K. MUSILEK. Synthesis and evaluation of frentizole-based indolyl thiourea analogues as MAO/ABAD inhibitors for Alzheimer's disease treatment. *Bioorganic and Medicinal Chemistry*. 2017, vol. 25, no. 3, pp. 1143–1152. IF<sub>2016</sub> = 2.923.
- A3** HROCH, L., O. BENEK, P. GUEST, L. AITKEN, O. SOUKUP, J. JANOCKOVA, K. MUSIL, V. DOHNAL, R. DOLEZAL, K. KUCA, T. K. SMITH, F. GUNN-MOORE and K. MUSILEK. Design, synthesis and in vitro evaluation of benzothiazole-based ureas as potential ABAD/17 $\beta$ -HSD10 modulators for Alzheimer's disease treatment. *Bioorganic and Medicinal Chemistry Letters*. 2016, vol. 26, no. 15, pp. 3675–3678. IF<sub>2016</sub> = 2.486.
- A4** BENEK, O., O. SOUKUP, M. PASDIOROVA, L. HROCH, V. SEPSOVA, P. JOST, M. HRABINOVA, D. JUN, K. KUCA, D. ZALA, R. R. RAMSAY, J. MARCO-CONTELLES and K. MUSILEK. Design, Synthesis and in vitro Evaluation of Indolotacrine Analogues as Multitarget-Directed Ligands for the Treatment of Alzheimer's Disease. *ChemMedChem*. 2016, vol. 11, no. 12, pp. 1264–1269. IF<sub>2016</sub> = 2.980.
- A5** LOVERIDGE, E. J., L. HROCH, R. L. HUGHES, T. WILLIAMS, R. L. DAVIES, A. ANGELASTRO, L. Y. P. LUK, G. MAGLIA and R. K. ALLEMANN. Reduction of Folate by Dihydrofolate Reductase from *Thermotoga Maritima*. *Biochemistry*. 2017, vol. 56, no. 13, pp. 1879–1886. IF<sub>2016</sub> = 2.876.